Geoscience Frontiers 7 (2016) 495–528

HOSTED BY

Contents lists available at ScienceDirect

China University of Geosciences (Beijing)

Geoscience Frontiers

journal homepage: www.elsevier.com/locate/gsf

Research paper

The Muruntau gold deposit (Uzbekistan) – A unique ancient hydrothermal system in the southern Tien Shan

Ulf Kempe [a], Torsten Graupner [b], Reimar Seltmann [c,*], Hugo de Boorder [d], Alla Dolgopolova [c], Maarten Zeylmans van Emmichoven [d]

[a] Institut für Mineralogie, TU Bergakademie Freiberg, Brennhausgasse 14, 09596 Freiberg, Germany
[b] Federal Institute for Geosciences and Natural Resources (BGR), Stilleweg 2, 30655 Hannover, Germany
[c] Centre for Russian and Central EurAsian Mineral Studies (CERCAMS), Department of Earth Sciences, Natural History Museum, Cromwell Road, London SW7 5BD, UK
[d] Faculty of Geosciences, Utrecht University, Heidelberglaan 2, 3584 CS Utrecht, The Netherlands

ARTICLE INFO

Article history:
Received 22 July 2015
Received in revised form
20 September 2015
Accepted 24 September 2015
Available online 23 October 2015

Keywords:
Muruntau
Gold deposit
Fluid inclusions
Isotope data
Gold composition

ABSTRACT

The Muruntau gold deposit in the Central Kyzylkum, Uzbekistan is one of the largest single gold deposits worldwide. Data available from the literature are reviewed with the aim to (1) integrate the present knowledge on this unique deposit from Russian and English literature; (2) show the considerable progress made in the understanding of the genesis of the Muruntau deposit during the last decades; and (3) point to problems still open for future research. Deposit formation occurred through a multi-stage process involving sedimentation, regional metamorphism including thrusting, magmatism with formation of hornfels aureoles and several stages of hydrothermal activity. According to recent knowledge, synsedimentary or pure metamorphic formation of gold mineralization seems unlikely. The role of granite magmatism occurring roughly within the same time interval as the main hydrothermal gold precipitation remains uncertain. There are no signs of interaction of matter between the magma(s) and the hydrothermal system(s). On the other hand, there was an intense, high-temperature (above 400 °C) fluid – wall rock interaction resulting in the formation of gold-bearing, cone-like stockworks with veins, veinlets and gold-bearing metasomatites. Several chemical and isotope indicators hint at an involvement of lower-crustal or mantle-related sources as well as of surface waters in ore formation. Deposit formation through brecciation involving explosion, hydrothermal or tectonic breccias might explain these data. Further investigations on breccia formation as well as on the exact timing of relevant sedimentary, metamorphic, magmatic and hydrothermal events are recommended.

© 2015, China University of Geosciences (Beijing) and Peking University. Production and hosting by Elsevier B.V. This is an open access article under the CC BY-NC-ND license (http://creativecommons.org/licenses/by-nc-nd/4.0/).

1. Introduction

The Muruntau gold deposit in western Uzbekistan is one of the largest individual gold deposits worldwide with resources in excess of 5000 mt (metric tons) of gold. It was discovered in 1958 by Mordvintsev Y.N., Khamyshkin P.V. and Luk'yanov S.I. by verification of an arsenic geochemical anomaly (Konstantinov et al., 2000). Interestingly, the discovery of a significant gold mineralization in that area was in contrast with generally accepted models for gold deposits at that time (Petrovskaya, 1968).

The history of scientific work on Muruntau may be subdivided into two main periods. In Soviet times, the area was closed to foreign visitors and few publications appeared in the Russian literature, sometimes even without providing the name and location of the deposit, or printed in local journals and books. At that time, extensive work had been performed by Soviet geologists from Uzbekistan and leading research institutes and universities in Moscow and Leningrad (now St. Petersburg) including field work, thin section studies by optical methods, chemical whole rock analyses (mostly focused on main compounds and gold contents), studies on heavy mineral fractions and fluid inclusions (including

* Corresponding author.
E-mail addresses: kempe@mineral.tu-freiberg.de (U. Kempe), Torsten.Graupner@bgr.de (T. Graupner), r.seltmann@nhm.ac.uk (R. Seltmann), H.deBoorder@uu.nl (H. de Boorder), allad@nhm.ac.uk (A. Dolgopolova), M.J.ZeylmansVanEmmichoven@uu.nl (M. Zeylmans van Emmichoven).
Peer-review under responsibility of China University of Geosciences (Beijing).

http://dx.doi.org/10.1016/j.gsf.2015.09.005
1674-9871/© 2015, China University of Geosciences (Beijing) and Peking University. Production and hosting by Elsevier B.V. This is an open access article under the CC BY-NC-ND license (http://creativecommons.org/licenses/by-nc-nd/4.0/).

decrepitation and homogenization methods) and first isotope research. The main objectives of those studies were (1) characterization of magmatic and metamorphic host rocks, (2) clarification of the age relationships (according to paleontological and first K-Ar and Rb-Sr isotope data), (3) study of gold types and distribution and (4) understanding of tectonic controls of gold mineralization. The relationship of hydrothermal activity to granite magmatism and related contact metamorphism was also investigated to some extent. A comprehensive overview on the results and outcomes of this period is given in Shayakubov (1998). This review paper will therefore repeatedly refer to Shayakubov's book.

The first research period ended with a cooperative scientific agreement between the U.S. Geological Survey and the Ministry of Geology of the Soviet Union in 1989 (Drew et al., 1996). Since that time, working groups from the U.S.A., Canada, Germany and Australia used modern methods of research to contribute to a better understanding of the genesis of this unique deposit along with the continuing studies by Uzbekian and Russian scientists. The knowledge on the genesis of the Muruntau deposit was reviewed to various extents and at various times by Kremenetsky et al. (1990), Kotov and Poritskaya (1991), Berger et al. (1994), Drew et al. (1996), Konstantinov et al. (2000) and others.

As will be demonstrated below, there is not a lot of controversy about the principal facts observed (while, of course, still ambiguity remains in the details), but there is much less agreement in data interpretations concerning the genesis and even the timing of gold mineralization at Muruntau. Naturally, works focused on one particular aspect of the problem stress this particular point not considering results obtained in other fields. It is therefore the aim of the present work to critically review results of previous studies on Muruntau with a focus on more recent research to demonstrate the progress and limitations in our recent understanding of the formation history of one of the most important gold deposit worldwide. A major point of our work is also to constrain unresolved problems open for future research.

2. Economic geology

With more than 5300 mt Uzbekistan hosts the fourth largest known gold reserves on earth (Safirova, 2014). The Muruntau deposit, exploited by the state-owned Navoi Mining and Metallurgical Combinat (NMMC), is one of the world's largest open-pit gold mines. The deposit accounts for a total resource (past production, reserves and resources) in excess of 170 Moz (million oz) of gold (5246 mt; Goldfarb et al., 2014). It has produced over 50 Moz of gold (1600 mt) since the beginning of production in 1967 (Toovey, 2011).

Estimated annual production of gold from the open-pit mine over the past decades was 1.8–2.0 Moz. Based on available production data, the mining complex, comprising the open pit, underground mining and heap leach operations, is believed to have had in 2014 about 2.6 Moz of gold production, which would be the first rank in the 2014 list of the world's top ten gold operations (Basov, 2015).

Presently, the fourth stage of mining from the Muruntau open pit with a surface size of 3.35 km × 2.5 km and a depth of 560 m is active (extension of mining depth planned to >1000 m; combining open pit and underground mining). Joining up of the Muruntau and Myutenbai open pits is planned in 2015, and the length of the open pit will increase to 4.27 km (NGMK, 2015). Due to depletion of reserves, NMMC has recently commissioned the world biggest BIOX® plant.

A new mine, Besopan, will be launched in a part of the deposit that the company has been exploring recently. The mine will be commissioned in 2016–2017 with a capacity of about 5–10 mt/year (preliminary information; Vorotnikov, 2014). Overall production of gold at NMMC's Muruntau open-pit mine is expected to grow by 30% to 2.5 Moz/year. The reserves at Muruntau are expected to last until approximately 2032 (Toovey, 2011 – GoldInvestingNews.com).

Gold mining at Muruntau is conducted using a truck and conveyor ore transportation system. The Muruntau processing plant treats ore with an average head grade of 2.4 g/t Au at the rate of 2.2 kt/day.

3. Regional geology

3.1. Cessation of accretionary tectonics and formation of gold deposits in Central Asia

The closure of the ocean basins between the Siberian craton and the Kazakhstan, Tarim and North China blocks controlled the final amalgamation of the Central Asian Orogenic Belt (CAOB) also known as the Altaid Orogen (Natal'in and Şengör, 2005). This process created in the western part of the area – now represented by the southern Tien Shan belt – favourable conditions for the formation of gold deposits. The southern Tien Shan gold belt includes large deposits such as Zarmitan, Jilau, Taror and Savoyardy that like Muruntau occur as large vein and stockwork systems often hosted by older, competent intrusive bodies or along the sheared margins of the intrusions (Goldfarb et al., 2014, Fig. 1). The distribution of middle to late Paleozoic gold ores is generally controlled by the final closure of the Turkestan Ocean, another basin developed along the northern Paleotethys Ocean, located between the Tarim–Karakum (e.g., Zonenshain et al., 1990) and Kazakhstan microcontinents during the Devonian to early Permian (e.g., Heubeck, 2001). The closure was contemporaneous with subduction of Paleotethys oceanic crust beneath the Tarim–Karakum block and of the Turkestan Ocean crust below the Kazakhstan block (Goldfarb et al., 2014).

Almost all the larger gold deposits, from Uzbekistan eastward to southern Mongolia, formed mainly during a brief 10–20 Ma long episode roughly at the Carboniferous–Permian time boundary and were classified as orogenic by Goldfarb et al. (2014). This episode reflects the well-defined cessation of compressional accretionary tectonics and the onset of large-scale strike-slip movement (Allen et al., 1995; Laurent-Charvet et al., 2003) along the many terrane suture zones of the Tien Shan, which were previously marked by thrust faulting (Goldfarb et al., 2014). Timing for this compressional to strike-slip transition in the CAOB, marking a change from subduction-related calc-alkaline to post-subduction more alkaline magmatism, is best placed at ca. 280–290 Ma (e.g., Ecomomos et al., 2012).

Late Paleozoic accretionary orogenesis on the southern side of the Kazakhstan block led to the formation of gold deposits mainly seaward of the Valerianov–Beltau–Kurama continental arc (Fig. 1). Where the western part of the Turkestan Ocean basin was closed, several world-class deposits and numerous smaller deposits formed in the southern Tien Shan, an area, typically considered the most outboard part of the western CAOB (Goldfarb et al., 2014). The rocks of the southern Tien Shan are dominated by carbonate platform sequences on the northwestern margin of the Tarim–Karakum block and clastic sedimentary rocks from the closing ocean basin to the south, with some intercalations of felsic to intermediate volcanic rocks.

Muruntau, situated in the westernmost part of the mountain range (Fig. 1), is the largest of the known gold deposits of the southern Tien Shan. Other significant gold deposits of probably similar age include the adjacent Kokpatas, Amantaitau, and Daugyztau. This important group of deposits is located to the south of a major offset within the Turkestan suture between the Kazakhstan

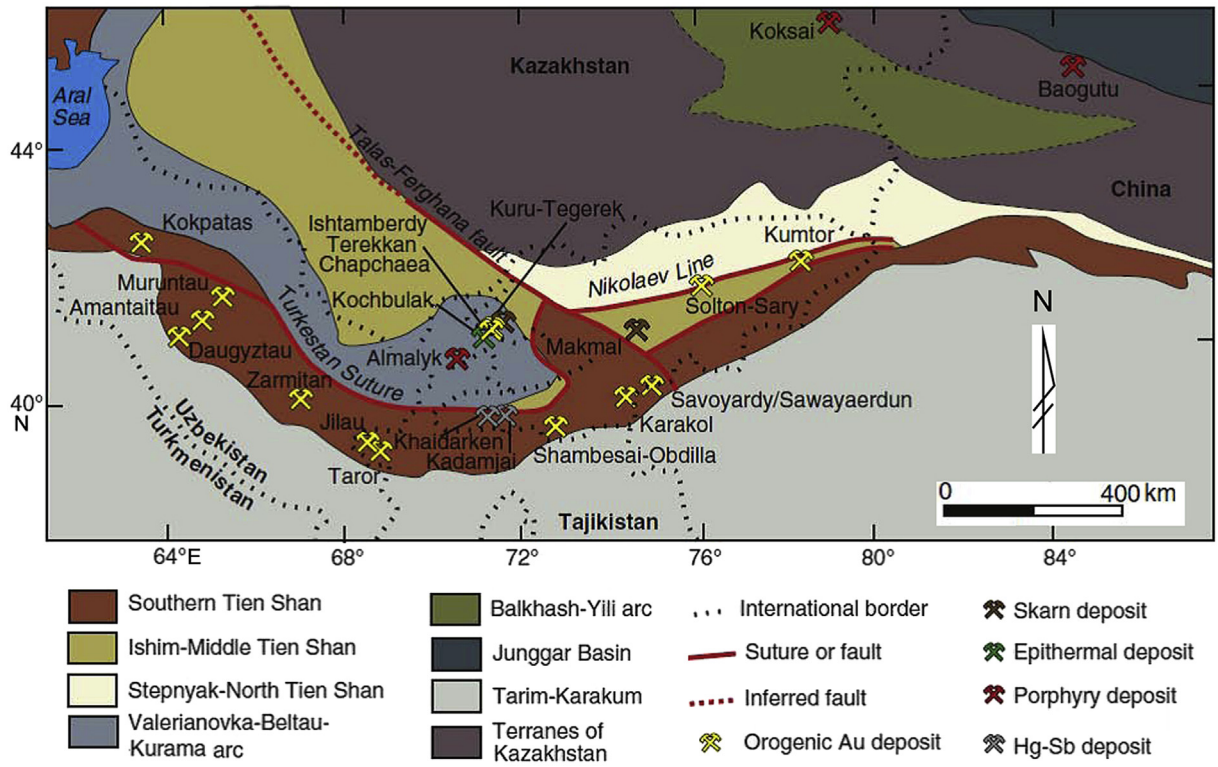

Figure 1. Present day configuration of the geology of the Tien Shan, central Asia, showing the most significant late Paleozoic Au-bearing mineral deposits. Map from Goldfarb et al. (2014) based on Yakubchuk et al. (2002), Konopelko et al. (2007) and Windley et al. (2007).

and Tarim–Karakum blocks (e.g., Fig. 1 in Natal'in and Şengör, 2005).

3.2. Regional-scale characteristics of gold deposits setting

The order of magnitude of Muruntau requires drawing attention to three regional-scale phenomena that highlight the unique location of the Kyzylkum gold district within the Tien Shan belt and which may shed further light on its geological background and uniqueness: features of morphology, magnetic field anomalies and mega-scale structures (De Boorder, 2012).

3.2.1. Morphology

Multi-resolution satellite imagery (Fig. 2a) illustrates the location of the Kyzylkum gold district where the morphological expression of the ore-bearing complexes is characterized by distinctly annular outlines which may relate to two underlying broad anticlinoria, the Tamdytau anticlinorium hosting Muruntau and the Bukantau anticlinorium hosting Kokpatas, in whose cores 280–295 Ma granitoid complexes have been emplaced (Kotov and Poritskaya, 1991; Seltmann et al., 2003, 2015; Wall et al., 2004). In a regional map view, the cupola-like structure in the Tamdytau area is expressed by gently curved fold axes parallel to the contact with the surrounding sediments to the north (Fig. 2a). The outline of the outcropping ore-hosting complexes may, therefore, have its origin in the underlying structures, the more so because the same trends are observed in the magnetic anomaly pattern (Makarova, 1974; see section 3.2.2 below), and in both the gravity anomaly pattern and the distribution of granitic complexes (CERCAMS Central Asia map 1:1,500,000, Seltmann et al., 2015).

The Cretaceous and Cenozoic sediments surrounding the ore-hosting crystalline complexes generally show subhorizontal attitude. The sediments are distributed northward from the Samarkand-Nukus belt into the flat, arid areas towards Kyzyl Orda. Although the outcrops of the crystalline complexes permit local correlation with lithologies of the southern Tien Shan, the extensive cover of Mesozoic–Cenozoic sediments towards Kyzyl Orda and Nukus obstructs detailed surface examination of the regional structural configurations. Consequently, it is not yet possible to trace structural relations between the Tien Shan and the Urals to the north of the area under consideration.

The multi-resolution imagery provides further indication of complex configurations in the subsurface, which at the regional scale reside in:

(1) a split in the west-north westerly structural Tien Shan grain north of Samarkand, with one branch continuing along strike and expressed by the ranges along the Central Ust Yurt Fault towards Nukus and a second branch diverging from the southern Nuratau Mountains to a more northwesterly direction towards the Tamdytau and Bukantau areas (Fig. 2a),
(2) the continuation of the latter structural grain into a semi-circular westward trend with east-west diameter of some 80 km particularly defined by the contacts between the Mesozoic and Cenozoic sediments with the crystalline complex of Tamdytau (Fig. 2a), while
(3) further northwest, the crystalline complex of the Bukantau hills is surrounded by a ring of younger sediments, with a diameter of about 100 km (Fig. 2a).

Compared to the easterly structural grain of the southern Tien Shan of eastern Uzbekistan, Kyrgyzstan and north-western China, the above patterns represent a notable break in the morphological expression of the mountain belt. Moreover, the multi-scale satellite imagery suggests that the structural grain of the crystalline complexes of Bukantau and Tamdytau is more variable and

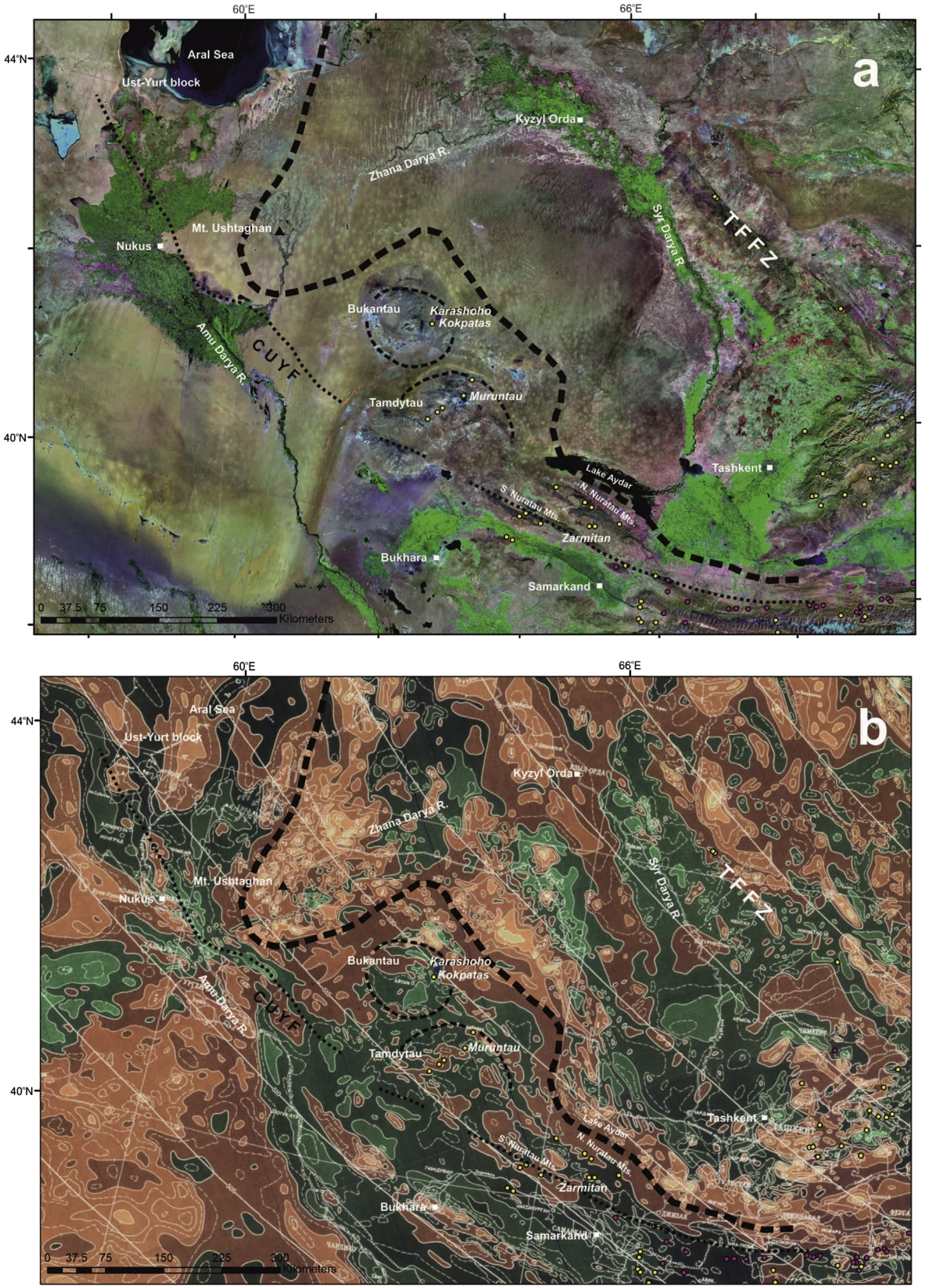

Figure 2. (a) Overview of the Kyzylkum region (TM7 – 7 red, 4 blue, 2 green), with the divisions inferred from the magnetic anomaly map in Fig. 2b. The medium dashed lines of the Muruntau and Kokpatas anomalies, derived in Fig. 2b, find support in the morphology of the surface features. The anomaly expresses the Valerianov – Beltau-Kurama volcanic arc and the suture of the Turkestan Ocean. TFFZ – Talas-Fergana Fault Zone. The finely dotted line represents the Central Ust Yurt Fault (CUYF) whose trace is probably located along the southern margin of the South Nuratau range (Fig. 2b). The medium dashed lines represent the annular outlines of the Muruntau and Kokpatas anomalies. Yellow dots represent gold deposits and purple dots represent mercury and mercury-antimony deposits. The Karashoho lamproite near Kokpatas is diamondiferous. (b) Magnetic anomaly pattern of the Kyzylkum region between the Amu Darya and Syr Darya Rivers after Makarova (1974) with interpretation of the major structures, also showing ore deposits, towns and rivers. Positive anomalies are in brown to white colour pattern, and negative anomalies are in dark to light blue colour pattern. Heavy dashed line separates the high-frequency eastern part of the main Kyzylkum anomaly from the lower-frequency western part of the anomaly.

disharmonious than is apparent from small-resolution geological maps (e.g. Seltmann et al., 2015). In the multi-resolution imagery, the morphology of the two crystalline complexes also reflects some of the features observed in the field (e.g. Drew et al., 1996 and references therein; Yakubchuk et al., 2005). In particular, these include Devonian to Carboniferous carbonate bands, shear zones with sinistral offset and outcrop configurations in unidentified lithologies. The Sangruntau-Tamdytau and Muruntau-Daugyztau shear zones controlling the Muruntau ore deposit (Drew et al., 1996; see section 4 below) cannot be defined in the imagery. On the basis of the surface configurations alone, the deformation mechanisms remain obscure exacerbating the puzzle of the nearby continuity from the Tien Shan to the Urals. Yet, the reality of the surface phenomena finds support and explanation in regional potential field anomalies, associated with structures in deeper levels as demonstrated below.

3.2.2. Magnetic anomalies

The regional magnetic anomaly map (Makarova, 1974) has been included in the digitally available Magnetic Map of the World (Korhonen et al., 2007) which depicts the same larger features as the original maps but does not clearly express its fine details. For the purposes of the present study, we have scanned the original magnetic anomaly map which, georeferenced to geographical coordinates, permits comparison with satellite imagery and other digital maps. In this way, the elongated morphological elements in the Palaeozoic complexes of the Nuratau Mountains and the Mesozoic–Cenozoic sediments towards Muruntau and Kokpatas are seen to coincide with a prominent curvilinear magnetic anomaly between Samarkand, Kyzyl Orda and the Aral Sea (Fig. 2b), hereafter called the Kyzylkum magnetic anomaly. This anomaly can be traced from south of Tashkent through Lake Aydar, to the northwest as far as latitude 44°N, southwest again as far as the Amu Darya river in the Mt. Ushtaghan area where it turns north across the Aral Sea and beyond. It corresponds to the connecting element of the Urals and the Tien Shan and resides in the Valerianovka – Beltau-Kurama (VBK) arc bordering the Kazakh-Kyrgyz continent to the east (Zonenshain et al., 1990). The N–NE striking Valerianovka branch of this arc, north of Mt. Ushtaghan, is part of the Trans-Uralian Zone. This branch is made up of Andean-type volcanics and intrusives and hosts prominent Kiruna-type iron deposits, copper-molybdenum porphyry systems and gold-copper skarns (Koroteev et al., 1997; Herrington et al., 2005, 2008). East of Mt. Ushtaghan, the Beltau-Kurama branch of the arc is located just north of Kokpatas and Muruntau. It connects eastward to the Middle Tien Shan. While the Valerianovka – Beltau-Kurama arc is largely obscured by the sediments of the Syrdarya Basin, the regional magnetic anomaly maps clearly show a continuous delineation across the Basin towards the Talas-Fergana Fault Zone (TFFZ, Figs. 1 and 2) in the east.

In the region of interest, the magnetic response of a broad segment of the Beltau-Kurama branch, standing out with its three obvious bends (Fig. 2b) shows that the arc encloses the Tamdytau and Bukantau areas with the Muruntau and Kokpatas ore deposits, respectively. These bends are viewed as oroclines, albeit of different orders (see Rosenbaum, 2014). There is a first order orocline, which links the Tien Shan ranges to the Urals backbone, and some superimposed higher order oroclines in the Mt. Ushtaghan-Bukantau-Tamdytau area.

In addition to the principal regional features, the magnetic anomaly map by Makarova (1974) showed a number of small anomalies which provide some further insight in regional structures in combination with data from multi-resolution imagery and field observations. In the Bukantau-Tamdytau area, the inner perimeter of the principal Kyzylkum magnetic anomaly encloses a domain characterized by numerous smaller anomalies which, where elongate, are seen to follow the surrounding arcuate trend. This domain has a NE–SW diameter of some 150 km measured between Kokpatas and the Central Ust Yurt Fault. It shows two compartments, located over the mineralized Tamdytau and Bukantau areas, respectively, which correspond to the two annular morphological features discussed in the previous section. In addition, the principal Kyzylkum magnetic anomaly shows a multitude of small anomalies along its eastern margin (Fig. 2b). In the southeastern limb of the Mt. Ushtaghan orocline, the frequency of these small anomalies decreases notably to increase again to the north. The latter abrupt change may represent a NE–SW-striking tectonic offset of the source of the anomaly, the volcanic Beltau-Kurama arc.

Summarizing, the host complexes of the Kyzylkum gold district are lodged in oroclinal structures, between first order orogenic and plate tectonic elements. The high-frequency magnetic linears on the eastern side of the Kyzylkum magnetic anomaly and within the enclosed ore-hosting domain between Kokpatas and the Samarkand-Nukus zone may witness a fragmented nature of parts of the volcanic Beltau-Kurama–Valerianovka arc and/or the Turkestan Suture, and of the enclosed complexes that host the gold deposits. The inferred fragmentation may be due to original variations in composition and/or to deformation. Since the early to mid Palaeozoic complexes exposed within the enclosed domain are comparable to those that make up the southern Tien Shan further east (where such magnetic anomaly patterns are not apparent), the fragmented appearance here may rather result from large-scale deformation.

3.2.3. Mega-scale structures

The dimensions of the Kyzylkum oroclines are modest compared with the known prominent oroclines of Central Asia (Yakubchuk et al., 2005; Van der Voo et al., 2006; Abrajevitch et al., 2007, 2008; Levashova et al., 2012). Yet, their location at the crossroads of three major orogenic systems – the northerly striking Urals, the easterly striking Variscides and the Tien Shan – lends the region a unique geodynamic focus. All three orogenic systems developed in the course of the Palaeozoic with the amalgamation of fragments of the Gondwana, Laurentia, Baltica, and Siberia continental masses across the Rheic, Palaeotethys, Palaeoasian and Neotethyan oceans.

On more regional scale, the Kyzylkum gold-hosting complex is wedged between the Beltau-Kurama arc with the Turkestan Suture to the north, the transcurrent Central Ust Yurt Fault to the south and the Ust Yurt Block to the west. To the east, there is the larger Kazakh-Kyrgyz block. The Kyzylkum complex, its internal structures and its ore deposits are therefore intimately connected with the interaction of major and minor continental lithosphere blocks (e.g. Biske and Seltmann, 2010). It owes its internal architecture to their collision and amalgamation in a framework of lithosphere-scale strike-slip dynamics, including clockwise and counter-clockwise rotation of the Siberian Craton during the Permian (Allen et al., 1995). In the Kyzylkum region itself, this strike-slip framework is witnessed by the geometrical configurations in the ranges between Nukus and Samarkand along the Central Ust Yurt Fault (Fig. 1). The sinistral sense of movement is consistent with reports by Yakubchuk et al. (2005). To the north of the Kyzylkum, Allen et al. (2006) inferred right-lateral slip and associated pull-apart basins in the subsurface of the West Siberian Basin on the basis of magnetic anomalies. In view of the widely spread lithosphere-scale, strike-slip deformation during the Permian, the principal magnetic Kyzylkum anomaly suggests large-scale, lateral buckling which probably also effected the entire Kyzylkum lithosphere column. The associated deformation of the trace of the Turkestan Suture suggests that the contortion reflected by the magnetic anomalies took place after the closure of the Turkestan

Ocean, estimated between 290 and 295 Ma (Biske and Seltmann, 2010; Glorie et al., 2010).

This conclusion confirms similar suggestions by Drew et al. (1996). Considering the translithospheric nature of the strike-slip deformation which implicated the involvement of the early Permian asthenosphere, the setting of the Kyzylkum ore district reinforces the 'buttress' hypothesis of Yakubchuk et al. (2005). The involvement of mantle sources is illustrated by the occurrence of 272–280 Ma old diamondiferous lamproite at Kokpatas (Golovko and Kaminsky, 2008, 2010).

3.3. Regional tectonics and Nd-Hf isotope data of granitoids

Results of Nd-Hf isotope mapping combined with U-Pb zircon SHRIMP geochronology and geochemical studies of granitoids from a sampling profile across terrane boundaries, including Kyzylkum of Uzbekistan and the Muruntau area under consideration, revealed distinct reservoir types (cratonic vs. turbiditic), corresponding to a diverse nature and origin of granitic magmatism (Seltmann et al., 2008; Dolgopolova et al., 2013). The studies tested three main tectonic domains (here described from N to S):

(1) Northernmost (as part of middle Tien Shan), the Beltau-Kurama tectonic zone with recycled crust of continental arc (lower Carboniferous to mid-Permian, C_1–P_2), represented by the giant Kalmakyr Cu-Au porphyry (~315 Ma, Seltmann et al., 2014) emplaced within massive Devonian to Carboniferous sediments and volcano-plutonic units. To the west, the North-Bukantau tectonic zone is located which is characterised by lower Devonian to late Carboniferous (middle Carboniferous according to former Soviet stratigraphy; D_1–C_2) oceanic arc tholeiites with slivers of Cambrian oceanic crust and early to late Carboniferous (or middle Carboniferous according to the alternative system; C_1–C_2) bimodal volcano-plutonic arc rocks with volcanomictic carbonate-terrigenic series.

(2) Following to the SW, there are exposed middle Paleozoic turbidites of the southern Tien Shan accretionary complex, represented by the Turkestan-Alai tectonic zone hosting the Zarmitan intrusion-related gold deposit (286 ± 2 Ma; Seltmann et al., 2011) in the Nurata region, and the Muruntau giant gold deposit (~290 Ma; see sections 7.1 and 8.4) in the Kyzylkum.

(3) Southernmost follow the Zarafshan-Alai and South Gissar tectonic zones, late Ordovician to late Carboniferous (alternatively, middle Carboniferous according to former Soviet timescale; O_3–C_2) back arc basins stitched by post-collisional granites of late Carboniferous to Permian (C_3–P) ages developed on pre-Cambrian cratonic crust of the Karakum microcontinent.

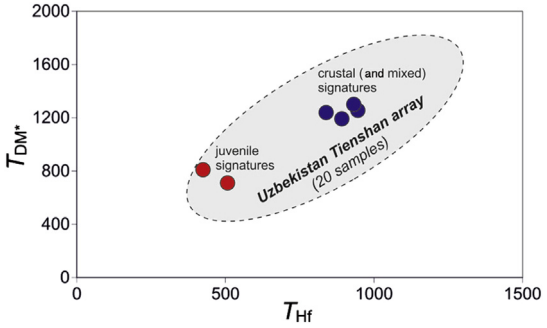

Figure 3. Nd model age (T_{DM^*}) vs. Hf-based ages (emplacement age plus previous crustal residence estimated from Hf isotope compositions of the dated zircons) for granitoid samples from a profile through the Tien Shan belt (grey array) including the Muruntau (Kyzylkum) area that is shown by coloured symbols (Data from Dolgopolova et al., 2013).

Nd isotopes (whole-rock) of granitoids from all domains show a wide range of ε_{Nd} (−5 to +7) indicating involvement of both mantle-derived material (subduction of oceanic crust) and older crustal sources (Mesoproterozoic model ages; Fig. 3). The large variations of Hf-isotope compositions found in zircons of the granites suggest recycling of older heterogeneous crustal protolith(s). In the southern Tien Shan, involvement of subducted oceanic crust is exemplified by juvenile ε_{Hf} values of up to +14 (Sultan-Uvais) and +16 (Teksquduk-Kyzylkum). However, Permo-Carboniferous granitoids occurring in all terranes exhibit predominantly crustal signatures indicating Neoproterozoic protoliths.

For the Kyzylkum profile, the Syrdarya Unit in the north is a cratonic Paleoproterozoic terrane, overlapped/stitched by a Paleozoic arc (this may explain the old ages reported by Mirkamalov et al., 2012a,b; see section 4.1.1.3). Muruntau is located at the northern margin of the turbidite terrane that formed the accretionary complex between the Syrdarya and Alai Units.

Nd–Hf model ages for studied samples from Kyzylkum (Dolgopolova et al., 2013) are shown in Fig. 3—the juvenile signatures of youngest intrusions (with early Paleozoic model ages of protolith) discriminate nicely against the cratonic basement signatures of samples with middle to Neo–Proterozoic model ages (= recycled crust). There is a fairly good agreement between the Hf and Nd model ages. The general linear relationship is what is expected if the two isotope systems reflect the same evolutionary processes. This matches interpretations of crust recycling and is in agreement with new results of U-Pb SHRIMP zircon dating of granitoid and metamorphic complexes including accretionary complexes of the Turkestan paleo-ocean and its northern and southern active continental margins (Mirkamalov et al., 2012a,b).

3.4. Regional geology: tectonic analyses

The regional geology of the Tamdytau area hosting the Muruntau gold deposit (Fig. 4) has been described in numerous publications. Only a brief overview is given in this section with focus on the tectonic evolution. For more details of the geological setting of Muruntau see section 4.

The deposit occurs within a pile of imbricated thrusts that was deformed into W–E-trending synforms and antiforms exposed in the Tamdytau (Tamdy Mountains) at the westernmost end of the southern Tien Shan (Drew et al., 1996). This structure consists of tectonically superimposed lithologies (Savchuk et al., 1991; Drew et al., 1996), which represent an early–middle Paleozoic oceanic to accretionary and fore-arc complex rocks thrust onto Vendian–middle Paleozoic passive margin sedimentary rocks whose Vendian–lower Paleozoic part was metamorphosed in the amphibolite to green schist facies (see section 4).

Drew et al. (1996) pointed out that the fold and fault belt of the Tien Shan system (Fig. 1) is extremely complex with various components that represent different orogenic events that span much of the Paleozoic and were later affected by an Alpine orogenic event (cf. Zonenshain et al., 1990). Drew et al. (1996) highlighted that in the central to western Tien Shan, a 5–6 km wide structural zone strikes over 1000 km north-westerly from the Fergana Valley in easternmost Uzbekistan, along the northern flank of the Nurata Mountains in the eastern Kyzylkum desert and thence northeast of the Tamdytau into the eastern Bukantau (Akhber and Mushkin, 1976). This structure is the suture zone that juxtaposes two continental masses, the Karakum massif to the southwest and the central Kazakhstan-North Tien Shan continent to the northeast (Zonenshain et al., 1990). A characteristic feature of the suture zone are the W–NW-striking shear zones that splay off to the west from the main zone that subdivides the Kyzylkum desert region into a series of tectonic blocks. The main suture and

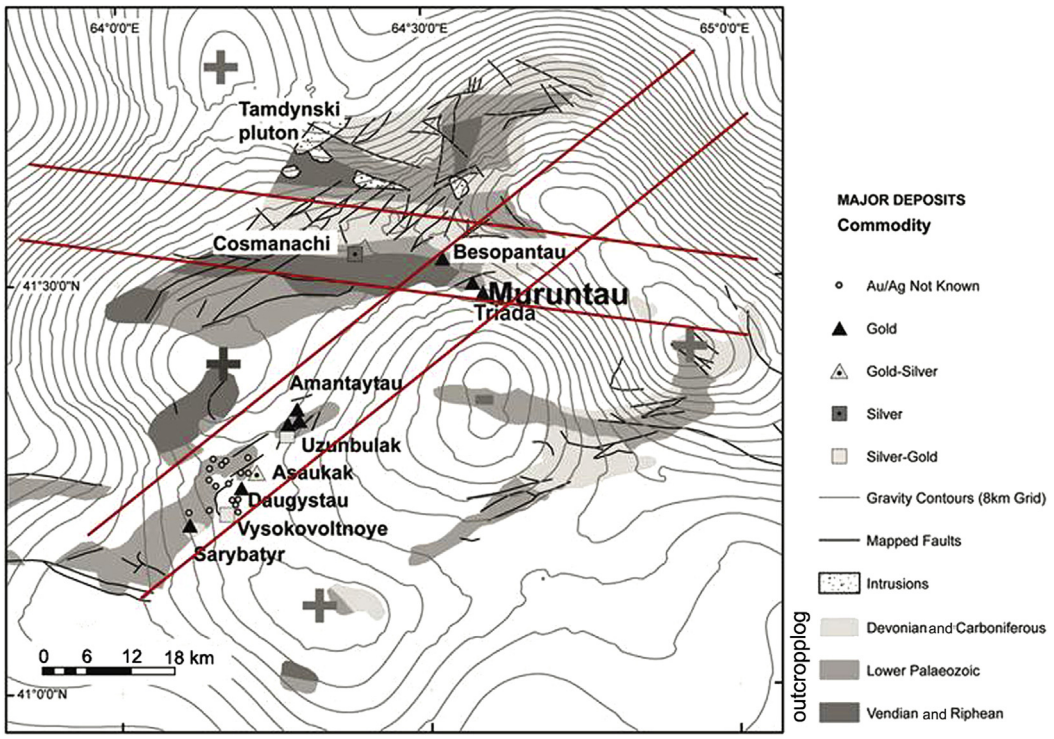

Figure 4. Position of gold and silver deposits in the Central Kyzylkum area aligning along the general northeast structural trend (see Fig. 1 for location). Gravity contour grid (centres of negative anomalies and positive anomalies indicated by symbols) has been draped over the geological sketch map (modified from Bierlein and Wilde, 2010). Muruntau is located at the junction of two main structural zones (in red), the northeast structural trend supposedly representing a trans-crustal shear zone and a subhorizontal structural trend reflecting the E–W strike of thrusted stratigraphy and fold axes (cf. Fig. 5).

the splays are offset by transverse northeast-striking shear zones (Mushkin et al., 1975).

In the vicinity of Muruntau, two regional shear zones, the northwesterly striking Sangruntau-Tamdytau and the transverse Muruntau-Daugyztau, developed during the 'Hercynian' (late Carboniferous–early Permian) at the time of the continent-to-continent collision of the Karakum plate and the central Kazakhstan-North Tien Shan continent (Zonenshain et al., 1990). The Hercynian compression led to the formation of north-dipping nappes. Two of these nappes transect the Tamdytau – a regional-scale syncline in the central part of the range and a regional-scale anticline in the south. Additional evidence for this continent-to-continent collision in Uzbekistan includes the occurrence of fragments of oceanic crust (Sabdyushev and Usmanov, 1971). A refraction seismic survey (Ivanov and Sabdyushev, 1974) and two USSR Deep-Geodynamic Drilling Program holes located near the center of the Tamdytau confirmed the synclinal structure in the central and northern parts of the range (Sabdyushev and Voronov, 1990).

Subsequent Hercynian transpression caused movement along the west-northwest-striking, left-lateral Sangruntau-Tamdytau shear zone and subsequently along the newly formed southwest-striking, left-lateral Muruntau-Daugyztau shear zone (Drew et al., 1996, Fig. 4). The interplay of movements along these shear zones changed the strike of the eastern nose of the antiformal nappe, which resulted in a Z-like-shaped fold near the southeastern tip of the Tamdytau that is best observed in the so-called Besapan-3 unit (bs_3; see section 4). The core of this Z-fold is transected by brittle faults of the Muruntau-Daugyztau shear zone and it is within this area that the current Muruntau open pit mine was developed.

Carboniferous–Permian granitoid intrusions were emplaced into the nappes, into the regional shear zones and transecting the inferred suture zone. Citing the work of Porshnyakov (1983), Kotov and Poritskaya (1991) stated that the intrusion of the granitoids was controlled by deep-seated, basement-penetrating faults. The numerous intrusions shown directly to the west of the Tamdytau indicate that a zone of dilatancy must have existed in the regional synclinorium, presumably created by the same tectonic forces that formed the Z-shaped structure (Drew et al., 1996).

The Muruntau-Daugyztau shear zone, along which there has been ductile and brittle deformation, is located in the southeastern portion of the Tamdytau. This fault strikes northeast-southwest and has been mapped over a length of 75 km and a width of about 5 km. Parallel faults were mapped to the northwest of the main fault zone in the same nappe and further to the northwest in the overlying synformal thrust package of Devonian and Carboniferous carbonate rocks. The movements on the Muruntau-Daugyztau faults are left lateral, as may be seen from the movement of the fault-bounded slices of Devonian carbonate rocks located to the northeast of the Muruntau open pit. The evolution in tectonic stress from the thrusting to the strike-slip regimes is demonstrated by the imposition of steeply dipping left-lateral faulting on the previously developed nappes. Intense hydrothermal alteration occurs in areas within and adjacent to the Muruntau-Daugyztau shear-zone. The orientation of the swarm of fault segments of this shear-zone system in the Muruntau area is parallel to the axis of the nappe south of the Tamdytau, which suggests that they have been developed along axial fractures and (or) thrust faults formed during the 'Hercynian' continent-to-continent collision (Drew et al., 1996).

Besides the large nappe structures discussed above, Proterozoic and Paleozoic formations in the Tamdytau show several generations of deformation that record a history of transition from ductile to brittle deformation styles (Drew et al., 1996). Alekseyev (1979) identified several distinct deformation events in rocks in the

Amantaitau region southwest of Muruntau, the oldest of which consists of small- and large-amplitude isoclinal folds overturned to the east and north that fold the original bedding. Facing determinations indicate that some of the folds, which are about 2 km wide, were transformed subsequently into a series of tectonic slices (Alekseyev, 1979).

According to Drew et al. (1996), this isoclinal folding was followed by metamorphic recrystallization and, in turn, by more-open folding without significant metamorphism. Several subsequent kink-fold events preceded the final shear-zone deformation described above. Because of the direction of isoclinal folding and the transposition of schistosity fabric by the 'Hercynian' compression, much of this deformation is interpreted to be 'Caledonian' (The term "Caledonian" is frequently used in the Russian language literature as synonym for 'early Paleozoic' orogenic events that could have taken place along the margins of the northern continents or along the northern margins of Gondwana. In today's geography, although formally, Caledonian events are restricted to the Caledonides of Scandinavia, Scotland and Ireland.). These deformation events, including the tectonic slicing, are of great importance for structural controls on veining and the stratabound nature of some of the ore bodies in the Muruntau and adjacent Myutenbai deposits as demonstated in the sections below. Yakubchuk et al. (2002) suggested – based on their structural analysis of the regional and detailed maps by Kotov and Poritskaya (1991) and by Drew (1993) – that there are two stratigraphically or tectonically controlled levels of highly silicified rocks in the Vendian-lower Paleozoic unit (Fig. 5). The upper silicification level, which hosts Muruntau and all small satellite deposits in the area, e.g., Kosmanachi, Besopan, Myutenbai, Triada, etc., forms a more than 7 km-long lens-shaped unit matching with the east-west tending Tamdytau-Sangruntau shear zone (Drew et al., 1996; Graupner et al., 2000, 2001a). The silicification developed along structures of the regional Dzhanbulak antiform and the Muruntau deposit occurs exactly at the eastern closure of this antiform whose pattern suggests that there were several superimposed deformational events (D1–D4; Fig. 5a–d). In particular, the density of the D3 fold axes is much greater at the eastern closure of the antiform where the Muruntau deposit occurs and where Drew et al. (1996) recorded the Z-shaped folds and their offset by the youngest strike-slip faults (D4). This structural framework was a path-way for entrapment of fluids (Yakubchuk et al., 2002). Seltmann et al. (2003) developed a tectonic model for the local formation of the ore-bearing structures at Muruntau in relation to the structural evolution of the area and the major alteration phases present as illustrated in Fig. 6.

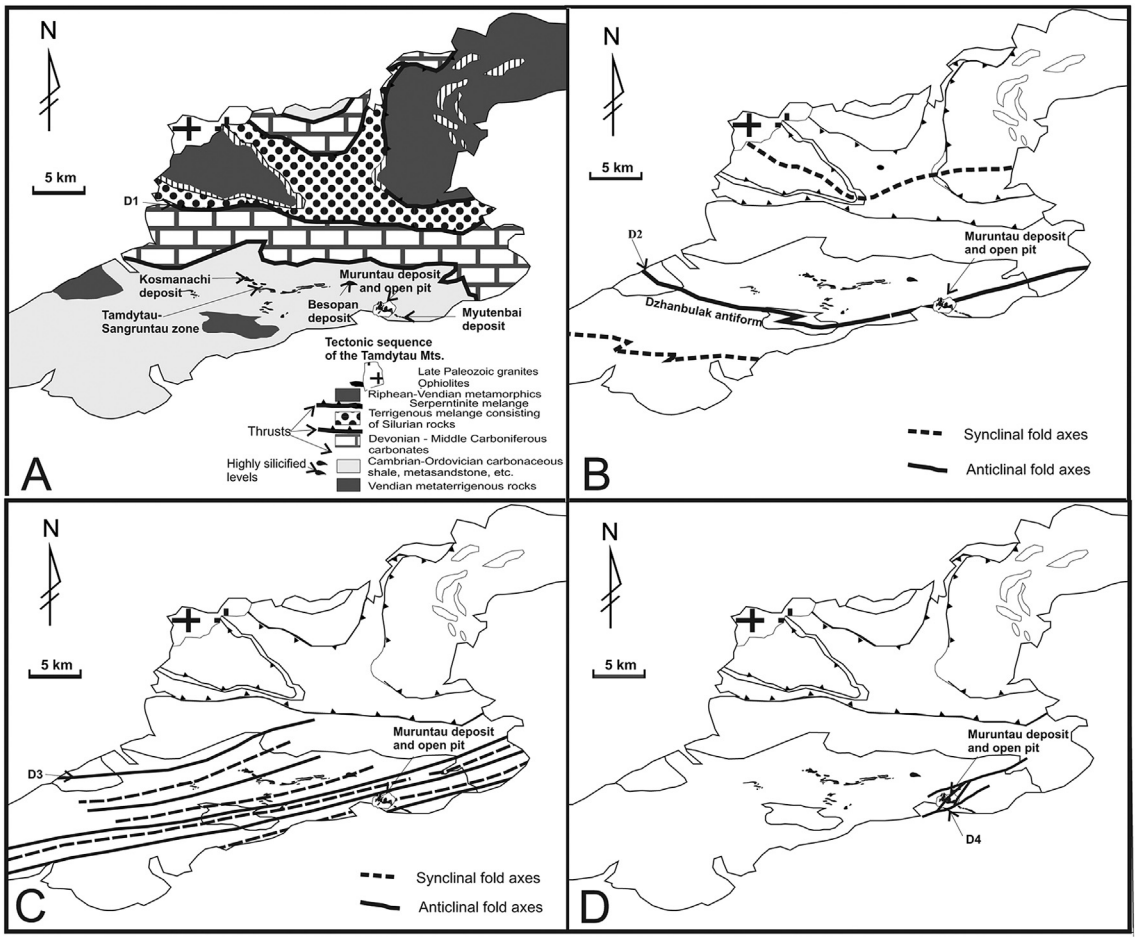

Figure 5. Structural scheme of the Tamdy mountains (from Yakubchuk et al., 2002; compiled using Drew et al., 1996). The structure consists of a series of D1 imbricated thrusts (A) with Paleozoic rocks constituting the nappes occurring between the Precambrian rocks both in the base and in the uppermost allochthons. The latter is accompanied by serpentinite melange. This structure was deformed into WE-trending folds during the D2 event (B) and into NE-trending folds during the D3 events (C). Note that the Muruntau deposit occurs in the hinge of the Dzhanbulak antiform, an apparently best place for entrapment of fluids. These late Paleozoic multiple episodes are responsible for tighter spacing of D3 folds at the closure of the Dzhanbulak antiform, location of fluids, and possibly granitoid intrusions. This structure was strike-slip faulted during D4 tectonic event (D), which supposedly took place in the Mesozoic (Yakubchuk et al., 2002).

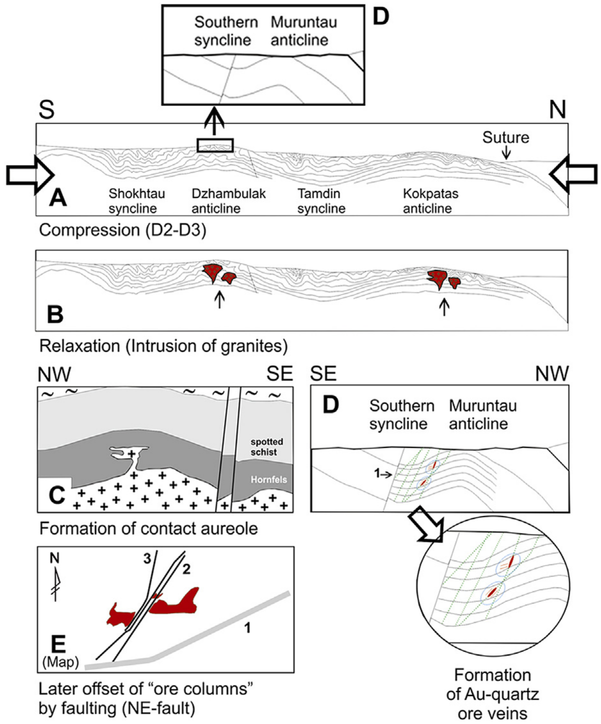

Figure 6. Model for the formation of the ore-bearing structures at Muruntau in relation to the structural evolution of the area and the major alteration phases present (Seltmann et al., 2003). Map E: 1 – Southern fault zone; 2 – Northeastern fault zone; 3 – Meridionalnyi fault.

4. Geological setting

The area around Muruntau is formed by a more or less flat landscape with only a few moderate elevations. The most important elevations are the Tamdytau (Tamdy-Mountains) about 30 km to the northwest of the deposit and the Aristantau (Aristan-Mountains) about 50 km to the south. Most of the area is covered by platform sediments (gravel, sand and clay) of Mesozoic to Cenozoic ages. Topographic elevations and their surroundings form large tectonic windows within the sedimentary cover with outcrops of Caledonian to Hercynian fold and thrust rocks (Kraft and Kampe, 1995). Two main groups of the latter may be distinguished in the surroundings of Muruntau. The underlying group is composed of a sequence of rocks metamorphosed in amphibolite-to green schist-facies intruded by Hercynian magmatites and hosting the gold mineralization (Fig. 7). The overall thickness of the sequences, and also of their units, are disputed because there is intense folding, a lens-like appearance of some units and additional complication of the profile due to thrust and fault tectonics (Mukhin et al., 1988; Kremenetsky et al., 1990; see section 4.1). Gar'kovets (1969) and Bel'kova and Ognev (1971) quoted an overall thickness of about 2000 m while other authors suggested thicknesses of up to 4000 m (Loshchinin et al., 1986) or even more (Mukhin et al., 1988; Kremenetsky et al., 1990; Drew et al., 1996). To the north and east of the Muruntau deposit, this lower group is unconformably overlain by dolomite and limestone with an overall thickness of about 3000 m (Marakushev and Khokhlov, 1992; Fig. 7). Because the latter rocks show no strong tectonic deformation and are apparently not cut by intrusions, dikes or mineralized veins (although some quartz veins were reported by Kotov and Poritskaya, 1991), some workers assumed that this sequence may have acted as a low permeability "cap" sealing the underlying metamorphic rocks during Hercynian magmatism and extensive hydrothermal activity (Mukhin et al., 1988; Konstantinov et al., 2000; Wall et al., 2004; Ezhkov and Rakhimov, 2012).

Outcrops of magmatic intrusions or dikes are scarce in and around the Muruntau deposit. The area was even referred to as "intrusion-free" in earlier works (Gar'kovets, 1975). There are three swarms of dikes outcropping in the Muruntau open pit and in adjacent areas. One swarm occurs to the south and one to the north of the deposit, respectively. These swarms strike nearly east-west and are composed of alkaline rocks including diabase, lamprophyre, spessartite, kersantite and granite (Bendik, 1969; Yudalevich and Levchenko, 1981; Kotov and Poritskaya, 1990; Drew et al., 1996; Golovanov et al., 1998a). A third northeast-striking swarm cross-cuts the deposit area and is exposed within the Muruntau open pit. Here, dikes are classified as granodioritic to granitic in composition (Zarembo, 1968; Bendik, 1969; Yudalevich and Levchenko, 1981; Kotov and Poritskaya, 1990; Kostitsyn, 1996; Golovanov et al., 1998a) although strongly affected by hydrothermal alteration. Nevertheless, classification as granitoids is in accordance with whole rock composition, immobile trace element contents and zircon morphologies (Kempe et al., 2015). The nearest outcrop of a magmatic intrusion is the Tamdytau granite and is located about 30 km northwest of Muruntau. However, three concealed granite intrusions were found adjacent to Muruntau by drilling: (1) the so-called Murun granite was recovered by the super-deep drill hole SG 10 about 1 km southeast of Muruntau near the Myutenbai deposit (depth interval below 4005 m down to the hole bottom at 4294 m), (2) the Sardarin pluton located 15 km southeast and (3) the Kurukkuduk granite 25 km south-southeast of Muruntau were both found by exploration drilling (cf. Kempe et al., 2015).

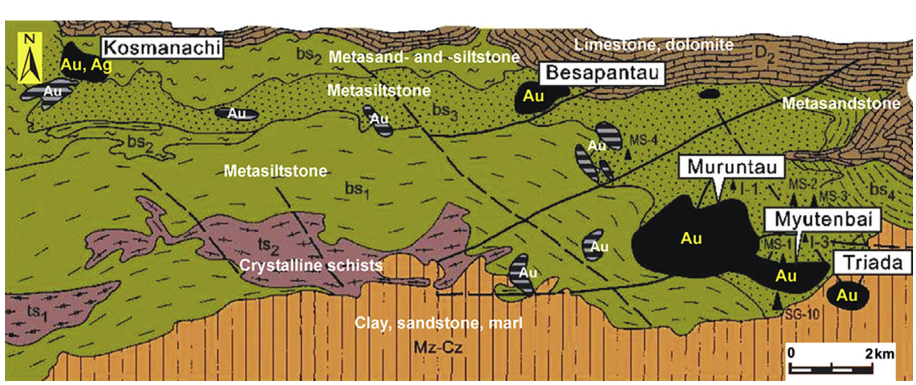

Figure 7. Geological sketch of the Muruntau region showing the main stratigraphic units and Au deposits (Au in yellow) and occurrences (Au in white): ts_1, ts_2 – Lower and Upper Taskazgan; bs_1 – Grey Besapan; bs_2 – Black Besapan; bs_3 – Variegated Besapan, ore-hosting; bs_4 – Green Besapan; Mz-Kz – Meso-to Cenozoic platform cover. Locations of deep boreholes (I-1, I-3), super-deep borehole SG 10 and deep satellite boreholes MS 1 to 4 are also indicated. Redrawn after Krementsky, written communication (1997).

4.1. Metamorphic and sedimentary rocks

4.1.1. Pre-Devonian rocks

The composition and petrography of pre-Devonian meta-sedimentary rocks is monotonous (Bendik, 1969; Bel'kova and Ognev, 1971; Loshchinin et al., 1986) and fossils are rare (Akhmedzhanov et al., 1979; Mukhin et al., 1988; Kremenetsky et al., 1990) or generally not suitable for correct age determination (Bukharin et al., 1984); significant visible unconformities within the sequences are absent (Gar'kovets, 1969). The metamorphic grade decreases continuously (Gar'kovets, 1969, 1971; Loshchinin et al., 1986; Kremenetsky et al., 1990; Marakushev and Khokhlov, 1992; Khokhlov et al., 1998) from the bottom (Taskazgan Sequence; lower amphibolites facies) to the top formed by the lower green schist-facies metamorphosed Besapan Sequence. The rocks under consideration are modified by contact metamorphism (see section 4.2.3 below) and metasomatic alteration in and around the Muruntau deposit (Sher, 1970; Kotov and Poritskaya, 1991; Marakushev and Khokhlov, 1992; Kol'tsov and Rusinova, 1997; Khokhlov et al., 1998; Wall et al., 2004). As a result, the stratigraphy is obscured.

Widely accepted by the scientific community is the subdivision of the basement rocks exposed in the area into two sequences: the Taskazgan Sequence (Ts; amphibolite facies; up to 900–1000 m thick; Gar'kovets, 1969; Mukhin et al., 1988; up to 2300 m thickness; Bukharin et al., 1984) forming the lower part and the Besapan Sequence (Bs; green schist facies; 1200 m thickness; Gar'kovets, 1969, more than 3000 m up to 5000 m; Bukharin et al., 1984; Mukhin et al., 1988) forming the upper part (Fig. 7). The Taskazgan Sequence commonly includes the former Auminzin Sequence (Bukharin et al., 1984; Kremenetsky et al., 1990).

The Besapan Sequence is further subdivided into four suites (Bukharin et al., 1984; Mukhin et al., 1988; Kremenetsky et al., 1990; Kostitsyn, 1991b; Berger et al., 1994; Drew et al., 1996; Kostitsyn, 1996; Khokhlov et al., 1998; Kempe et al., 2001a): bs_1 (Grey Besapan; mainly schists after siltstone), bs_2 (Black Besapan; mainly meta-sandstone or carbonaceous meta-sandstone with grit and gravel and abundant dark biotite), bs_3 (Variegated Besapan; intercalations of phyllitic meta-siltstone, meta-sandstone and meta-tuff, some meta-carbonate) and bs_4 (Green Besapan; mainly meta-sandstone with meta-siltstone, some meta-carbonate). The names of the suites relate to the rock colors in the outcrops after weathering. The Black Besapan and the Grey Besapan are considered to form a single rock package by some authors (Loshchinin et al., 1986; Kremenetsky et al., 1990; Marakushev and Khokhlov, 1992).

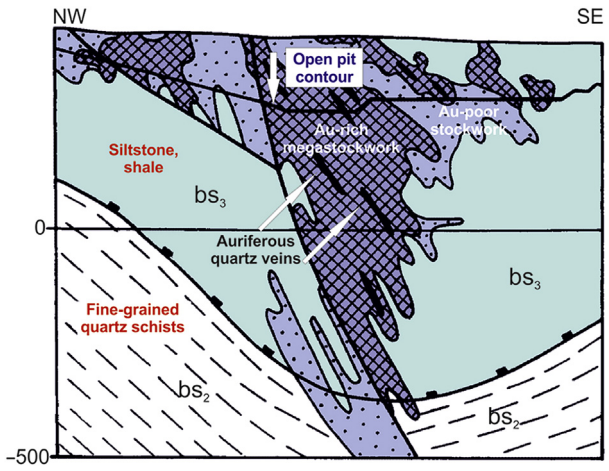

Figure 8. Schematic cross-section through the central part of the Muruntau deposit illustrating the formation of ore columns by veins, stockworks and metasomatites. bs_2 – Black Besapan; bs_3 – Variegated Besapan. After Obraztsov (1998).

The assignment of the Variegated Besapan bs_3 to a normal sedimentary rock package within the Besapan Sequence is controversial (Akhmedzhanov et al., 1979; Loshchinin et al., 1986; Kremenetsky et al., 1990; Bojtsov et al., 1996; Shayakubov, 1998). According to Loshchinin et al. (1986), the contact between the Variegated bs_3 and Green Besapan Bs_4 Suits represents a tectonic discordance. Similarly, Wilde et al. (2001) recognized the contact between the Variegated bs_3 and Green Besapan bs_4 as a tectonic one, which is interpreted to trace the regional, flat dipping Sangruntau-Tamdytau shear zone. This zone is of apparent Carboniferous age (Drew et al., 1996) and related to the regional continent-continent collision and formation of thrust sheets (see section 3). According to Khokhlov et al. (1998), the lower contact of the Variegated Besapan also represents a mylonite zone (Fig. 8). Mukhin et al. (1988) have shown that the Besapan Sequence may be understood as a stack of nappes and the Variegated Besapan Suite bs_3 itself as a tectonic lens or mélange formed along with other lenses and wide zones of blastomylonites in the adjacent Besapan units, in particular, in the area of the Muruntau deposit. Accordingly, the Variegated Besapan bs_3 is referred to as the Kosmanachi (former Muruntau) Suite in recent publications and the underlying Grey bs_1 and Black Besapan bs_2 as the Rokhat Suite (Shayakubov, 1998; Mirkamalov et al., 2012a; Rafailovich et al., 2013). Drew et al. (1996) reported a local inversion within the thrust sheets in the Tamdytau area to the north of Muruntau, where rocks of the Taskazgan Sequence overly the green schist rocks within a mélange including lenses of ophiolite and chert.

The Taskazgan Sequence (Fig. 7) comprises garnet-bearing schists with some intercalations of mafic meta-volcanics, quartzite and meta-carbonate rocks (skarnoids; Kremenetsky et al., 1990; Kol'tsov and Kostitsyn, 1995). The Besapan Sequence including the Kosmanachi Suite consists of meta-sediments typical of a passive shelf with interbeddings of meta-siltstones, meta-sandstones, gritstone, chert and minor meta-carbonates (Gar'kovets, 1973; Bukharin et al., 1984; Marakushev and Khokhlov, 1992; Wall et al., 2004) as quoted above in this paragraph. The whole-rock composition of the pre-Devonian rocks was examined by Kremenetsky et al. (1990) and Marakushev and Khokhlov (1992).

4.1.1.1. Carbonaceous matter. In Russian literature, the metamorphic rocks hosting the Muruntau deposit (Besapan and/or Kosmanachi Suites) are often referred to as black shales (e.g. Bel'kova and Ognev, 1971; Gar'kovets, 1978; Loshchinin et al., 1986; Kotov and Poritskaya, 1990, 1991; Kremenetsky et al., 1990; Kostitsyn, 1991b; Protsenko and Rubanov, 1991; Rusinova et al., 1996) implying a significant role of organic and/or carbonaceous matter in the processes of concentration and remobilization of gold. One popular genetic concept suggests primary gold enrichment in sedimentary rocks by sorption on organic matter resulting in the formation of gold-rich black shales (Gar'kovets, 1978; Loshchinin et al., 1986; Zairi et al., 1998; see discussions below in sections 7.2 and 8.1). The classification of the rocks under consideration as black shales is mainly based on the results of optical microscopy indicating a dispersed occurrence of organic matter especially in the Variegated Besapan (Kosmanachi Suite) and the upper Green Besapan (Khokhlov et al., 1998). However, the content of organic carbon in these rocks is mainly within the first hundreds of ppm and rarely exceeds one thousand ppm (Uspenskiy and Aleshin, 1993; Bojtsov et al., 1996; Rusinova et al., 1996; Khokhlov et al., 1998; Seltmann et al., 2003). The content of organic carbon is even higher in the Taskazgan sequence (Kol'tsov and Kostitsyn, 1995; Bojtsov et al., 1996). However, Kremenetsky (1994) quoted concentrations of 1–3 wt.% C_{org} for the Besapan sequence at Muruntau similar to Gar'kovets (1975). The high carbon values may be explained by secondary redistribution in the Muruntau deposit

with significant carbon depletion within the hydrothermal alteration halo and a related local enrichment in other parts of the sequence and in faults and brecciation zones (cf. Loshchinin et al., 1986; Rusinova et al., 1996; Kol'tsov and Rusinova, 1997; Khokhlov et al., 1998). In conclusion, the classification of the host rocks as black shales (Tourtelot, 1979) is questionable. Rusinova et al. (1996) studied the distribution and redistribution of carbonaceous matter (which, in fact, comprises high-to low-ordered graphite) as well as the degree of ordering of the graphite in greater detail. According to these authors, carbon commonly occurs highly dispersed and represents well-ordered graphite in unaltered metamorphic rocks. Modifications resulting from later, hydrothermal redistribution will be considered below in section 6.1.

4.1.1.2. The "Muruntau lens". The metamorphic rocks hosting the giant Muruntau gold deposit and exhibiting some peculiarities adjacent to ore mineralization, are often referred to as the "Muruntau lens" ("Muruntau Sequence" in earlier work; Mukhin et al., 1988) according to their lens-shaped appearance (Fig. 7). However, the exact meaning of this term varies between authors and may be related to (1) the tectonic nature of the Z-like-shaped fold hosting the Muruntau deposit (Mukhin et al., 1988; Kremenetsky et al., 1990), (2) the character of the assumed tectonic mélange (Mukhin et al., 1988; Bojtsov et al., 1996; Kempe et al., 2001a; Rafailovich et al., 2013), (3) the rock package modified by metasomatic alteration (mainly silicification; Berger et al., 1994; Drew et al., 1996; see also Wilde et al., 2001) and (4) the lens-shaped morphology of the stratiform, low-grade gold ore body (Savchuk et al., 1987). Earlier, Voronkov (1976) speculated that the sediments forming this lens-shaped body may have originally derived from an ancient river delta.

4.1.1.3. Sedimentation ages of meta-sedimentary rocks. There is no consensus among various authors on the stratigraphic ages of the rocks under discussion. At the end of the 1970s, a special conference decided to assign a late Proterozoic age to the Taskazgan Sequence (Tz) based on fossils found in some meta-carbonate rocks (supported by later fossil findings; Mukhin et al., 1988), leaving open the poorly constrained age of the Besapan Sequence Bs (Ordovician-Silurian) and, in particular, of the Variegated Besapan Suite bs_3 (with apparent ages ranging from Silurian to Carboniferous; Akhmedzhanov et al., 1979). Loshchinin et al. (1986) assumed a Vendian to Cambrian age for the Grey and Black Besapan ($bs_1 + bs_2$) and a Paleozoic (Ordovician O to Silurian S) age for the upper two suits only (Variegated and Green Besapan $bs_3 + bs_4$). According to Mukhin et al. (1988), the Grey and Variegated Besapan Suites are older (middle Cambrian $Є_2$–middle Ordovician O_2) than the Black and Green Besapan Suites (middle Ordovician O_2–lower Silurian S_1). Bukharin et al. (1984) inferred Ordovician (O_1–O_2) ages for the Gray and Black Besapan (Rokhat Suite) adopted by recent authors (Rafailovich et al., 2013). Because of the principal significance of the Variegated Besapan Suite bs_3 as the host rock of the gold mineralization at Muruntau, Bukharin et al. (1984) have studied fossils in this and adjacent units in greater detail and revised some older fossil and age definitions. According to their data, the age of the Taskazgan Sequence extends from Cambrian (Є) into the Ordovician (O) in the upper part. The mixture of Proterozoic (PR) to Silurian (S) ages found in the Besapan Sequence and, in particular, in the Variegated Besapan Suite, may be explained by the isolated development of the related sedimentary basin according to these authors. Bukharin et al. (1984) assumed an upper Ordovician (O_3) to lower Silurian (S_1) age for the upper two Besapan Suites in agreement with Loshchinin et al. (1986).

Mirkamalov et al. (2012a,b) carried out SHRIMP U-Pb dating on zircon from one sample of the Variegated Besapan Suite Bs_4 (Kosmanachi Suite). They defined three age groups of 2332–3729 Ma (upper Archean to lower Proterozoic), 631–1025 Ma (upper Proterozoic) and 526–559 Ma (upper Proterozoic to lower Cambrian $Є_1$) placing a Cambrian (Є) upper age limit on these rocks, much older than the generally assumed Ordovician (O) to Silurian (S) ages. Summarizing, the ambiguity in the stratigraphic position of the rocks under consideration is most probably related to their mixed nature as a tectonic mélange and the difficulty in the identification of microfossils suitable for a more exact biostratigraphy.

4.1.2. Devonian to Carboniferous carbonate rocks

Devonian (D) to Carboniferous (C) rocks are weakly deformed – only some subhorizontal faults are present – and consist of bituminous dolomite and marble of the Zhivachisaj Sequence (Bel'kova and Ognev, 1971; Rusinova et al., 1996). The age of the sediments is well constraint by fossils (middle Devonian to upper Carboniferous, D_2–C_3, Kostitsyn, 1996; Rusinova et al., 1996; or lower Devonian to middle Carboniferous, D_1–C_2, Mukhin et al., 1988; Kremenetsky et al., 1990; Carboniferous classified according to Soviet stratigraphy). Wilde et al. (2001) discussed the presence of buried rift margins within this unit. According to Kotov and Poritskaya (1991), the limestone experienced contact metamorphism during the intrusion of the Sardarin pluton. The nature of these carbonate rocks was studied in more detail by Abramovich (1969). This author concluded on a biochemical precipitation of the carbonates based on measured trace element distribution and the low contents of terrigenous material. According to Drew et al. (1996), the deposition of this carbonate sequence marked the beginning of continent-continent collision between the Central Kazakhstan-North Tien Shan continent and the Karakum massif within the middle Carboniferous (C_2).

4.1.3. Basal conglomerates or tectonic breccia?

Rock fragments of a diversity of rocks including fragments containing gold-bearing quartz veins or granitic material embedded in a carbonate matrix occur in the footwall of the Devonian to Carboniferous dolomites and limestones. Some workers interpreted these apparent basal conglomerates as proof of a pre-Devonian age of gold mineralization (upper age limit D_1; Askarov and Bigaeva, 1965; Bendik et al., 1969a; Gar'kovets, 1969, 1971, 1973; Gar'kovets et al., 1970; Rakhmatullaev, 1980). However, later investigation revealed the tectonic nature of this breccia related to thrusting of the carbonate rocks onto the older metamorphic sequences (Kotov and Poritskaya, 1991; Drew et al., 1996; Wilde et al., 2001). According to Golovanov et al. (1998b), quartz pebbles from the "conglomerate" exhibit properties of quartz from ductile deformed, so-called "flat" veins as described below in section 5.2.

4.1.4. Platform cover

Meso-to Cenozoic cover sequences which are represented by surficial gravels, sands and clay, may also contain sandstone, mudstone and siltstone at greater depth (e.g., Graupner et al., 2000). Not much work has been done on these late sedimentary rocks although their study may be of importance in the search for hidden deposits below the platform cover (Kremenetsky et al., 1990; Fig. 7).

4.2. Magmatic rocks

4.2.1. Dikes

Surprisingly, there is only few data on the magmatic rocks in the Muruntau area and in particular, on the dikes. On the other hand, the swarm of dikes crossing the Muruntau open pit is of special

interest because (1) it is assumed to have formed more or less contemporaneously with the sequence of gold-bearing quartz veins and (2) it is interpreted to separate at least two main stages of gold ore formation (Zarembo, 1968; Bendik, 1969; Rakhmatullaev, 1980; Yudalevich and Levchenko, 1981; Kostitsyn, 1991b; Kotov and Poritskaya, 1991; Uspenskiy and Aleshin, 1993; Drew et al., 1996; Golovanov et al., 1998b; Konstantinov et al., 2000). Kremenetsky et al. (1990) recorded the additional occurrence of dikes in cores from deep drilling operations close to the deposit. All dikes show evidence of hydrothermal alteration and are cross-cut by sulfide-rich veinlets and by late veins (Bendik, 1969; see section 5.3 below). Kostitsyn (1996) mentioned that the compositional variability of the dike rocks in the open pit is at least partly a result of their heterogeneous metasomatic alteration. According to our data (Kempe et al., 2015), the dikes are affected by late alteration with formation of sericite, chlorite and sulfides, but no clear remnants of early biotitization or microclinization could be found. This may support the inference of an "intra-ore" formation of those dike rocks in accordance with field observations by Bendik (1969) and Yudalevich and Levchenko (1981); alternatively, late alteration developed in and adjacent to the dike zone may have completely erased all characteristics of early metasomatism because the dikes form a zone bordered by intense albitization of the wall rocks. Golovanov et al. (1998a) reported similar alteration features with albitization, sericitization and chloritization and secondary sulfides for the dikes. According to the latter authors, alteration assemblages resembling K-metasomatic alteration may be sometimes detected in the rocks. Yudalevich and Levchenko (1981) have studied the relationships between dikes and gold mineralization in Western Uzbekistan including the Tamdytau area and the Muruntau deposit in greater detail. According to their data, the dikes of alkaline type (from spessartite to alkaline granite) are widely exposed. They experienced alteration (albitization) contemporaneous with the formation of gold-bearing quartz veins in other places. For Muruntau, however, Yudalevich and Levchenko (1981) concluded a post-ore age of lamprophyre and diabase. Similarly, Vikhter et al. (1986) reported gold mineralization to post-date granitic dikes but to preceed diabase dike formation. In contrast, relative age relations between alkaline dikes and gold mineralization, with the latter superimposed on the alkaline dikes as commonly found in other areas of the Kyzylkum, were established by Kotov and Poritskaya (1990) based on detailed work on gold showings to the west of the Muruntau deposit. Golovanov et al. (1998a) mentioned alteration of mafic dike rocks by biotitization, chloritization and sericitization.

Gusev and Gusev (2012) published whole rock and petrographic data on dikes of various types. According to these authors, all of those rocks belong to the K-rich magmatic series. Golovanov et al. (1998a), reviewing the analytical data by Yudalevich, stressed the bimodal character of the dike magmatism. However, these authors assigned all dikes to a single series according to their tectonic position. Relative age relations between dikes of different composition were not yet established.

4.2.2. Granite intrusions

The granodioritic to granitic dikes may be genetically related to the large intrusions of similar composition developed in the region (Kotov and Poritskaya, 1991; Kempe et al., 2015). The late Paleozoic magmatism produced large intrusions in the Kyzylkum area ranging in composition from diorite to leucogranite (Yudalevich et al., 1991; Golovanov et al., 1998a; Shayakubov and Dalimov, 1998). The intrusions are late-to post-collisional in tectonic setting (Kempe et al., 2015). Some of them show seriate textures, others are seriate-porphyritic. The rocks display geochemical and petrological characteristics of I-type intrusions (Gusev and Gusev, 2012; Kempe et al., 2015). All samples investigated (including those of granitoid dikes) contain ilmenite, but no magnetite (Gusev and Gusev, 2012; Kempe et al., 2015). The intrusions (as well as the dikes) belong to "shoshonitic", K-rich magmatic series (Golovanov et al., 1998a; Gusev and Gusev, 2012; Kempe et al., 2015). The Th and U contents are high and variable (3.5–68 ppm U and 11–57 ppm Th) with variable Th/U ratios (0.35–6.3) probably because of the mobility of uranium during metasomatic alteration (Kempe et al., 2015; see section 5.6 below). A comprehensive study of the granitoid magmatism in the Muruntau area is still lacking.

4.2.3. Contact metamorphism

Alteration of metamorphic rocks by contact metamorphism caused by the intrusion of the granitoids was studied by several authors (Palej and Sher, 1970; Sher, 1970; Loshchinin et al., 1986; Kotov and Poritskaya, 1991; Uspenskiy and Aleshin, 1993; Drew et al., 1996; Kol'tsov and Rusinova, 1997; Khokhlov et al., 1998; Wall et al., 2004; Bierlein and Wilde, 2010). The thermal aureole is traced by hornfels in the innermost zone and spotted or knotty schists in the outer one. Characteristic mineral assemblages contain biotite, cordierite and andalusite (Loshchinin et al., 1986; Kotov and Poritskaya, 1991; Drew et al., 1996; Kol'tsov and Rusinova, 1997). Kotov and Poritskaya (1991) mapped the contact metamorphic halo in the area of the Muruntau deposit using outcrops and around the Sardarin pluton using drilling data. Above the Sardarin pluton, hornfels occurs while a zone of spotty and knotty schists may be traced to the northwest extending into the Muruntau open pit (cf. Drew et al., 1996). According to Sher (1970), the hornfels zone below the Muruntau deposit is located about 700 m below the recent surface as established by drilling data. It is therefore possible that the Sardarin intrusion or another intrusion extends below the deposit and is in some way related to the Murun granite intersected in the super deep drill hole. The existence of a hypothetic intrusion or extension from the Sardarin and/or Murun pluton below the Muruntau deposit is also supported by the occurrence of the dikes exposed within the open pit because such dikes normally extend from the related intrusion to not more than several hundreds of meters. Similar conclusions were drawn by Golovanov et al. (1998a) based on geophysical data. Kol'tsov and Rusinova (1997) estimated the horizontal extent of the hornfels aureole around the known contour of the Sardarin pluton below the sedimentary cover to 1–3 km. Above the Murun granite, the hornfels zone extends to about 500 m. The apparent difference is probably related to variations in the inclination of the granite contact. The formation of the aureole of contact metamorphic rocks is of great importance for preferred subsequent veining as stressed by several authors (Petrovskaya, 1968; Kremenetsky et al., 1990; Wall et al., 2004; see also Drew et al., 1996). The brittle behavior of these compact rocks during deformation in an area where two prominent fault and shear zones intersect, has promoted the formation of the large stockworks inside the Muruntau deposit.

5. Ore veins and ore bodies

5.1. Types of ore bodies

The Muruntau deposit may be seen as a giant stockwork hosted by rocks of the Variegated Besapan (bs_3; Golovanov et al., 1998c, Fig. 8). Mineralization is most intense in psammopelite- and psammite-dominated, thin-to-medium bedded lithological packages characterized by strong biotite-feldspar-quartz alteration. Ore-stage veining, mineralization and metasomatism are focused at several levels within the hornfelsed bs_3 package (Wall et al., 2004). Berger et al. (1994) and Drew et al. (1996) assumed a

formation of the Muruntau ore-bearing system in the brittle/ductile transition zone of the crust within transpressional shear zones. In contrast, Wall et al. (2004) described the Muruntau system not to represent a shear zone-hosted or -related system. Instead, these authors characterize the tectonic setting of Muruntau as localized in a fold–fault system akin to those hosting other giant gold deposits worldwide.

The concepts on the dimension, shape and structural control of the ore bodies changed considerably during the history of exploration, mining and scientific investigation of the deposit (Golovanov et al., 1998c; Obraztsov, 2009). While, in an earlier time, extensive zones of sulfide-bearing quartz veins and zones of albitization were regarded as the principal ore bodies, stratiform-like structures became more important when the high gold contents within the host rocks adjacent to the veins were explored. Later on, detailed analysis of the gold distribution revealed the role of metasomatic alteration and of cross-cutting stockwork structures.

The assumed morphology of the ore bodies strongly depends on the cut-off grade (Golovanov et al., 1998c). Obraztsov and co-workers developed the "ore columns concept" to describe the distribution and characteristics of the closely spaced ore bodies in the stockwork based on a cut-off of 2 ppm Au (Obraztsov and Belenko, 1997; Obraztsov, 1998; Obraztsov, 2009). The nearly vertical columnar structures host >70% of the total gold reserves, but occupy less than 30% of the total stockwork volume (Shayakubov et al., 1999; Obraztsov, 2009). The "ore columns" within the Muruntau system were crosscut and offset by ENE to NE trending small and large displacement (300–500 m), sinistral-reverse faults (Wall et al., 2004; cf. Kempe et al., 2001a).

Continued study on the ore bodies revealed that there are several structures controlling the localization of the ore bodies (Fig. 9) as summarized by Golovanov et al. (1998c). One type of structural control is related to the bedding and schistosity of the host rocks including the development of parallel "metamorphic" quartz veins which are complicated by intense folding and boudinage (Fig. 9a). Other controlling structures are located sub-parallel to the first but relate to later flat-dipping zones of thrust, shear and mylonitization. A third type of structure is controlled by brittle deformation behavior of the rocks after regional and thermal metamorphism with both sub-parallel and cross-cutting vein structures and alteration zones (Fig. 9b–d). In the case where gold mineralization was mainly controlled by "flat" veins or ore-bearing metasomatites, the ore bodies are stratiform-like. Around the "Central" veins with cross-cutting stockwork veinlets (Fig. 9d), the ore bodies are cone-like and steeply dipping (Golovanov et al., 1998c; Obraztsov, 2009).

Gold-bearing structures may be subdivided into two basic types: (1) large quartz veins on the one hand, and (2) vein and veinlet-"impregnated" lithological packages of metasomatosed meta-sedimentary rocks on the other. According to Golovanov et al. (1998c), the ore stockworks present in the four ore bodies of the Muruntau deposit are combined types of ore structures controlled by a number of structural elements and formed at different stages.

5.2. Vein types: mineralogy and evolution

The ores and veins in the Muruntau deposit are generally low-sulfide. Three major types of gold-bearing quartz-dominated veins can be recognised, which reflect the general observations and classifications as reported by various authors, but, otherwise, differ in important details (e.g. Zarembo, 1968; Rakhmatullaev, 1980; Uspenskiy and Aleshin, 1993; Drew et al., 1996; Golovanov et al., 1998c): (1) veins that experienced ductile deformation during shearing and folding (concordant and sub-concordant "flat veins" and parts of the "banded veins" in the stockworks; Fig. 9a); these

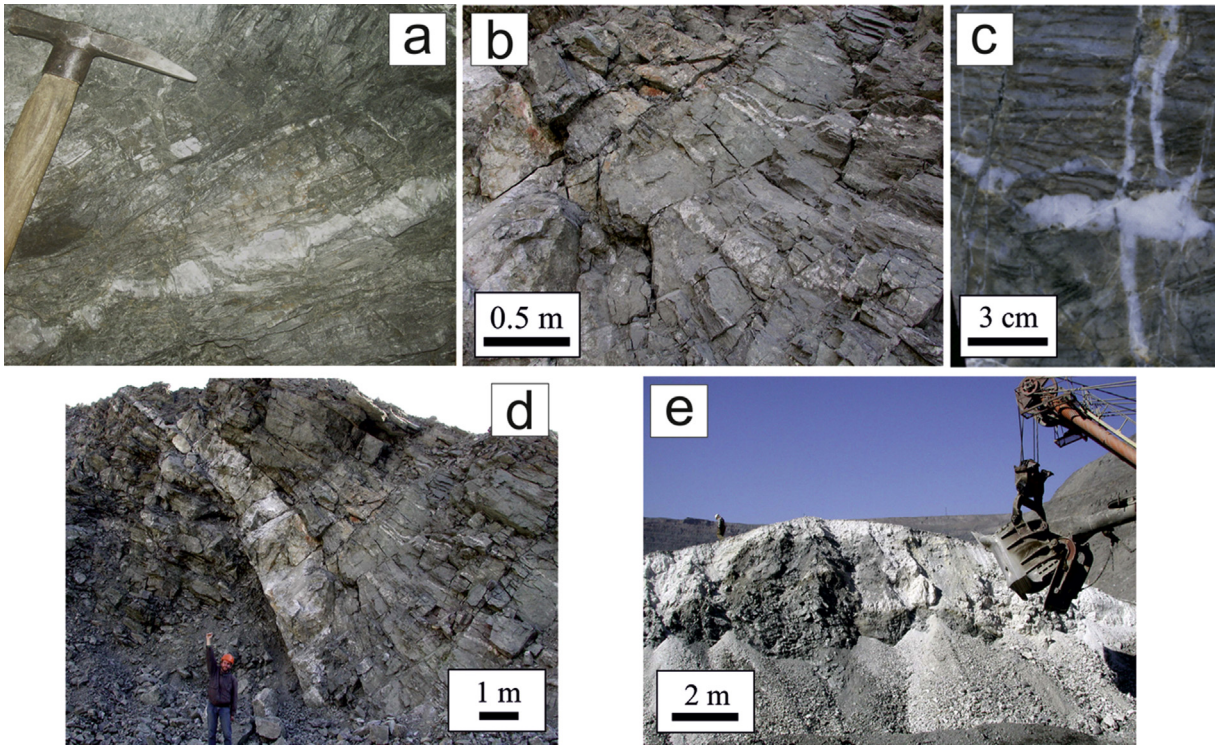

Figure 9. Major vein types of the Muruntau deposit: (a) flat, boudinaged, low grade gold-mineralized quartz vein, Muruntau Shaft M, 0 m level; (b) shallow dipping auriferous stockwork veinlets, Muruntau pit, +120 m level; (c) quartz stockwork veinlets, Muruntau pit, +140 m level; (d) steeply dipping Central quartz vein surrounded by flat dipping stockwork, Muruntau pit, +120 m level; (e) shallow dipping Central quartz vein, Muruntau pit, +120 m level (Fig. 9b,d,e are from joint field work with V.J. Wall in 2003; in Wall, 2004).

are cross-cut by later veins and dikes; (2) veins and veinlets of stockworks with characteristic pyrite-arsenopyrite association present in variable quantitative proportions (typical short veinlets of variable strike and dip with both shallow and sub-vertical dip (Fig. 9b–d); reactivated segments of "banded veins"; longer extending steeply dipping veins bearing arsenopyrite and/or pyrite and, finally, "Mother Lode"-type, so-called "Central" veins; Fig. 9d, e); (3) locally occurring late veins of various compositions with low gold contents and enrichment in silver, tourmaline, calcite, adularia etc. All three groups of veins are described in more detail below in this section.

According to Bierlein and Wilde (2010), the low iron content in sphalerite, the arsenic concentrations in arsenopyrite and the presence of Ni-Fe-S phases in the ore veins point to relatively high formation temperatures between 350 and 450 °C, which is in accordance with fluid inclusion data and alteration assemblages in adjacent metasomatites (see sections 5.4 and 6.1 below). Bierlein and Wilde (2010) have suggested a generalized paragenetic sequence of mineral precipitation in the veins of the deposit based on textural relationships observed in thin sections, which is shown in Fig. 10. Note, however, that it is difficult to establish correct general paragenetic sequences because of the general low contents of sulfides, their uneven distribution in the veins and the occurrence of minerals present in several or all vein types. It is, therefore, difficult to establish "key" minerals, which allow a clear definition of a particular vein type.

(1) The earliest, ductile deformed "flat" quartz I veins (Fig. 9a) occur parallel to sub-parallel to the foliation of the host rocks and are cut by all other vein types (Zarembo, 1968; Rakhmatullaev, 1980; Mukhin et al., 1988; Kremenetsky et al., 1990; Kotov and Poritskaya, 1991; Uspenskiy and Aleshin, 1993; Khokhlov et al., 1998; Golovanov et al., 1998c; Shayakubov et al., 1999; Graupner et al., 2000). Flat veins comprise about 3–5% of the rock volume

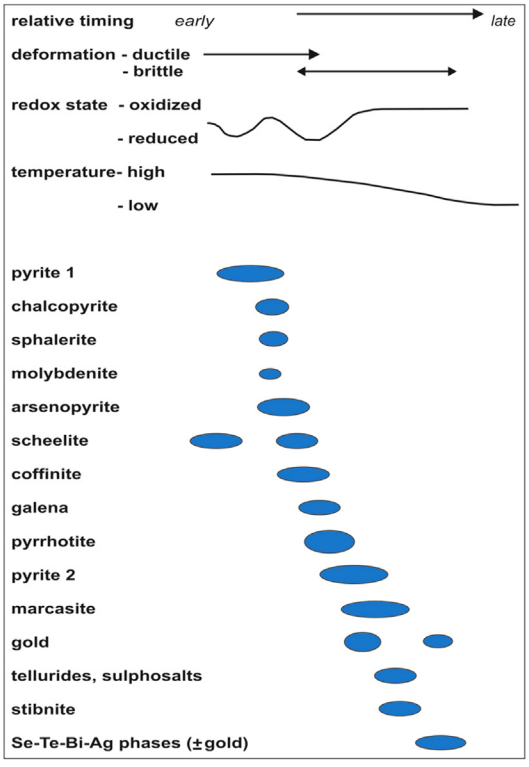

Figure 10. Generalized sketch of paragenetic sequences inferred from textural relationships in thin sections (from Bierlein and Wilde, 2010).

(Kotov and Poritskaya, 1991; Kol'tsov and Rusinova, 1997; Khokhlov et al., 1998), but may reach locally 30% as a result of reactivation of older structures within the stockworks (Golovanov et al., 1998c; Graupner et al., 2000), especially in psammopelites (Wall et al., 2004). These commonly millimetre-to several centimeter-width veins and lenses show mainly non-brittle deformation features, like intense isoclinal folding and boudinage (e.g. Mukhin et al., 1988; Zairi and Kurbanov, 1992; Uspenskiy and Aleshin, 1993; Khokhlov et al., 1998). Greyish quartz I predominating in these vein structures is always intensely recrystallized and displays typical "metamorphic", brownish luminescence colours (Graupner et al., 2000). Flat veins contain low amounts of sulfides (pyrite, pyrrhotite, chalcopyrite) and, occasionally, low Au concentrations (0.03–0.30 ppm; Khokhlov, 1990; sometimes up to 2.0 ppm). Furthermore, carbonates, microcline, chlorite and a brownish-grey to white scheelite I occur. Uspenskiy and Aleshin (1993) found no indication for a genetic link between this scheelite I and gold as suggested by Protsenko and Rubanov (1991). Scheelite I usually occurs in small, disseminated grains in quartz I and adjacent wall rocks and shows similar ductile deformation features as observed for quartz (Uspenskiy and Aleshin, 1993; Kempe et al., 2001a). All scheelite-bearing quartz vein types (scheelite I and II; see section 5.6 below) probably have been assigned to the early Au-W geochemical association by Koneev (Koneev, 2003; Koneev et al., 2005, 2010) and are represented by the mineral assemblage scheelite-gold-carbonate-chlorite-quartz according to these authors. However, scheelite II formation differs significantly in time and style from scheelite I resulting in another mineral association in the later veins (Kempe et al., 2001a; see sections 5.6 and 7.1.4 below).

The second group of veins (2a–c) comprises the vast majority of the vein quartz in the deposit:

(2a) The high grade gold-bearing stockworks are made up by shallow to steeply S/SE dipping vein networks dominated by coarse grained quartz II (Fig. 9b, c). The veins range in thickness from less than 1 mm to several centimeters; distances between the veins of less than 1 cm are not unusual. The vein networks seem to be almost unaffected by ductile deformation; features resulting from brittle deformation dominate here (Zarembo, 1968; Drew et al., 1996; Graupner et al., 2000). Often, essentially undeformed stockwork veins cross-cut mesoscopic crenulation folds in biotite altered metasediments (e.g. Wall et al., 2004). According to Golovanov et al. (1998b) such veins are arranged parallel to each other or are interlocking and are characterized by rather even contacts, a persistent thickness and considerable extent. Quartz II constitutes up to 90% by volume of the quartz deposited at Muruntau (Zarembo, 1968; Zairi and Kurbanov, 1992). In general, all quartz II is much less influenced by recrystallization processes compared to quartz I although it is strongly altered by brecciation and hydrothermal alteration as evidenced by cathodoluminescence (CL) studies (Graupner et al., 2000; Bierlein and Wilde, 2010). A hydrothermal origin of the quartz II in the stockworks is indicated by its transient blackish blue luminescence colours; primary growth zoning was identified using CL imaging in a few restitic grain fragments only (Graupner et al., 2000, 2005a). The mineralogy of the veins is characterized by the subordinate occurrence of K-feldspar (sometimes sericitized), predominantly low sulfide contents (pyrite, arsenopyrite), native gold, a brownish to orange scheelite II, late Bi-tellurides, apatite and titanite (Bendik et al., 1969a; Kotov and Poritskaya, 1991; Golovanov et al., 1998c; Bierlein and Wilde, 2010). Commonly, quartz II, arsenopyrite, scheelite II and zircon from the stockwork veinlets are brecciated (e.g. Graupner et al., 2000, 2005a; Kempe et al., 2001a). According to some authors, Bi-tellurides, sphalerite and galena, although associated with gold, formed at a later stage after the main

arsenopyrite-pyrite-gold precipitation (Petrovskaya, 1968; Bendik et al., 1969a; Bierlein and Wilde, 2010). Rakhmatullaev (1980) subdivided the stockwork veins into two types – scheelite-bearing and scheelite-free veins. According to this author, formation of both vein types is separated in time by the intrusion of granodioritic dikes. The wall rocks hosting the stockwork veinlets show, in general, biotite stable margins. However, close to the vein margins and also inside the veins, aggregates of carbonate and chlorite were found probably related to cross-cutting carbonate-pyrite-chlorite-sericite-quartz veinlets; the latter late veinlets (belonging to the third group) are common (Seltmann et al., 2003).

(2b) The "Central" veins ("axial" veins, Shayakubov et al., 1999; "Mother Lode"-style veins, Drew et al., 1996) making up the central parts of several stockwork zones (Bendik et al., 1969b; Sher, 1972; Golovanov et al., 1998c), are composed of lenticular, vein-like quartz bodies, which predominantly strike E–W or SE–NW and dip at moderate (30°) to steep angles (70–75°) to the S (Fig. 9d, e). They seem to be related to small displacement, mainly E–W striking dip-slip (probably reverse) faults in an essentially low strain, brittle deformation environment (Wall, 2004; Wall et al., 2004). The four largest quartz bodies have thicknesses of ≤14 m (mostly ≤ 5 m) and strike dimensions of ≤300 m (Golovanov et al., 1998c). The vein structures are rimmed by marginal breccias and microcline-quartz-dominated alteration zones or lenses (e.g. Zarembo, 1968; Graupner et al., 2005a). For a number of smaller veins, a simple, regularly formed subtype and a complex subtype, with segments enriched in angular xenolithes of wall rock fragments and the presence of apophyses, are distinguished (Golovanov et al., 1998c; Graupner et al., 2005a). The above quartz veins exhibit rather massive textures and their margins commonly lack foliation (Wall et al., 2004). Cathodoluminescence and structural data do not indicate zoning or lamination within the massive "Central" veins (Graupner et al., 2005a). These data indicate that they are essentially tensile features and not 'shear' veins (Wall et al., 2004). Kremenetsky et al. (1990) described an occurrence of arsenopyrite-pyrite-rich veinlets ("zones") either arranged along a vein margin or located in the central segment of the "Central" vein or even cross-cutting it. These authors interpret such observations in terms of a more than one-stage hydrothermal process of vein formation. Evidence for intense brecciation was recognized in central segments of the "Central" quartz veins using CL microscopy of quartz (Graupner et al., 2000). Besides massive, transient bluish luminescent hydrothermal quartz II these veins contain ≤2–3% of sulfides. Pyrite, pyrrhotite and arsenopyrite are commonly present in minor amounts, as well as rare nests and later, crosscutting veinlets of calcite, dolomite and chlorite (e.g. Kempe et al., 2001a). Native gold, apatite, scheelite II, allanite, rutile, ilmenite, monazite, zircon and bismuthinite are accessory minerals (cf. also Golovanov et al., 1988a). The gold content in the "Central" veins is rather variable but may locally reach very high values (5.6 to > 100.0 ppm Au) with an average grade of ~13 ppm for bulk samples from the +78 m level (Shayakubov et al., 1999).

(2c) Veins and systems of veinlets with locally increased sulfide contents are commonly related to reactivated fault zones (e.g., the southern Fault zone), with total sulfide contents in veins not exceeding 10%. They are considered as a separate vein type by several authors (Kremenetsky et al., 1990; Shayakubov et al., 1999). These quartz-arsenopyrite veins are generally 10–20 cm thick (very rarely up to 0.5–1 m; Shayakubov et al., 1999); the veinlets trend sub-E–W and the thicker veins trend NE and both are moderately to steeply dipping (40–90°; Golovanov et al., 1998c). The gold contents in arsenopyrite from these veins are locally high, but extremely variable (several tenths to less commonly hundreds of ppm of gold in fine-grained arsenopyrite; Zarembo, 1968). For example, 120–130 ppm of gold was determined in two samples used for Re-Os dating (Morelli et al., 2007). These veins and veinlets may be related to the Au-As(-S) geochemical association of Koneev (2003, 2010; gold-arsenopyrite-pyrite-quartz mineral assemblage). Koneev et al. (2010) emphasized that the Muruntau deposit was referred to as a quartz-pyrite-arsenopyrite-gold type deposit at a time shortly after its discovery.

Together with the adjacent gold-bearing metasomatites, group 2 veins contain about 70–80% of the gold in the deposit (Protsenko et al., 1998). However, these veins and vein systems are differently treated by various authors. Rakhmatullaev (1980) distinguished two types of quartz veins with gold, pyrite, arsenopyrite and K-feldspar not separating "Central" veins as a sub-group. Kremenetsky et al. (1990) separated arsenopyrite-bearing and pyrite-bearing veins, but there are veins with characteristics of both types and an identical mineral association may be found in the "Central" veins as mentioned above in this paragraph. Berger et al. (1994) and Drew et al. (1996) suggested that "Central" veins cross-cut the stockwork veins, however, observations made on outcrop scale suggest a more or less similar formation of both vein structures (e.g. Graupner et al., 2005a). Summarizing, all veins of types (2a) to (2c) may be regarded as gold-bearing quartz veins cross-cutting the bedding of the wall rocks and older "flat" veins and are related to a single, extensional veining stage.

(3) Finally, several types of late, widespread, but only locally occurring veins with low gold contents, are summarized under a group 3. These veins are often silver-rich, but of very limited importance for the gold mining operations at Muruntau. Golovanov et al. (1998b) distinguished: (a) a pyrite-quartz IIIa-albite-tourmaline association in veins (up to 4 m in width), veinlets and zones of brecciation cemented by albite, quartz IIIa, tourmaline, pyrite, chlorite and subordinate arsenopyrite (this vein type was also described by Rakhmatullaev, 1980; Uspensky and Aleshin, 1993; Berger et al., 1994; Drew et al., 1996 and Kostitsyn, 1996), (b) a polysulfide-carbonate-quartz IIIb association with veins and veinlets restricted to the southern flank of Muruntau and the Myutenbai deposits, as well as (c) a silver-adularia-carbonate-quartz IIIc association forming veins with width up to 1.5 m, veinlets and breccias cements concentrated at the southern and eastern flanks of the ore field. This latter type was also described by Rakhmatullaev (1980), Uspenskiy and Aleshin (1993) and Kostitsyn (1996). The latest vein associations at Muruntau are represented by (d) the scarce stibnite-pyrite-calcite and cinnabar-quartz IIId-dickite veinlets and the more common (e) quartz IIIe-carbonate association containing relicts of ore minerals (Golovanov et al., 1998b). However, calcite(-brookite?) veinlets without significant amounts of quartz III also occur (e.g. Drew et al., 1996). These latest veinlets probably represent three of the mineral assemblages in the classification scheme of Koneev et al. (2010): silver-adularia-carbonate-quartz (Au-Ag association), stibnite-pyrite-calcite (Au-Sb association) and cinnabar-quartz-dickite (Au-Hg association) and may be paralleled with the two latest vein formations distinguished by Bendik (in Rakhmatullaev, 1980).

5.3. Interrelations between veins and dikes

The interrelations between dikes and the various vein types exposed in the open pit are of principal importance for (1) the understanding of the role of granite magmatism for deposit formation and (2) the timing of gold mineralization. Several authors concur that dikes formed subsequent to a first period of gold precipitation, but before late stages of vein formation. There is, however, considerable disagreement in the details. According to Zarembo (1968) and Uspenskiy and Aleshin (1993), dikes intruded after the formation of the concordant to sub-concordant quartz I veins and ore bodies, but before formation of the giant

stockworks, hosting the low-sulfide gold–arsenopyrite–pyrite association. In contrast, Bendik (1969), Palej and Sher (1970) and Drew et al. (1996) inferred that the dikes crosscut all stockwork-type veins of group 2, including the "Central" veins. Based on Rb-Sr dating, Kostitsyn (1991b, 1996) assumed that one magmatic pulse represented by granitoid intrusions and dikes (at about 286 Ma) preceded another pulse with alkaline dikes related to gold mineralization (at about 274 Ma) (see section 7.1.3 below). Alternatively, Shayakubov and Dalimov (1998) concluded from extensive field observations and literature data that granitoid intrusions and dike formation preceded all hydrothermal events at Muruntau, with the latter largely disturbing and/or resetting the K-Ar and Rb-Sr isotope systems. Some other authors have not constrained the relative age relationships between the dikes and various vein types, but inferred clear age relations between metasomatic alteration and dike formation. Kotov and Poritskaya (1991) and Protsenko et al. (1998) suggested that potassic alteration preceded dike formation, while albitization was superimposed on the dike rocks. According to Rakhmatullaev (1980), dikes intruded repeatedly during formation of the various vein types. Summarizing, there are no unequivocal data in the literature to constrain relative age relationships between dikes, metasomatic alteration and vein mineralization (Golovanov et al., 1998b,c). Although there is some evidence that dike formation may be intimately related with alteration and veining in time, the only fact clearly established is that all dikes are strongly affected by formation of a late sulfide-bearing alteration assemblage.

5.4. Characteristics of the vein fluids

In the last two decades, a large number of studies focused on the investigation of fluid inclusions from the Muruntau hydrothermal system have been published (e.g. Kotov et al., 1993; Berger et al., 1994; Ermolaev et al., 1994; Graupner et al., 2001a,b, 2005a, 2006; Wilde et al., 2001; Kryazhev, 2002). There are some conclusions from these studies, which are generally accepted, whereas others remain controversial. The most important problems involved with earlier Russian studies (e.g. Zarembo, 1968; Kotov and Poritskaya, 1991; Zairi and Kurbanov, 1992) are the classification of the fluid inclusion types, which is often unclear, and the lack of analytical data on individual fluid inclusions (e.g. bulk analytical data are presented only and Laser Raman data on the non-aqueous volatiles are missing); both problems are critical for a careful interpretation of the data. Furthermore, significant differences regarding the degree of deformation and recrystallization of the quartz hosting the fluid inclusions were observed in the different vein types at Muruntau (Graupner et al., 2000); the latter observation does not support an occurrence of primary inclusions in quartz I of the ductile deformed "flat" quartz veins as suggested by some authors. The study published by Wilde et al. (2001) has some limitations due to the use of key samples with a not well constrained origin (stockpile samples).

Generally accepted by most workers is the wide range of homogenization temperatures (Th) found for the discrete populations of fluid inclusions at Muruntau. According to different authors, three to six populations of fluid inclusions are present, with Th values ranging from 450 to about 100 °C (e.g. Kotov and Poritskaya, 1991; Alyoshin, 1994; Ermolaev et al., 1994; Graupner et al., 2001a, 2005a). Alyoshin (1994) found the highest salinities (Na^+, K^+, Cl^-) for trapped fluids in quartz I and much lower salinities for the fluids from the main gold ore stage (quartz II).

Special attention of the more recent studies was directed at the composition of the non-aqueous volatiles in the trapped fluids. According to most authors, the fluids contain CO_2, CH_4, N_2 and occasionally C_2- and C_3-hydrocarbons and H_2S (e.g. Wilde et al., 2001; Graupner et al., 2001a). Importantly, a change from a more CH_4-rich (low CO_2/CH_4 values) to a less CH_4-rich (higher CO_2/CH_4 values) fluid was observed for the fluid present during the main stage of hydrothermal activity and economic gold deposition (Alyoshin, 1994; Graupner et al., 2001a; Wilde et al., 2001; Kryazhev, 2002). However, the mechanisms responsible for this change remain controversial (e.g. presence of two discrete two-phase fluids or evolution of a single fluid by fluid phase separation). Using gas chromatography for bulk quartz samples from "Central" veins, high CO_2/CH_4 ratios were found in all vein quartz containing a later anhedral gold II (see next section for details on gold II occurrence and composition), whereas low CO_2/CH_4 ratios are typical of samples containing an earlier, mostly euhedral gold I only (Graupner et al., 2005a). Detailed microthermometric data confirmed these results and proved that H_2O-CO_2 inclusions in samples from the marginal parts of these vein-like quartz bodies always contained significant amounts of CH_4, whereas H_2O–CO_2 inclusions with a relatively wide range in volatile compositions occurred in quartz from central, strongly deformed segments of the vein-like bodies; however, almost pure CO_2-subsystems predominated in the latter segments.

A very important point to be addressed by the fluid inclusion work is the origin of the fluids involved in the alteration and mineral precipitation processes at Muruntau. Constraints may be derived from Br/Cl and noble gas analyses, but also from trace element and stable isotope characteristics of ore and vein minerals. For examples, the composition of the ore-forming fluids may be reconstructed by trace element analysis of minerals coexisting in the veins. Kempe et al. (1999) compared Y, REE, U and Sr contents in coexisting scheelite and quartz from group 2 stockwork and "Central" ore veins. Note that Sr and Y + REE may enter the scheelite structure while, in quartz, these elements are most probably adsorbed on internal surfaces or contained in fluid inclusions. The results demonstrated an enrichment of Sr in both minerals and, thus, in the fluids, which are non-metamorphic in composition according to their Rb-Sr characteristics. A non-metamorphic character of the fluids is also suggested by the variability in the REE distribution patterns for quartz and scheelite including the occurrence of positive Eu anomalies in Myutenbai samples and their absence in samples from the central Muruntau deposit (Kempe et al., 1999).

Extensive studies on stable isotopes have been carried out by various authors. Organic carbon from the host rocks displays $\delta^{13}C$ values of $-25.4 \pm 1.9‰$ ($n = 175$; Kostitsyn, 1991b). Carbonates within metasedimentary rocks of the Variegated Besapan yielded higher and more variable values: $\delta^{13}C$: $-8.9‰$ to $-19.7‰$ as well as variable oxygen isotope characteristics of $\delta^{18}O$ ranging from $+16.0‰$ to $+11.5‰$ (Kryazhev, 2002). The stable isotope data ($\delta^{13}C$) for carbonates from the main stage of hydrothermal activity are within error indistinguishable from that from the wall rocks but less variable ($\delta^{13}C$: $-8.5 \pm 2.5‰$, $n = 91$; Kostitsyn, 1991b) while the $\delta^{18}O$ values display a very large scatter (-5 to $+27‰$, Kostitsyn, 1991b). Similarly to carbon in carbonates, $\delta^{34}S$ values of sulfides from the ore-free packages ($2.9 \pm 3.5‰$, $n = 478$) correspond closely to those of sulfides from the ore veins ($2.4 \pm 3.3‰$, $n = 349$; Kostitsyn, 1991b). According to Berger et al. (1994) preliminary results of stable isotope work on the quartz veins yielded relatively wide ranges for oxygen isotope values ($\delta^{18}O_{fluid}$: $+4$ to $+9‰$; when assuming vein formation at 400 °C), probably indicative of variable water:rock ratios or mixing of different fluids in local structures. Vein quartz II containing gold I and secondary gold II and showing increased fluid CO_2/CH_4 values (~ 9.0) yielded $\delta^{13}C$ values of the fluid between $-4.3‰$ and $-5.4‰$. These data indicate an input of fluids from a juvenile source into the Au-bearing stockwork including high-grade auriferous "Central" veins (Kryazhev, 2002; Graupner et al., 2006).

Fluid-wall rock interactions within the meta-sedimentary rocks are considered as the main factor controlling fluid composition during deformation of the early flat quartz I veins at Muruntau as indicated by halogen ratios (Br/Cl vs. Cl) for fluids trapped in inclusions in quartz I (Graupner et al., 2001a). The halogen characteristics of the fluids in group 2 ore veins (log Br/Cl: −2.64 to −3.23) lend further support for the activity of juvenile fluids during the main ore stage (Graupner et al., 2001a). From the halide geochemistry (fluid inclusion Br and Cl data), mixing of fluids from different sources may also be inferred (Graupner et al., 2001a).

Helium trapped in gold-related early arsenopyrite from higher-grade auriferous zones, which has preserved the original fluid signature better than associated scheelite and quartz, indicates a small input from a mantle source (≤5% of total He; Graupner et al., 2006; Morelli et al., 2007). However, the overwhelming majority of the He in the fluid (~95%) is from crustal sources. The noble gases Ne, Kr and Xe in the sample fluids are dominated by gases of atmospheric origin (Graupner et al., 2006). In general, fluids trapped in sulfides from meta-sedimentary rock-hosted gold systems within the Tien Shan gold province (Muruntau, Kumtor and Amantaitau deposits) plot at similar $^{3}He/^{36}Ar$ and $^{40}Ar/^{36}Ar$ ratios as the vein samples in meta-sedimentary rocks from the Charmitan deposit; in contrast, sulfides from intrusive rock-hosted auriferous veins at Charmitan contain lower proportions of meteoric fluids (i.e. higher $^{3}He/^{36}Ar$ fluid ratios) than the latter ones (Graupner et al., 2006, 2010 and new data; Fig. 11).

5.5. The native gold: modes of occurrence, morphology and chemical composition

For Muruntau, several data sets related to gold ores and characteristics of native gold are available: (1) publications focussed on the gold ore composition in the mine and a systematization of these data using data for other deposits in the region and (2) studies providing a detailed insight into the individual stages of formation of the deposit presenting the modes of occurrence of individual gold grains and aggregates and their typical major and minor element compositions.

Koneev et al. (2010) compared gold ores from the Muruntau and Myutenbai deposits to data from various gold and gold-silver deposits of Western Uzbekistan and emphasized the elevated contents of Te (8.6–20.3 ppm), Bi (46–270 ppm), Se (17.3–24.2 ppm) and W (74–375 ppm) in addition to high As contents (1.11–1.58 wt.%) in the Muruntau system. These authors also presented elemental ratios for Muruntau and Myutenbai with Au:Ag = 2:1 and 3:1, Te:Se = 1:2 and 1:1 as well as Pt:Pd = 1:12 and 1:4, respectively. A constant occurrence of native gold in micro-assemblages together with Bi-tellurides and sulfoselenides in these deposits (e.g. Kotov et al., 1995; Vasilevsky et al., 2004) is discussed to explain the above ore-compositional data.

All investigators of the native gold at Muruntau emphasized its high purity, which is ensured by the dominating early ore-stage gold with high purity (840–980; Golovanov et al., 1998b; Graupner et al., 2005a). The highest purities were analyzed for native gold in quartz veins associated with scheelite, subordinate sulfides, molybdenite and tellurides. Inside the Muruntau stockwork, a significant variability concerning the purity of the native gold with depth cannot be established (e.g. Musin, 1981).

Zarembo (1968) published an early review on the vein and gold types present in the Muruntau ore system. He mentioned a wide distribution of gold in the ores, but emphasized its irregular distribution. For the quartz I of the above vein classification the author made no statement on gold occurrence and distribution at all. Zarembo assigned the bulk of the gold at Muruntau to the quartz II and the quartz-arsenopyrite veins, probably based on compositional data for technological ore samples. Data of L.A. Nikolaev, cited by Zarembo, prove a dominance of euhedral grains amongst the precipitated gold having a grain size ranging from 0.05 to 0.30 mm, an average fineness of 940 and admixtures of Ag and of Cu, Bi, Pb, As, Sb, Se and Te in trace amounts; however, these gold data were not assigned to an ore stage or vein type by the latter author, although the morphology, size and chemical composition of the gold closely resembles Au I as later defined by Graupner et al. (2005a). Zarembo (1968) investigated rounded and irregular gold grains and aggregates associated with fine grained quartz in very fine veinlets. These gold occurrences are assigned to deformed segments of quartz II and quartz-sulfide veins and to rock fragment-enriched parts of vein structures in this work. Zarembo (1968) characterized post-ore carbonate veins to be barren, but reported on a spatial association of gold with the latest polymetallic association in the deposit. Based on these data, Zarembo inferred that strong deformation of the quartz II and quartz-arsenopyrite formations resulted in good conditions for subsequent gold precipitation. However, the author also stated that the predominance of individual euhedral crystals as found by Nikolaev contradicts his inference. Furthermore, Zarembo (1968) inferred a late redistribution of parts of the gold. The large, irregularly-shaped gold as described by Zarembo (1968) may be

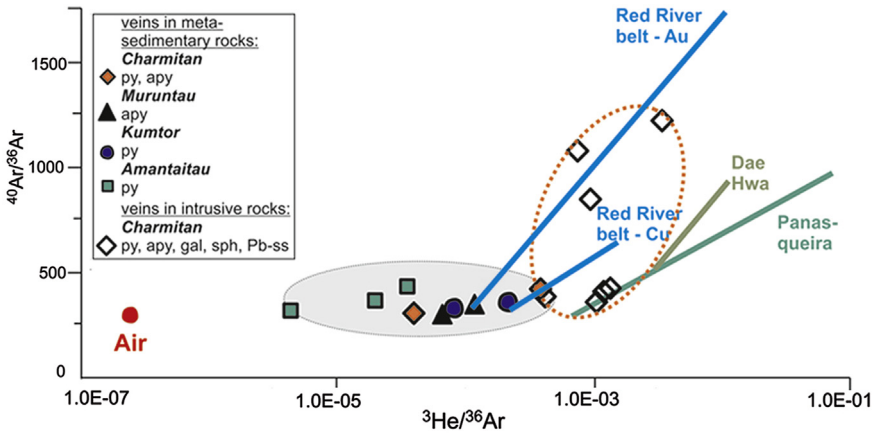

Figure 11. $^{40}Ar/^{36}Ar$ – $^{3}He/^{36}Ar$ plot for fluid inclusions in sulfides from Muruntau compared to those from Amantaitau, Charmitan (Uzbekistan) and Kumtor (Kyrgyzstan) Au deposits and inclusion data for the Red River Au and Cu deposits (China), Dae Hwa W-Mo deposit (South Korea) and the Panasqueira W deposit (Portugal). The data illustrate the involvement of mantle- and wall rock-related as well as atmospheric fluids. Figure after Graupner et al. (2010) with new data.

entirely assigned to the gold II type as defined by Graupner et al. (2005a).

Kremenetsky et al. (1990) presented a detailed study focussed on the gold occurrences in veins and veinlets of the quartz stockwork at Muruntau. These authors' distinguished two pre-ore quartz vein types (Q1+Q2) – both corresponding to the quartz I of the above vein classification, two ore stage quartz vein types (Q3+Q4) – both corresponding to the quartz II of the above vein classification, and one post-ore calcite vein type (Ca); in addition, one arsenopyrite (Apy) and one pyrite vein type (Py), both assigned to the ore stage (quartz II), were presented with data for the contained gold. The (Q1) and (Q2) syn-metamorphic vein structures contained individual hypidiomorphic (rounded) gold grains (size: 0.02–0.04 mm) having a mean fineness of 842 (Ag_{mean} = 158; n = 5); trace elements like Sb, Bi and Cu were generally below LOD of the X-ray method applied. The steeply dipping (Q3) stockwork veins contained fine gold (grain size up to 0.05 mm) concentrated at the vein – wall rock contacts. The moderately dipping (Q4) stockwork veins contained hypidiomorphic crystals or accumulations of anhedral dust-like particles in quartz or inside the vein salvage zone. Native gold in (Q3) and (Q4) ore stage veins ranged in its fineness from 853 to 955 (mean 891; n = 15); admixtures of Sb were rare (≤0.03 wt.%), Bi and Cu contents were more common (≤0.11 and ≤ 0.08 wt.%, respectively; n = 4 for both elements above LOD). Gold grains in (Apy) veins either had a finely dispersed distribution (grain size: <0.005–0.001 mm) and a high fineness, or, when associated with epigenetic Bi mineralization, a small grain size (≤0.08 mm × 0.05 mm) and a low to very low fineness (285–683; n = 11). Native gold in (Py) veinlets appeared finely dispersed and had a high fineness (873; n = 3) and contained no admixtures of Sb, Bi or Cu. The post-ore (Ca) veinlets contained rare, redistributed inclusions of finely dispersed gold (grain size <0.008 mm) having a low fineness.

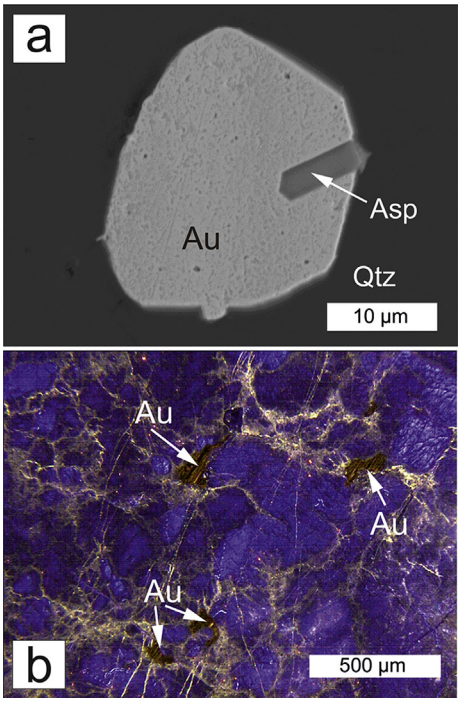

Figure 12. Two morphological types of gold in the Muruntau "Central" veins: (a) euhedral Au I with broken, ingrown arsenopyrite crystal included in a quartz grain; secondary electron image; (b) anhedral Au II aggregates (arrows) located in a network of secondary microstructures revealed by CL optical microscope imaging (Figures from Graupner et al., 2005a).

Graupner et al. (2005a) studied native gold in the main ore stage quartz stockworks (quartz II of the above vein classification) from the second and third ore bodies at Muruntau using optical and CL microscopy, SEM and electron microprobe. Three profiles across near E–W striking "Central vein" bodies in one vein zone at different mining levels, including the brecciated wall rocks, have been investigated. In addition, stockwork veinlets were examined. Two types of native gold have been observed (Fig. 12). A type I gold occurred randomly distributed in quartz, associated with deformed scheelite, Bi-tellurides and arsenopyrite, and characterized by euhedral crystals (size: 0.01–0.04 mm) showing combinations of cubic and octahedral forms (Fig. 12a). Gold I had a high fineness (870–915; n = 205 in 23 grains) and commonly contained Hg (≤0.73 wt.%); admixtures of Bi (≤0.42 wt.%), Sb (≤0.30 wt.%), Cu (≤0.20 wt.%) and Fe (≤0.56 wt.%) occurred occasionally. In general, gold I from the veins did not show clear compositional zoning, although the crystal rims were often somewhat enriched in Ag. A clear association between gold I and microcline in the altered wall rocks was recognized. Gold II in quartz veins appeared as anhedral grains at boundary surfaces and in interstitial spaces between partly to intensely dynamically recrystallized and often finer grained quartz together with calcite, dolomite and chlorite (Fig. 12b). It showed a large range in grain sizes (0.01–0.25 mm). Gold II displayed a large variation in fineness (770–940; n = 190 in 16 grains) and always contained Hg (0.10–0.72 wt.%). Admixtures of Bi, Sb and Cu occasionally occurred (≤0.36, ≤0.30 and ≤0.20 wt.%, respectively).

Summarizing the published data on the gold composition and distribution at Muruntau it is obvious that in a large number of available studies (e.g. Petrovskaya, 1968; Zarembo, 1968; Bierlein and Wilde, 2010) only the later (commonly larger sized and spatially more concentrated) gold II grains are considered in greater detail. This fact is clearly supported by the characteristics on the native gold (size, shape and chemistry of gold grains/aggregates; distribution characteristics of the grains) described by the cited authors.

5.6. Association of gold with uranium and tungsten

High contents of W, U and Th are typical of the metasomatites and mineralization at Muruntau (Uspenskiy and Aleshin, 1993; Bojtsov et al., 1996; Konstantinov et al., 2000). According to the trace element analyses of whole rock samples, the U and Th contents within the deposit are on a high level, similar to typical high-heat production (HHP) granites and close to the contents found for the granitoids and dikes present in and around Muruntau (see section 4.2.2 above). According to Bojtsov et al. (1996), the uranium content in the metasomatites is commonly at about 11 ppm (average of 115 samples). We found average contents of 11.3 (5.5–23.0) ppm Th and 15.7 (1.5–23.4) ppm U (18 samples; Kempe et al., 2000). The Th/U ratios are highly variable similar to the magmatic rocks, and range from 0.56 to 2.8. Again, this variability hints at a high mobility of uranium during the metasomatic alteration processes.

Bojtsov et al. (1996) discovered lens-shaped, stratiform-like bodies, several meters thick and several tenths of meters long with even higher uranium contents (240 ppm on average; 105 samples). These zones of high radioactivity are significantly enriched in Y, Mo, V, Ni and Au compared to the surrounding rocks although no correlation was found between the uranium and gold contents. According to mineralogical investigations, the main carrier of the uranium in these U-rich "lenses" is uraninite. The importance of the extremely U-rich zones is twofold. On the one hand, the area of the Central Kyzylkum is well known for large unconformity uranium deposits, for example, in the Uchkuduk region northwest of

Muruntau (Kraft and Kampe, 1995). On the other hand, we have found that gold-quartz mineralization may show enhanced uranium contents as evidenced by increased uranium contents in type II scheelite from various deposits worldwide (Kempe and Oberthür, 1997). This Au-U association is not yet appropriately considered and explained in the literature.

Similarly, there is an interesting association of gold (native gold) with tungsten (scheelite II) at Muruntau. The scheelite content is so high that tungsten was mined as a by-product (Uspenskiy and Aleshin, 1993). Whole rock analysis of metasomatites shows enhanced (470 ppm on average, 18 samples) but highly variable tungsten contents – from below the dectection limit of 4 ppm to up to 3000 ppm (Kempe et al., 2000). This high variability is in accordance with the findings by other authors (Uspenskiy and Aleshin, 1993; Golovanov et al., 1998b). We have not found a correlation between the tungsten and the gold contents according to whole rock data, which is also in accordance with the authors cited above and Kostitsyn (1991b). The carrier of the tungsten in metasomatic rocks, quartz veins and veinlets is scheelite. In earlier works, the association between tungsten and gold was regarded as coincidental (Badalova and Palej, 1965; Petrovskaya, 1968; Vikhter et al., 1986) while Protsenko and Rubanov (1991) inferred a genetic link between gold and scheelite precipitation. Uspenskiy and Aleshin (1993) have studied the tungsten distribution as well as the characteristics of scheelite in the Muruntau deposit in greater detail. According to these authors, the tungsten mineralization forms near-concordant ore bodies similar in appearance to that described by Bojtsov et al. (1996) for uranium. The scheelite is mainly confined to skarnoids and "flat" veins and shows no correlation with lens-shaped gold ore bodies in these occurrences. On the other hand, there is a close association between scheelite and gold in columnar ore structures, were both minerals occur in stockwork veinlets and "Central" veins. According to Golovanov et al. (1998b), gold in these veins is found as inclusions in scheelite. Uspenskiy and Aleshin (1993) recognized three stages of scheelite formation: The earliest scheelite I is found in the stratiform-like skarnoids and veins and may be distinguished by its light coloration, average small size, yellowish fluorescence (enhanced Mo content, high Sr concentrations) and the position in the "flat" structures. Scheelite II formed in the Au-rich quartz veins of the stockwork and the "Central" veins. There is a slight dominance of scheelite II over scheelite I in the deposit. Scheelite II, apart from its position in the mineral sequence, may be also distinguished by its darker (yellowish- to brownish-orange) coloration and bluish luminescence. Scheelite III occurs at Muruntau and Myutenbai only occasionally in late veins with albite, tourmaline and calcite. Its appearance is similar to that of scheelite II.

The scheelite types described by the above authors may compare to the two scheelite types established by Kempe et al. (2001a): scheelite I of light coloration is confined to "flat" veins and scheelite II of darker coloration to the stockworks. However, there are some discrepancies in the characteristics described by us and by the previous authors for scheelite I: Although we also found enhanced Sr contents in scheelite I, these contents are significantly lower than in scheelite II. Furthermore, the luminescence in the samples studied by us was always bluish in accordance with the low Mo content (below 4 ppm; Kempe et al., 1999). In contrast, the Sr content in scheelite II was found to be very high (>400 ppm) and the luminescence is always yellowish (despite the low Mo contents below 4 ppm) and quenched. Both scheelite types are distinguishable by their characteristic REE patterns: Low REE contents with flat patterns and some enrichment of the heavy REE in scheelite I and higher REE contents with bell-shaped patterns for scheelite II (Kempe et al., 1999). Scheelite III was not considered by Kempe et al. (1999, 2001a). We argue that the discrepancies between our results and those reported by Uspenskiy and Aleshin (1993) may be explained, on one hand, by differences in sampling of scheelite I. We have not sampled scheelite I from skarnoids. It is well known that skarn scheelite often shows enhanced Mo contents which may explain discrepancies in the luminescence behavior and Mo concentrations. On the other hand, analytical methods used by Uspenskiy and Aleshin (1993), in particular, the luminescence method, are not appropriate for quantitative trace element analysis, in particular of the REE, in scheelite (Kempe et al., 1991).

Summarizing, the sources of the gold and the tungsten seem to be different as can be seen from the different behavior in early, stratiform-like ore bodies of gold and tungsten. Nevertheless, in the main ore stage gold and tungsten precipitated together in the quartz veins of the stockworks.

6. Fluid – wall rock interaction

The rocks of the Besapan Sequence hosting gold mineralization were intensely altered during various post-sedimentary events. The first was regional metamorphism leading to the formation of schists, sandstones, siltstone, phyllites and locally meta-carbonates as described above in section 4.1.1. Afterwards, hornfelses formed locally as a result of Hercynian granite magmatism. Alteration finally occurred during various hydrothermal events adjacent to the vein zones. The wall rock alteration is difficult to study because its character may vary from meter-down to the decimeter- and millimeter-scale (Voronkov, 1976; Mukhin et al., 1988; Marakushev and Khokhlov, 1992; Protsenko et al., 1998; Kempe et al., 2000, Fig. 13b and e) depending on variations in the initial host rock composition (plagioclase and mica content, carbonate lenses or cement etc.) and the structural fabric. Repeated changes in textures, chemical composition of whole rocks and their mineral composition make it difficult to characterize exactly each single alteration event. For example, biotite formed during contact metamorphism and during hydrothermal alteration as well (Kol'tsov and Rusinova, 1997). However, Gar'kovets (1969) assigned biotite formation exclusively to higher-grade regional metamorphism neglecting possible contact metamorphism. The same author found almost no signs of any significant metasomatic alteration (Gar'kovets, 1971, 1973). Khokhlov et al. (1998) also questioned contact metamorphic biotite and reported metamorphic biotite for the lower two Suites of the Besapan and for the Tazkasgan Sequence. Mukhin et al. (1988) have reported biotite formation during regional metamorphism for the Taskazgan Sequence only. Kremenetsky et al. (1990) considered all biotite including that in spotted aggregations as metasomatic in origin. In contrast, Bojtsov et al. (1996) regarded all biotite including that developing along schistosity as a result of contact metamorphism. As shown by Kol'tsov and Rusinova (1997) and Drew et al. (1996), biotite formed during metasomatic alteration may be distinguished from that formed in the hornfels aureole by its lower iron and aluminium contents. In section 4.2.3, we considered the formation of the thermal aureole to some extent mainly because of its possible role in later wall rock alteration and veining.

6.1. Metasomatic alteration: alteration types and sequences

Most authors agree that the formation of gold-bearing quartz veins of various types was accompanied by intense wall rock alteration (Palej and Sher, 1970; Kremenetsky et al., 1990; Kotov and Poritskaya, 1991; Marakushev and Khokhlov, 1992; Kol'tsov and Rusinova, 1997; Protsenko et al., 1998; Kempe et al., 2000; Wilde et al., 2001; Wall et al., 2004; Graupner et al., 2005b; Bierlein and Wilde, 2010). Field observations show that alteration is often developed along or subparallel to stratigraphic units and/or

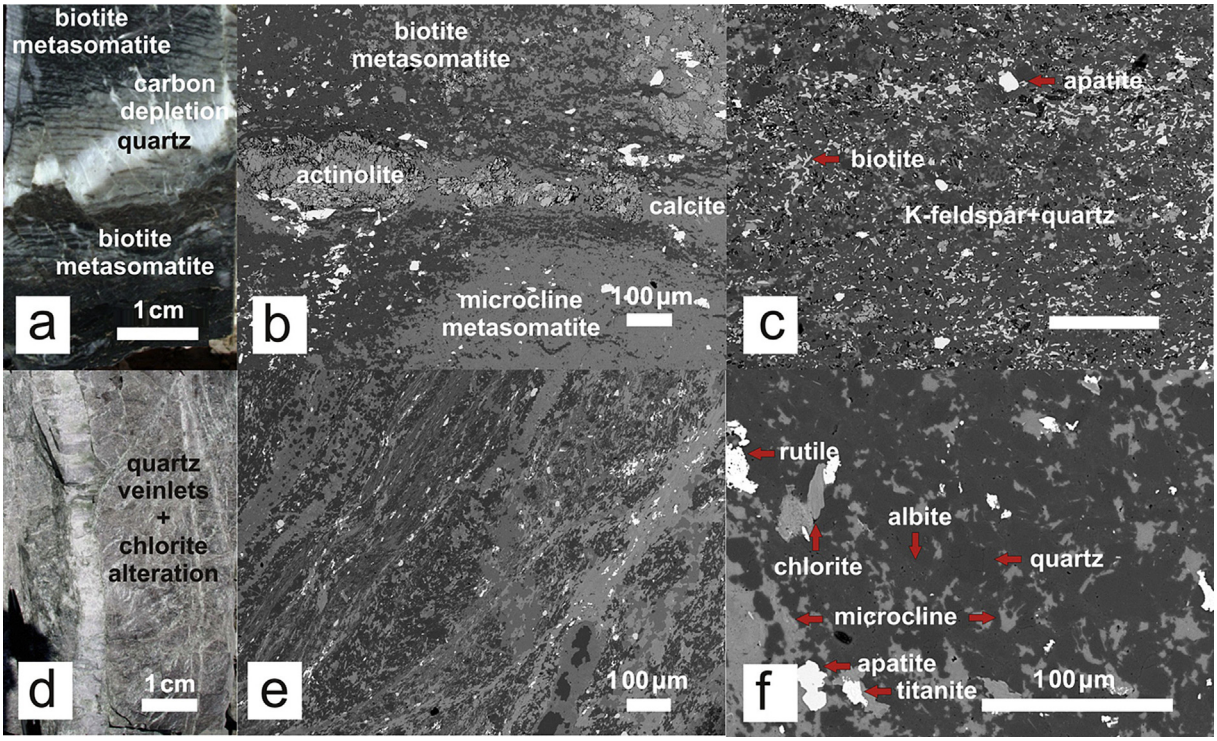

Figure 13. Alteration features in the wall rocks of the Muruntau deposit. Outcrop photographs with scale bars 1 cm: (a) Biotite(-microcline) metasomatites adjacent to a vein; an aureole of carbon depletion of less than 1 cm from the vein selvages is clearly visible (borehole MS-3, −1495 m); (d) Chlorite and sericite alteration occurring in a network of late fractures adjacent to a quartz vein (Muruntau open pit, + 135 m level); Backscattered electron images with scale bars 100 µm: (b) Thin, boudinaged carbonate layers partly replaced by actinolite (skarnoid formation) in a matrix of biotite and microcline-quartz metasomatites (Muruntau open pit, First ore body, +300 m level); (c) Interrelations between biotite (upper and lower part) and microcline-quartz (centre) metasomatites (see b); (e) Small-scale alternating banded metasomatites with (from upper left to lower right) microcline-quartz, sericite-chlorite, biotite-quartz, chlorite-calcite, microcline-quartz, chlorite-calcite (Muruntau shaft M, Second ore body, +128 m level); (f) Albite-chlorite-quartz metasomatite (with rutile) replacing microcline-quartz metasomatite (with titanite and apatite; Muruntau shaft M, New ore body, +78 m level).

schistosity resulting in a stratiform-like character of alteration and related low-grade gold mineralization (Kremenetsky et al., 1990; Kotov and Poritskaya, 1991; Marakushev and Khokhlov, 1992; Bojtsov et al., 1996; Protsenko et al., 1998; Wilde et al., 2001; Fig. 14). During this process, a re-distribution of carbonaceous material took place which was removed from aureoles around the veins and from quartz-feldspar rich layers of the metasomatic rocks (Bendik, 1969; Bojtsov et al., 1996; Rusinova et al., 1996; Kol'tsov and Rusinova, 1997; Goloanov et al., 1998b; Protsenko et al., 1998; Fig. 13a). As a result, metasomatites display a pronounced banded character enhanced by the redistribution of other "mafic" minerals (mainly biotite; Kostitsyn, 1991b; Marakushev and Khokhlov, 1992; Kol'tsov and Rusinova, 1997). According to Rusinova et al. (1996), redistribution of carbon occurs under non-equilibrium conditions leading to the formation of low-ordered graphite. Note that an analogous re-distribution of gold with significant zones of gold depletion has not yet been found. In contrast, the whole area around the deposit and also the wall rocks within it display enhanced gold contents (Marakushev and Khokhlov, 1992; Bojtsov et al., 1996; Drew et al., 1996; Golovanov et al., 1998b; Khokhlov et al., 1998; Wall et al., 2004). According to calculations by Kotov and Poritskaya (1990), even a redistribution of all the gold contained in these "enriched" wall rocks cannot explain the extraordinary gold tonnages present in the Muruntau deposit. Clearly, an

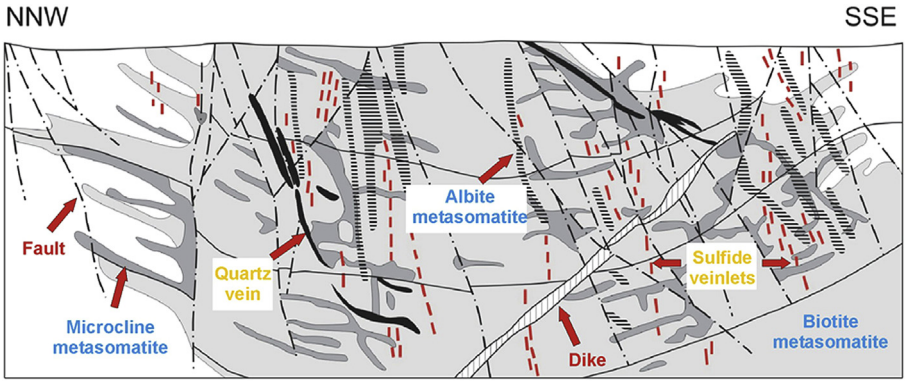

Figure 14. Cross-section (not to scale) through the Muruntau deposit illustrating the relations and distributions of the main alteration types (after Sher and Yudin, 1971, unpublished).

external (probably repeated) input of Au-rich fluids into the ore system should be considered.

During alteration, new biotite, microcline, albite, calcite, sericite, chlorite, apatite and titanite were formed at the expense of older biotite, chlorite, calcic plagioclase, K-feldspar and ilmenite (Sher, 1970; Kol'tsov and Rusinova, 1997; Kempe et al., 2000). As a result, the density and porosity of the altered rocks decreased significantly (Krementesky et al., 1990). According to the prevailing minerals, various types of metasomatites may be distinguished. However, there is no full agreement between various authors about this point. Even more complicated are the relative age relations between different alteration events because three overlapping factors may be responsible for the spatial control of alteration: (1) simultaneous veining, (2) repeated reactivation of older cleavages and vein systems and (3) variations in wall rock composition.

Several authors described the prevailing metasomatic assemblage as containing quartz, biotite and two feldspars (Kotov and Poritskaya, 1991; Marakushev and Khokhlov, 1992; Drew et al., 1996; Kol'tsov and Rusinova, 1997; Protsenko et al., 1998) ignoring the fact that potassic alteration (with formation of low-iron biotite and/or microcline) yielded opposite results compared to sodic (albite) or calcic (carbonate and/or apatite) alteration and that different types of metasomatic alteration may be distinguished according to the whole-rock and mineral composition (Kempe et al., 2000). This apparent ambiguity is probably related to the fact that different "leucocratic" alteration assemblages are often difficult to distinguish from each other in the field and, sometimes, even under the optical microscope (Sher, 1970). Such metasomatites with dominating microcline, albite or carbonate are collectively referred to as "pink metasomatites" by various authors despite the contrasting mineral compositions (Sher, 1970; Kotov and Poritskaya, 1991; Marakushev and Khokhlov, 1992; Kol'tsov and Rusinova, 1997; Protsenko et al., 1998). On the other hand, oligoclase or K-feldspar, respectively, may be present in the related metasomatites as restite phases (Protsenko et al., 1998; Kempe et al., 2000).

Biotite and microcline alteration (Fig. 13b, c) are the main processes involved (Marakushev and Khokhlov, 1992; Kol'tsov and Rusinova, 1997; Protsenko et al., 1998; Konstantinov et al., 2000) while albite alteration (Fig. 13f) is developed only locally (Fig 14). Sericitization (locally associated with chlorite alteration) is subordinate, late and lower in temperature (Rakhmatullaev, 1980; Kotov and Poritskaya, 1990, 1991; Zairi et al., 1998; Bierlein and Wilde, 2010; Kempe et al., 2015; Fig. 13d). This contrasts with the more common albite-sericite alteration assemblages (in the Russian literature described as "beresite") known from other hydrothermal gold deposits (e.g., Sher, 1970; Kremenetsky et al., 1996) and is indicative for the initially high temperatures of the ascending fluids (about 400–450 °C; Kryazhev and Kudryavtsev, 1995; Kol'tsov and Rusinova, 1997; Bierlein and Wilde, 2010). As shown by analysis of whole-rock composition of altered and unaltered rocks using paragenetic diagrams (Kol'tsov and Rusinova, 1997) and mass transfer calculations (Graupner et al., 2005b), potassic alteration resulted in increased potassium contents with K_2O concentrations of up to 7–8 wt.% (Sher, 1970; Marakushev and Khokhlov, 1992; Kol'tsov and Rusinova, 1997; Protsenko et al., 1998; Kempe et al., 2000). K-feldspar metasomatites may be seen as the "inner" zone of K-metasomatism compared to a more widespread, "outer" biotite alteration zone (Kostitsyn, 1991b; Marakushev and Khokhlov, 1992; Kol'tsov and Rusinova, 1997; Protsenko et al., 1998; Konstantinov et al., 2000; Fig. 14). According to Protsenko et al. (1998), there are two types of K-feldspar metasomatites: (1) more widely developed metasomatites with intermediate microcline closely related to biotite metasomatites and (2) pale pink to grayish metasomatites with maximum microcline occurring more restricted and adjacent to quartz veins. According to our data, primary orthoclase coexists with secondary microcline with the latter prevailing in pale pink, gold-rich samples (Kempe et al., 2000). K-feldspar metasomatites tend to form at the selvages of the veins (Zarembo, 1968; Palej and Sher, 1970; Sher, 1970; Drew et al., 1996; Protsenko et al., 1998) but may also form concordant lenses (Kol'tsov and Rusinova, 1997; Protsenko et al., 1998). Rb-Sr isotopic research confirms that both forms of appearance are essentially of the same type (Zairi et al., 1998). According to thermodynamic calculations by Kol'tsov and Rusinova (1997), fluids related to this potassic alteration should have a high alkalinity and the metasomatites were formed under large pressure gradients (decompression). Neither metamorphic fluids circulating in the host rocks, nor acidic fluids derived from a granite intrusion may be responsible for such an alteration style (Kol'tsov and Rusinova, 1997) in contrast to the suggestions made by Wall et al. (2004). Potassic alteration resulted in more extensive mass transfer in psammopelitic rocks compared to pelitic ones (Graupner et al., 2005b). While Yardley and Cleverley (2015) concluded that metamorphic fluids could only be liberated as potential metal carriers by decompression during exhumation, the sources of the fluids involved in the production of the above metasomatites and the causes of exhumation remain speculative.

A special type of alteration, probably related to potassic alteration, is the formation of skarnoids after meta-carbonate rocks (Kol'tsov and Kostitsyn, 1995, Fig. 13b). According to the latter authors, thermodynamic calculations in combination with Sr/Sr isotope data hint at a high-temperature (400–450 °C) formation under non-isochemical conditions and decompression. The exchange of matter during skarnoid formation occurred mainly with the other metamorphic host-rocks of the Besapan Sequence according to the Sr isotope data.

Albite metasomatites (albitites) formed probably later, replacing K-rich metasomatites (Bendik et al., 1969a; Sher, 1970, Rakhmatullaev, 1980; Kotov and Poritskaya, 1991; Protsenko et al., 1998; Konstantinov et al., 2000, Fig. 13f). Note, however, that Berger et al. (1994) and Wilde et al. (2001) have suggested a reverse relationship. The albite metasomatites developed mainly along vein selvages and some quartz-rich beds (Kotov and Poritskaya, 1991; Wilde et al., 2001). According to Protsenko et al. (1998) and Konstantinov et al. (2000), large zones of albitie alteration occur also around the dike zone and as vein-like bodies crosscutting the bedding (Fig. 14). It seems, however, that the latter type belongs to a much later alteration process because the related rocks are rich in tourmaline (Rakhmatullaev, 1980; Kotov and Poritskaya, 1991; Protsenko et al., 1998), which is not found in other albitites (Kempe et al., 2000; see above in this section). Albite alteration is accompanied by chlorite formation, precipitation of pyrite and some carbonate (Sher, 1970; Kotov and Poritskaya, 1991; Protsenko et al., 1998; Wilde et al., 2001). Sher (1970) suggested that this alteration style is also related to gold precipitation, although our data hint at an opposite conclusion (Kempe et al., 2000; see section below) in agreement with the findings by Protsenko et al. (1998).

Late alteration such as carbonate, apatite (Kempe et al., 2000), sericitic alteration (close to and within the southern Fault zone; Kotov and Poritskaya, 1991; Protsenko et al., 1998) and argillic alteration (Rakhmatullaev, 1980; Kotov and Poritskaya, 1991; Protsenko et al., 1998; Konstantinov et al., 2000) occur only locally, close to the recent surface and show no relation to economic gold mineralization.

6.2. Metasomatic alteration: veining and gold content

Biotite- and microcline-rich metasomatites may contain high, up to economic grade, gold contents of 1–3 ppm, occasionally up to

30 ppm (Marakushev and Khokhlov, 1992; Kol'tsov and Rusinova, 1997; Golovanov et al., 1998b; Protsenko et al., 1998; Kempe et al., 2000; Wall et al., 2004). Such concentrations are comparable to that of the ore veins. Therefore, various models suggested for the Muruntau deposit were influenced by the visible morphology of the veins and wall rock alteration haloes considered as gold-bearing ("stratiform"-type for flat veins and metasomatites and "stockwork"-type for cross-cutting veins and vein systems; cf. preceding section). However, the real gold distribution could be established only by detailed analysis of the gold content throughout the mine (Voronkov, 1976; Bojtsov et al., 1996; Protsenko et al., 1998, Fig. 8).

Several authors tried to relate wall rock alteration to the formation of particular vein types. Kotov and Poritskaya (1991) and Kol'tsov and Rusinova (1997) suggested that the formation of the early "flat" veins corresponded with potassic alteration. This is, however, in contrast with the general succession in the evolution of gold-bearing veins and also with the alteration assemblages found within the "flat" veins or zones adjacent to them (Petrovskaya, 1968; Golovanov et al., 1998b; Khokhlov et al., 1998; Graupner et al., 2001a). Uspenskiy and Aleshin (1993) related the formation of concordant and sub-parallel quartz veins to hornfels formation with amphibole and pyroxene. We have not found metasomatites with amphibole and pyroxene adjacent to flat veins as described by the latter authors, although amphibole (and rarely pyroxene) could be determined in various types of metasomatites (Kempe et al., 2000; Fig. 13b). Probably, skarnoids formed locally in the thermal aureole and adjacent to "flat" veins in meta-carbonate layers (Bendik et al., 1969a; Voronkov, 1976; Protsenko et al., 1998; Golovanov et al., 1998b). It seems that such larger lenses of skarnoids occurred more frequently in the upper part of the deposit (Kudrin et al., 1990; Uspenskiy and Aleshin, 1993; Kol'tsov and Kostitsyn, 1995). An interrelation between the formation of stockwork (or part of stockwork veins) and/or the "Central" veins on one hand and albite alteration on the other as suggested by Rakhmatullaev (1980), Kotov and Poritskaya (1991) and Uspenskiy and Aleshin (1993) is not supported by the data. In general, it is quite difficult to relate veining stages and alteration stages because alteration (including biotite and microcline) developed mainly along the rock bedding and formed lens-shaped bodies of various size not only, or not clearly, along particular vein selvages (Kotov and Poritskaya, 1991; Marakushev and Khokhlov, 1992; Kol'tsov and Rusinova, 1997; Protsenko et al., 1998; Kempe et al., 2000; Fig. 14).

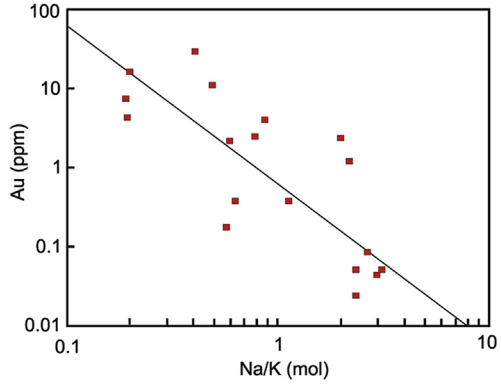

Figure 15. Relation between atomic Na/K ratios and Au contents in various types of metasomatic rocks from Muruntau and Mjutenbaj according to whole rock analyses. The Na/K ratio considers K-metasomatic alteration (biotitization and microclinization) and albitization, respectively, excluding the influence of SiO_2 mobility in these processes. Data from Kempe et al. (2000).

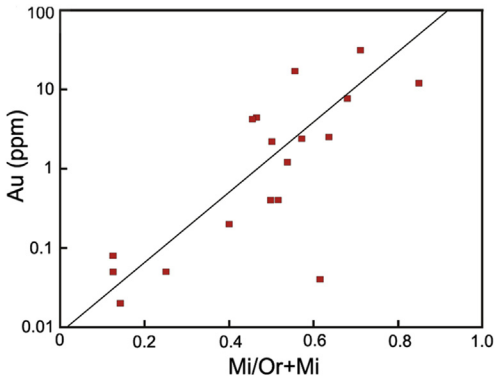

Figure 16. Relation between the degree of microclinization of K-feldspar (according to quantitative Rietveld analyses of the whole rock samples) and the Au contents. Data from Kempe et al. (2000).

There is also some dispute in the literature whether biotite and microcline or sericite alteration are the main processes related to the formation of the main economic gold concentrations (Wilde et al., 2001; Bierlein and Wilde, 2010), although there is a distinct interrelation between enhanced gold contents and high-temperature potassic alteration (Golovanov et al., 1998b; Protsenko et al., 1998; Kempe et al., 2000). High-temperature potassic alteration may be related to the main-stage or the second-stage gold precipitation (Au I or Au II according to Graupner et al., 2005a), but more probably to Au I not only because of similar temperature conditions (note the lower temperature for Au II precipitation of 230–330 °C; Graupner et al., 2005a), but also because there is a clear correlation between the gold content and the K/Na ratio for the whole rocks (Golovanov et al., 1998b; Kempe et al., 2000; Fig. 15). Furthermore, native Au I could be observed within these rocks (Graupner et al., 2005a). This indicates that the formation of the stockworks was paralleled by potassic (biotite and microcline) alteration of the wall rocks. There is a clear trend for enhanced gold contents with increasing degree of microclinization (Kempe et al., 2000; Fig. 16). Similar conclusions were reached by Rakhmatullaev (1980), Drew et al. (1996), Golovanov et al. (1998b), Konstantinov et al. (2000) and Wall et al. (2004) based mainly on field observations and thin section studies.

6.3. *Fluid-wall rock interaction and isotope signatures*

The fluid-wall rock interaction may be traced by the signatures of the Rb-Sr and Sm-Nd isotope systems (Kostitsyn, 1991b, 1996; Kempe et al., 2001a). The Sr isotope signature of the fluids is best reflected by Ca minerals with low to very low Rb contents as calcite (Kostitsyn, 1991b, 1996) and scheelite (Kostitsyn, 1996; Kempe et al., 2001a). These fluid signatures may be compared to the initial Sr isotope composition of the wall rocks (Besapan Sequence), the dolomites of the older Taskazgan Sequence and of the younger Devonian to Carboniferous Zhivachisaj Sequence and to those of the granitoid intrusions and dikes (Kostitsyn, 1991b, 1996; Fig. 17a). The Sr isotope composition of the fluids was in equilibrium with the wall rocks and distinctly different from that of the dolomites and granitoids. This finding points to very intense fluid-wall rock interactions during vein formation. The Sr was probably derived from wall rock carbonates and the anorthitic feldspar component during their replacement by secondary silicates when K-rich and/or later albite metasomatites were formed. Similarly, the initial Nd isotope composition of scheelite II was in equilibrium with that of the wall rocks during vein formation with samples of the latter plotting on

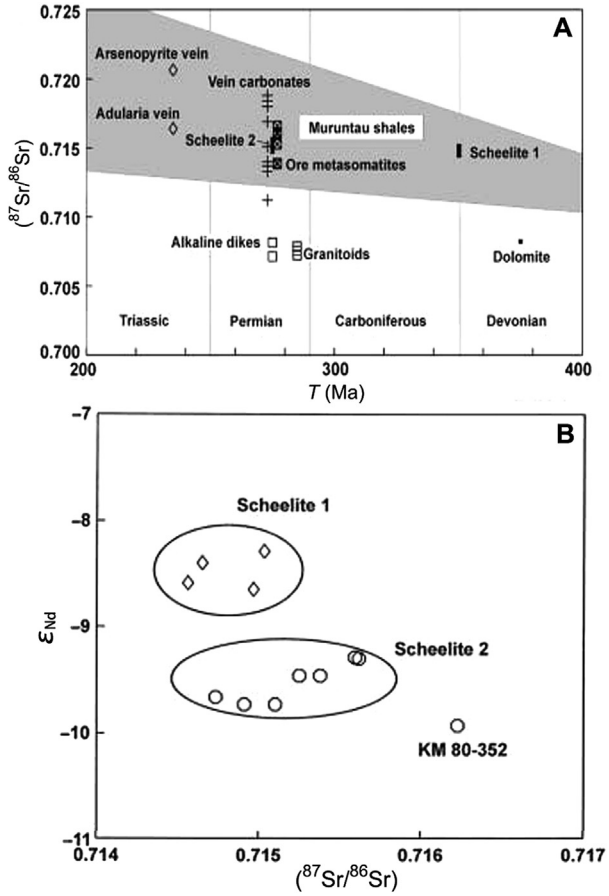

Figure 17. Sr and Nd isotope signatures of scheelite from Muruntau and Kosmanachi: (A) Initial Sr isotope ratio of scheelite I ("flat" veins) and scheelite II (stockwork and "Central" veins; data from Kempe et al., 2001a) compared to Sr signatures of rocks, veins and vein carbonates from the Muruntau deposit and adjacent areas (data from Kostitsyn, 1991b). The Sr isotope signatures of both scheelite types are similar to that of schists, metasomatites, veins and vein carbonates, but dissimilar to the isotope signatures of granitoids and Devonian – Carboniferous carbonates. (B) Diagram comparing initial Sr isotope ratios and ε_{Nd} values of scheelite I, scheelite II from Muruntau/Mjutenbai and scheelite from Ag-rich veins in Kosmanachi. The differences in the isotope signatures stick to significant age differences between the three scheelite types. Probably, scheelite from Kosmanachi corresponds to scheelite III of Uspenskij and Aleshin (1993) from Muruntau. Figure from Kempe et al. (2001a).

or close to the Sm-Nd isochron defined by Scheelite II samples (Kempe et al., 2001a). These isotope constraints indicative of intense fluid-wall rock interaction, however, cannot be applied in the same fashion to all other elements mobile during the hydrothermal processes, in particular, to the gold (Kostitsyn, 1996; Kempe et al., 2001a). As discussed in section 6.1, gold from the veins cannot be derived by simple redistribution from the wall rocks by analogy to the Sr. More complicated scenarios are also indicated for Nd by the REE distribution patterns of scheelite II (Kempe et al., 1999; see section 5.6 above).

7. The gold: when and from where?

7.1. Timing of mineralization

Up to now, there is no consensus concerning the absolute age relations between gold mineralization and the several other geological processes established in the deposit itself and in its surroundings (regional metamorphism, magmatism, metasomatic alteration and veining) although considerable work has been done in this direction. Note that such a state of affairs is not uncommon in the study of gold deposits (Kempe et al., 2001a; Brown et al., 2002) because it appears difficult to define any undisturbed isotope system directly related to the precipitation of the gold. In the particular case of the Muruntau deposit, the situation is even more complicated due to the complex history of magmatism, metamorphism, hydrothermal alteration and veining as demonstrated by the data presented in the previous paragraphs. Isotope age data obtained in the early period of studies at Muruntau were reviewed by Kostitsyn (1991b), Zairi et al. (1998) and Kempe et al. (2001a). At that time, the K-Ar and Rb-Sr systems of whole rocks, rock fractions and mineral separates were examined. In more recent studies, the Sm-Nd system of scheelite, the Ar/Ar system of sheet silicates, the Re-Os system of arsenopyrite and the U-Pb system of zircon and monazite were tested in order to constrain absolute ages of ore-forming or ore-related processes within the deposit (Kempe et al., 2001a,b; Wilde et al., 2001; Morelli et al., 2007; Kempe et al., 2015). Considering all published age data, two particular points are acknowledged at the beginning of our short review:

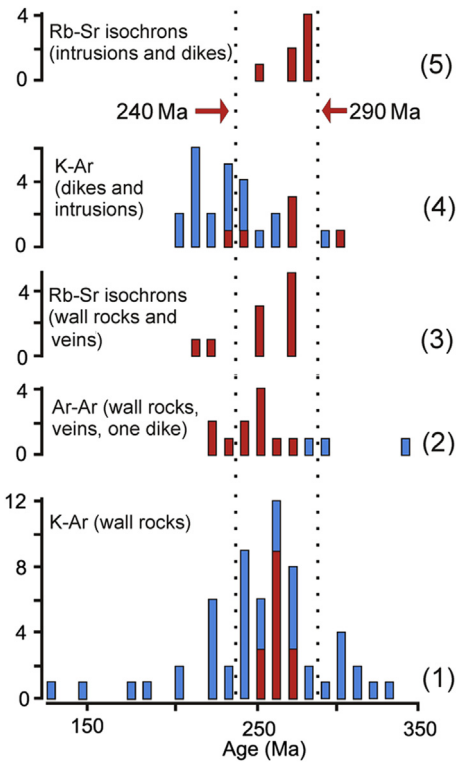

Figure 18. Compilation of K-Ar, Ar-Ar and Rb-Sr literature data for rocks and minerals from the Muruntau area (from bottom to top): (1) K-Ar data for wall rocks (metamorphic and metasomatic): red – minerals (biotite, amphibole, adular, muscovite); blue – whole rock samples; data compiled by Kostitsyn (1991b), Zairi et al. (1998) and Kempe et al. (2001a); (2) Ar-Ar plateau and integrated ages for wall rocks, veins and one dike sample from Muruntau: red – sericite and adular; blue – whole rock samples; data from Wilde et al. (2001); (3) Rb-Sr "density isochron" ages for metasomatites and veins from Muruntau (Kostitsyn, 1991b, 1996); (4) K-Ar ages for granitoid intrusions and dikes from the Muruntau area: red – minerals (biotite, amphibole); blue – whole rock samples; data compiled by Kostitsyn (1991b), Zairi et al. (1998) and Kempe et al. (2001); (5) Rb-Sr whole-rock and "density" isochron ages of granites and dikes from Muruntau (Kostitsyn, 1991b, 1996). Two reference lines are shown for comparison: (1) The line at 290 Ma is close to the zircon alteration ages for granitoids obtained by U-Pb SHRIMP analysis and Pb-Pb evaporation (290–294 Ma) and discussed by Kempe et al. (2015) and to the Re-Os arsenopyrite age (287.5 ± 1.7 Ma) reported by Morelli et al. (2007). (2) The reference line at 240 Ma is close to a precise conventional U-Pb zircon age (236.5 ± 1.4 Ma) reported by Nemchin (2002, personal communication cited in Kempe et al., 2015) for a dike sample.

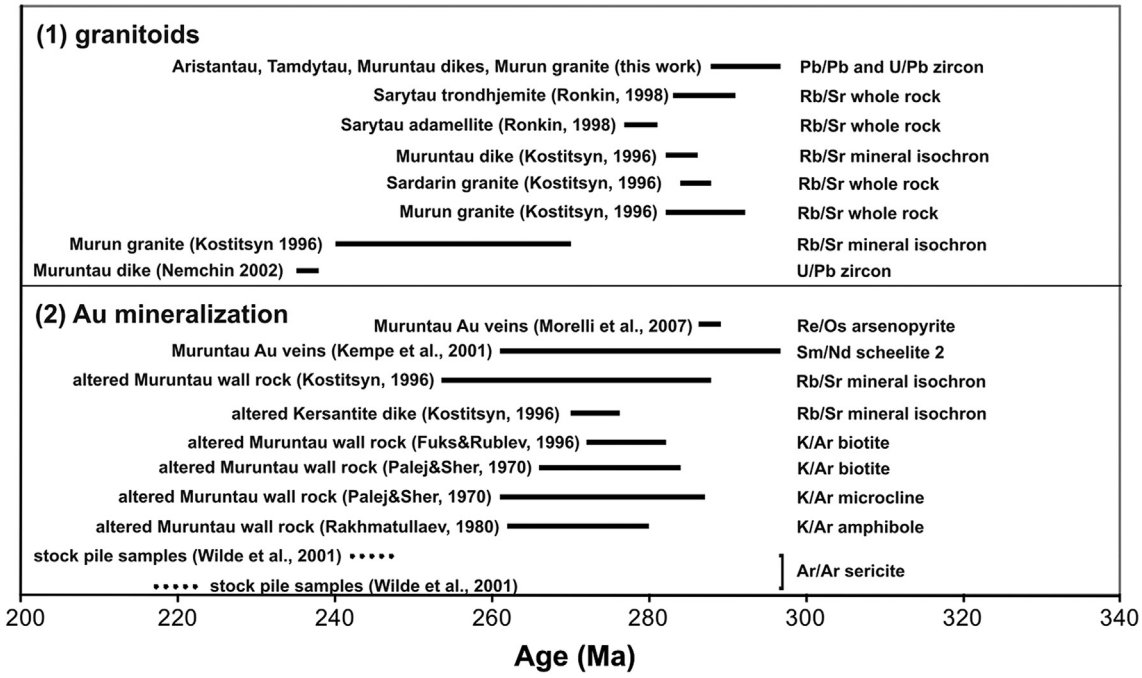

Figure 19. Compilation of absolute age data for (1) granitoid intrusions and dikes in Muruntau and adjacent areas and (2) Au mineralization (minerals and rocks) at Muruntau. The main magmatic activity cannot be clearly resolved from Au mineralization although the latter seem to be somewhat younger. Younger magmatic and hydrothermal activity is indicated for Triassic times. Figure from Kempe et al. (2015).

(1) There is some apparent "increase" in the defined ages when passing on from K-Ar and Ar-Ar to Rb-Sr, Sm-Nd, Re-Os and U-Pb ages. This is not difficult to understand considering the "closure" temperatures of the related isotope systems or, more exactly, the susceptibility of the minerals or rocks to secondary alteration. Before interpreting isotope age data for systems with complicated histories, it appears useful to recall the two prerequisites which are necessary to obtain reliable age information: the "starting" and the "boundary" conditions (e.g., Faure, 1986). The first ("starting") condition is the state of homogenization of the isotope system under study (rock, mineral, part of crystal etc.) in respect of the initial isotope ratios of the daughter element. The second ("boundary") condition demands that the isotope system remained closed to exchange of the related elements or isotopes after the "isotopic clock" started to work. Caution is therefore generally advisable in the interpretation of absolute age data. Below, we will evaluate published ages keeping this point in mind.

(2) Although there is a large spread in the data, the absolute ages defined by various methods and isotope systems cluster at 260–300 Ma (Figs. 18 and 19) indicating that a peak of tectonic, magmatic and/or hydrothermal activity occurred at that time. This point was acknowledged earlier by Zairi et al. (1998) when evaluating available K-Ar and Rb-Sr data.

Considering early K-Ar data, we found that many analyses were conducted using whole rock samples – a method commonly not suitable for age determination because of the frequent open system behavior of feldspars (excluding late adularia) and some other minerals and the common occurrence of "excess" Ar. Therefore, we focus in our discussion on the analyses of mineral separates of mica and amphibole (Kostitsyn, 1991b; Kempe et al., 2001a). The K-Ar ages from the literature were recalculated according to recently used decay constants for the K-Ar system if necessary (Kempe et al., 2001a).

An extensive study of the Rb-Sr isotope system of metamorphic, magmatic and metasomatic rocks and ore veins was undertaken by Kostitsyn (1991b, 1993, 1994, 1996). Kostitsyn and Rusinova (1987) developed a method for samples with sub-microscopic mineral intergrowths using the density fractions of a sample to obtain Rb-Sr isochrons ("density isochrons"). This approach was subsequently applied by Kostitsyn to various rock and vein samples from the Muruntau ore field. However, such isochrons may represent mixing lines of two end-members (mineral isotope systems) because all fractions are obviously mixtures of two or more minerals. Note that the isotope systems of original rock and vein samples from Muruntau often appeared to be disturbed by alteration or by initial isotope heterogeneity (Kostitsyn, 1991b, 1993, 1994, 1996).

7.1.1. Geological age constraints

Before turning to a detailed discussion on the absolute age data obtained by various methods, it is useful to recall age constraints as derived from the geological observations reviewed above in sections 4 and 5:

(1) There are no clear geological constraints for the sedimentation ages of the rocks of the Besapan and Taskazgan Sequences besides the fact that they are intruded by the granitoids and dike series (upper age limit). The paleontological record allows large variations in possible sedimentation ages from late Proterozoic to late Ordovician (O). However, the zircon ages for the Kosmanachi suite may indicate an older sedimentation age. Clearly, the highly deformed rocks of the Besapan Suite are pre-Devonian because they are overthrust by almost unfolded Devonian (D) to Carboniferous (C) carbonates.

(2) Regional metamorphism predates magmatic intrusive event(s) because contact aureoles overprint the earlier metamorphic assemblages. It is, however, unclear when the stack of nappes, the Muruntau lens and the related flat-dipping shear zones including the prominent Sangruntau-Tamdytau zone may have

formed. Mukhin et al. (1988) suggested that the nappe structure formed in pre-Devonian time while Drew et al. (1996) assumed a Carboniferous (C) age for the Sangruntau-Tamdytau shear zone formation. The timing of the thrusting event involving Devonian (D) and Carboniferous (D) limestone and dolomite is also not well constrained from geological data (besides a defined late to post-Carboniferous maximum age). Whether or not these rock packages may have acted as a sealing "cap" promoting deposit formation remains ambiguous. Drew et al. (1996) inferred a late Carboniferous (C_2) to early Permian (P_1) age of the thrust based on apparent intrusive relationships between granites and the sediments.

(3) The age of the granitoids and related dikes is better constrained because of the distinct relative age relations elsewhere in the Central Kyzylkum area. According to Askarov and Bigaeva (1965), Kotov and Poritskaya (1990, 1991) and Kol'tsov and Rusinova (1997), it falls into a range between late Carboniferous (C_2) and Permian (P). Similarly, Kostitsyn (1991a) reported granitoids in the adjacent Altyntau region intruding clastic and carbonate sediments of Devonian (D) to middle Carboniferous (according to Soviet stratigraphy) age.

(4) According to Badalova and Palej (1965) and Palej (1968), geological data suggest different ages for low-sulfide gold mineralization, which is superimposed on the Hercynian granitoids and dikes (late Carboniferous C_2 to Permian P) on one hand, and for silver-rich high-sulfide mineralization which occurs in Triassic (T) sediments and volcanics, on the other. Similar conclusions were drawn by Voronkov and Yakovlev (1980).

7.1.2. Absolute age of metamorphism

According to tectonic analysis, the main folding and regional metamorphism are considered to be Caledonian (Drew et al., 1996). The Rb-Sr data reported by Kostitsyn (1996) suggest that the closure of this system in the metamorphic rocks occurred at about 400 Ma (one sample from Black Besapan Bs_2 and one from the Green Besapan Bs_4), while the K-Ar system yields similar numbers of 410–430 Ma (Loshchinin et al., 1986); i.e. upper Silurian to lower Devonian (D_1). This "closure" age may be regarded as a good age estimate for the final stage of regional metamorphism in the Muruntau area.

7.1.3. Absolute age of magmatism

K-Ar whole rock ages reported mainly for dike samples vary over a wide range from 200 Ma up to more than 300 Ma demonstrating a repeated opening of the related isotope system (Zairi et al., 1998, Fig. 18). K-Ar mineral ages defined for dikes in the ore field cluster around 240 Ma and may be related to late hydrothermal events overprinting that dikes (Kempe et al., 2001a, Fig. 18). Five K-Ar ages reported for the Tamdytau intrusion were also at least partly reset (Kempe et al., 2001a, 2015). There is a single K-Ar amphibole age of about 300 Ma for basalt from the nappe structure in the Tamdytau which possibly reflects a primary magmatic event (see compilation in Kempe et al., 2001a).

The Rb-Sr system of a sample from the Sardarin pluton as studied by Kostitsyn (1991b, 1996) seems not to be strongly affected by alteration. All fractions with feldspar and biotite as well as the whole rock sample plot on a single isochron defining an age of 286.2 ± 1.8 Ma and an initial Sr ratio of 0.70789 ± 12 (Kostitsyn, 1991b, 1996). This age is only slightly below the zircon alteration ages discussed below. Nevertheless, some disturbance of the isotope system seems to be present considering alteration features of mica and feldspar. In contrast, the Rb-Sr systems of samples from the Murun granite are strongly affected by alteration (Kostitsyn, 1996) in accordance with petrographic and mineralogical observations (e.g., Kempe et al., 2015). While eight whole rock samples of this granite defined an isochron (287.1 ± 4.6 Ma) with a remarkably high initial Sr isotope ratio (0.716 ± 15), a three-point mineral isochron yields a much lower age (255 ± 15 Ma) with an even higher initial Sr ratio.

"Density isochrons" for two dike samples from Muruntau underground mines are sub-parallel and define a similar age as for the granites of around 285 Ma (Kostitsyn, 1991b, 1996). However, two samples of an alkaline syenite and a kersantite dike yielded significantly younger ages by the density isochron method (average age 274.1 ± 3.9 Ma) similar to that of the gold-bearing metasomatites, but with lower initial Sr isotope ratios (0.70712 ± 39 and 0.70814 ± 12, respectively; Kostitsyn, 1991b, 1996, Fig. 18).

Nemchin (2002, personal communication cited in Kempe et al., 2015) reported a conventional U-Pb zircon age for a stock-pile sample of a dike of 236.5 ± 1.4 Ma – much lower than U-Pb zircon SHRIMP and Pb-Pb zircon evaporation ages discussed by Kempe et al. (2004, 2015) for one sample from the Aristantau granite, three from the Tamdytau intrusion, one from the Murun granite and one from a granodioritic dike sampled in the open pit (Fig. 19). Considering geological relations discussed above in section 5.3, it cannot be excluded that the age defined by Nemchin (2002, personal communication cited in Kempe et al., 2015) represents indeed a younger magmatic event. On the other hand, Kempe et al. (2015) argued that their U-Pb concordia ages between 290 and 294 Ma obtained for U-rich zircon or parts of zircon crystals (hydrothermal overgrowths) define the time of albitic alteration rather than that of intrusion. The somewhat higher U-Pb SHRIMP ages found for small crystals from the dike sample without overgrowth and not significantly affected by post-magmatic albitization (Kempe et al., 2015) may hint at an intrusion of the dike at about 305 Ma. Even older U-Pb SHRIMP concordia ages (327 ± 5 Ma) were reported by Mirkamalov et al. (2012a,b) for zircon from a migmatite-granite-gneiss complex in the Zarafshan zone of south Uzbekistan. The relation of the latter magmatism to that in the Muruntau region is, however, equivocal.

7.1.4. Attempts at absolute age determinations for metasomatic alteration and gold mineralization

K-Ar and Ar-Ar isotope analyses of mica and amphibole from the gold-bearing metasomatites and veins yielded a large scatter of ages between 230 and 280 Ma with a peak at about 250–260 Ma (Zairi et al., 1998; Kempe et al., 2001a; Wilde et al., 2001; Fig. 18). However, the K-Ar system provided precise age constraints only in some particular cases when the isotope system was not disturbed by late alteration as in the case of biotite from the biotite metasomatites (Palej and Sher, 1970) and of late adularia (see below in this paragraph). Note that the K-Ar and Ar-Ar ages are in good accordance with the Rb-Sr data for the latter mineral in the late veins. Wilde et al. (2001) attempted an Ar-Ar age determination for the gold mineralization using sericite mainly from vein selvages and metasomatites. However, as demonstrated in the preceding paragraphs, sericite was formed during late hydrothermal activity, subsequent to the main magmatism, high-temperature K-metasomatic alteration and the high-temperature stage of vein formation with the latter related to a first important event of gold precipitation. Accordingly, the ages defined by the Ar-Ar method cluster well below 290 Ma at two main values at about 245 and 220 Ma, respectively (Wilde et al., 2001, Fig. 18). Unfortunately, the samples used by these authors seemed not to be an ideal subject for Ar-Ar work due to the frequent absence of heating plateaus, the occurrence of excess Ar and later age disturbances (Wilde et al., 2001).

Kostitsyn (1991b, 1993, 1994, 1996) studied the Rb-Sr isotope system of metasomatic rocks and of vein samples. Often, the isotope system of the metasomatites showed initial isotope

heterogeneity for Sr or later disturbances. Nevertheless, Kostitsyn (1991b, 1994, 1996) succeeded in the definition of "density isochrons" for four rock samples of K-feldspar and biotite metasomatites defining an average age of 272.6 ± 3.8 Ma with relatively high initial Sr isotope ratios at about 0.716. The average age is close to that obtained for alkaline dikes by the same method (Fig. 18). Considering the metasomatic nature of the "alkalinity" of the dikes (Kostitsyn, 1991b), we suggest that the Rb-Sr "intrusion ages" obtained for these dikes may simply reflect alteration ages as in the case of the metasomatites (cf. Kempe et al., 2001a). The Rb-Sr isotope system of a sample of banded metasomatite showed initial isotope heterogeneity (Kostitsyn, 1991b, 1994). The sericite-bearing density fractions of another sample defined a distinctly younger isochron age (256.8 ± 9.9 Ma; Kostitsyn, 1991b, 1994, 1996) compared to the other fractions. In this latter case, the initial Sr isotope ratio also displayed enhanced heterogeneity varying between 0.713 and 0.714 at somewhat lower values than for the other samples of metasomatitic rocks studied (Kostitsyn, 1994).

Density isochron ages were also defined for three vein samples representing late, group 3 vein types: a quartz − tourmaline vein (257 ± 13 Ma), a quartz − arsenopyrite vein (230.2 ± 3.5 Ma) and a quartz − adularia vein (219.4 ± 4.2 Ma; Kostitsyn, 1993). Note that the latter value is in good accordance with Ar-Ar data for adularia (221.8 ± 0.9 Ma; Wilde et al., 2001) and K-Ar ages of sericite (224 ± 10 Ma) from this vein type, although there are some other K-Ar data for adularia suggesting slightly higher ages at about 242–247 Ma (cf. Kempe et al., 2001a).

Kempe et al. (2001a) used the Sm-Nd system of scheelite II associated with gold to constrain the absolute age of the early gold mineralization. The obtained isochron defined an age of 279 ± 18 Ma (MSWD 1.5; $\varepsilon_{Nd} = -9.5 \pm 0.3$). This is close to the ages defined by the Rb-Sr method for the ore-bearing metasomatic rocks. However, the precision of the Sm-Nd age is relatively low due to the weak spread in the Sm/Nd ratios of the analyzed scheelite samples. For scheelite 1 from the "flat" veins, another isochron with a related age of 351 ± 22 Ma was obtained. Although this may be a "mixing line" formed by alteration during later gold mineralization, this apparent isochron indicates the existence of a distinctly older mineralization event. Such an inference is confirmed by the analysis of the ε_{Nd} values which are distinctly different for scheelite I (−8.4) and scheelite II (−9.5) and remain so even when re-calculated for a time at 280 Ma for both systems (Kempe et al., 2001a, Fig. 17b).

The Re-Os isotope system of arsenopyrite from larger arsenopyrite- and pyrite-bearing gold-rich veins was studied by Morelli and co-workers (Morelli et al., 2004, 2007). Preliminary results for nine samples collected randomly from a single hand specimen defined an isochron age of 286 ± 5 Ma interpreted as the formation age of the arsenopyrite and the associated gold (Morelli et al., 2004). However, there was a large scatter in the data reflected by the error and the high MSWD of 5 despite a very large spread in the Re/Os ratios (from 500 up to 6000). Later, two additional samples were studied with the resulting three isochron ages overlapping with each other within error: 288.6 ± 5.6, 290.4 ± 4.5, 296.4 ± 6.1 Ma (Morelli et al., 2007). As discussed by the cited authors, there are indications for some heterogeneity in the Re-Os isotope systems. For example, it was not possible to include all three sample suites together in one regression procedure. It remains, however, unclear whether the obtained uncertainties and variations are related to initial isotope heterogeneity, late disturbances or some real age distributions. Note that a large spread in the mother/daughter element ratios normally indicates a fractionation degree not commonly reached in a homogeneous system, but often by mixing or alteration effects.

Summarizing, all isotope systems used to obtain age constraints at the gold mineralization at Muruntau suffer from effects of initial isotope heterogeneity and later disturbances. This applies not only to less stable systems as that of K-Ar in mica or of Rb-Sr in whole rock samples but also to more robust systems as the Sm-Nd system of scheelite, U-Pb system of zircon and the Re-Os system of arsenopyrite. Fortunately, the effect on the latter systems is not so large to prevent any absolute age determination (Fig. 19). However, the obtained values should be used with caution. On the other hand, the isotope data obtained clearly reflect the repeated pulses of tectonic and hydrothermal activity operative during the formation of this giant gold deposit.

7.2. Genetic concepts

Various conflicting genetic concepts have been developed for the formation of the giant Muruntau gold deposit in correspondence with the complexity of observations on geological structures, intrusive events, metasomatic processes and vein systems. However, due to this complexity, none of these authors succeeded to present a holistic model that addresses all the observations reported so far (Kotov and Poritskaya, 1990, 1991; Marakushev and Khokhlov, 1992; Zairi and Kurbanov, 1992; Kol'tsov and Rusinova, 1997; Wall et al., 2004; Hall and Wall, 2007). In the following discussion, we will consider for clarity separately the suggested sources of the gold and the inferred processes of enrichment and precipitation of native gold (Table 1).

Historically, the concepts of formation of the Muruntau deposit were strongly influenced by the knowledge on the gold distribution within various types of vein structures and host rocks. Originally, the gold mineralization was exclusively assigned to crosscutting quartz veins and stockworks (e.g., Zarembo, 1968; Palej and Sher, 1970) and the classical hydrothermal concept was the dominating one (e.g., Bendik et al., 1969a; cf.; Kremenetsky et al., 1990). Later, economic gold contents in the wall rocks and their stratiform-like distribution as well as enhanced "background" gold contents in the whole Variegated Besapan Suite were revealed by extended sampling (e.g., Protsenko, 1987). The prevailing concepts in this period focused on syn-sedimentary enrichment of gold culminating in the definition of a new "Kyzylkum-Type" of gold deposits related to black shales (Gar'kovets, 1971, 1973). More recently, the column-like character of the ore bodies resulting from a combination of stratiform-like wall rock alteration and cross-cutting vein formation was established (Bojtsov et al., 1996; Kremenetsky et al., 1996; Wall et al., 2004; Obraztsov, 2009). Accordingly, the developing views led to a renaissance of hydrothermal concepts, but often included the assumption of a deep-seated source of the ore-forming fluids (see below).

Most authors concur in the conclusion that deposit formation at Muruntau passed through several stages (Petrovskaya, 1968; Zarembo, 1968; Sher, 1970; Rakhmatullaev, 1980; Voronkov and Yakovlev, 1980; Loshchinin et al., 1986; Mukhin et al., 1988;

Table 1
Genetic concepts.

Gold sources	
1	Detrital gold (paleo-placer)
2	Gold-rich black shale
3	Granite magma
4	Sub-crustal (mantle) sources
Processes of enrichment and precipitation	
1	Circulation of near-surface brines
2	Metamorphic processes including shearing and circulation of metamorphic fluids
3	Activity of granite-related fluids or/and thermal aureoles around intrusions
4	Mantle-induced fluids
Polygenetic and polychronic concepts	

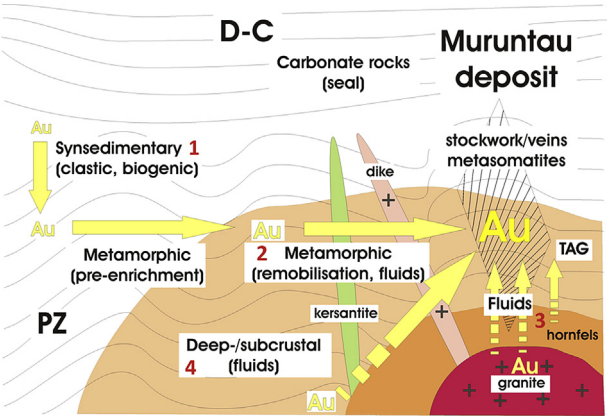

Figure 20. Sketch illustrating most popular genetic concepts for the formation of the giant Muruntau Au deposit: (1): Synsedimentary deposition of clastic or dissolved Au with sorption on biogenic carbon; subsequent pre-enrichment of Au during regional metamorphism; (2) Remobilization and precipitation of Au in the vein system during tectonic-metamorphic activity; (3) Precipitation of Au in the vein system and metasomatites by fluids generated by the granitoid intrusions or driven by the thermal aureole of such intrusions (TAG according to Hall and Wall, 2007); (4) Au supply into the vein system by fluids of deep- or subcrustal origin possibly related to mantle magmatism.

Berger et al., 1994; Konstantinov et al., 2000; Graupner et al., 2005a; Bierlein and Wilde, 2010; Rafailovich et al., 2013). However, there is no agreement in the definition of the main sources and the principal process leading to the enrichment and precipitation of the gold. It is also a point of controversy, whether various stages of deposit formation are part of a single evolutionary process or belong to different tectonic and/or hydrothermal events. Some authors even assumed a single tectonic/magmatic/hydrothermal process (although developing through several stages) to be responsible for the formation of this giant gold deposit (e.g., Kotov and Poritskaya, 1990, 1991; Drew et al., 1996).

Some authors have suggested that the principal process of gold enrichment occurred synsedimentary, prior to metamorphism, magmatism, and vein formation, i.e. during formation of the shelf sequences (Fig. 20). According to this viewpoint, all later processes of metamorphism, magmatism, metasomatic alteration and vein formation resulted just in a redistribution and final enrichment of the pre-existing gold. The latter processes are therefore considered isochemical in nature (Gar'kovets, 1978). Primary gold accumulation may have formed in placers (in particular, in a river delta; Voronkov, 1976), by sedimentation of fine-dispersed gold or by chemical sorption of the gold on organic carbon (Gar'kovets, 1969, 1971, 1973, 1975, 1978; Rafailovich et al., 2013). It has been suggested that the secondary redistribution and vein formation represent the result of long-lasting circulation of metamorphic fluids during brittle deformation of the Au-bearing rocks (Gar'kovets, 1969, 1971, 1973; Bel'kova and Ognev, 1971; Mukhin et al., 1988). Another group of authors favoured a supply and precipitation of gold entirely by metamorphic fluids (Loshchinin et al., 1986; Protsenko, 1987). The majority of workers concluded from their data that classical hydrothermal processes resulted in the formation of the giant Muruntau deposit (Petrovskaya, 1968; Zarembo, 1968; Bendik et al., 1969a; Kotov and Poritskaya, 1990, 1991; Kostitsyn, 1996; Kol'tsov and Rusinova, 1997; Graupner et al., 2001a, 2005a,b, 2006; Kempe et al., 2001a; Monecke et al., 2002; Wall et al., 2004). Nevertheless, hydrothermal systems may have been active within the deposit at different times (Bendik et al., 1969a; Kostitsyn, 1996; Graupner et al., 2001a; Kempe et al., 2001a; Bierlein and Wilde, 2010). There is no agreement among the authors in favour of a hydrothermal genesis of the deposit, whether the hydrothermal systems were driven by granitic magma and/or metamorphism, both triggering a thermal gradient responsible for creating "thermal aureoles" (Kremenetsky, 1994; Wall et al., 2004; Hall and Wall, 2007) or by a deep-seated, lower crustal- or mantle-related magmatic or any other juvenile source (Petrovskaya, 1968; Kotov and Poritskaya, 1990, 1991; Kempe et al., 1997; Kol'tsov and Rusinova, 1997; Graupner et al., 2006; Fig. 20). According to Kostitsyn (1991b, 1996), late magmatism and ore formation occurred more or less simultaneously but were not directly linked to each other. This inference is in agreement with suggestions made by Yudalevich and Levchenko (1981). Kotov and Poritskaya (1990, 1991) assumed a progressive involvement from moderate depth to lower crustal material in magma formation (evolution from granitic to kersantitic magmas) and in hydrothermal activity with only limited interaction between the magmas and the fluids. According to this model, fluid generation occurred at lower crustal levels, i.e. below the level of magma formation (so-called "transmagmatic fluids"). A similar model was favoured by Kol'tsov and Rusinova (1997), which compared biotite-K-feldspar metasomatites at Muruntau to similar metasomatic rocks common in porphyry-copper deposits and assigned to "transmagmatic fluids" in the Russian literature. In contrast, Kremenetsky et al. (1996) inferred that evolution of the Kyzylkum gold province started with formation of a mantle plume with later generation of local bimodal magmatic and related fluid systems resulting in gold deposit formation. This concept is in several aspects similar to the thermal aureole gold (TAG) concept (Wall et al., 2004; Hall and Wall, 2007) and that suggested by Bierlein et al. (2006). A rather vague hypothesis was presented by Marakushev and Khokhlov (1992). These authors suggested an infiltration of the gold-rich metamorphic shales by supercritical lamprophyric magmas (i.e. magmas with temperatures above the critical point for liquid and gas) resulting in "fluid-magmatic replacement" and formation of gold-rich "metasomatites". In accordance with Graupner et al. (2006) and based on Re-Os-He isotope data, Morelli et al. (2007) concluded that a mantle-related or other juvenile fluid was involved in formation of the auriferous veins. On the other hand, a time overlap between ore formation and granite magmatism is evident according to these authors. Note that the latter conclusion is in some accordance with findings by Kostitsyn (1996), Kempe et al. (2001a, 2015), Wall et al. (2004) and Hall and Wall (2007). Drew et al. (1996) stressed a structural control during ore formation changing in time by a transition from shearing along the Sangruntau-Tamdytau towards main deformation within the Muruntau-Daugyztau shear zone, accompanied by the intrusion of granites. The concept developed by Wilde et al. (2001) favoured deposit formation at a very late stage of tectonic evolution, namely in the Triassic (T), by long-lasting circulation of low-temperature near-surface brines involving a major rift with the fluid source within these Devonian (D) to Triassic (T) evaporites.

Consequently, there is substantial controversy on (1) the possible mechanism of primary Au enrichment during sedimentation, metamorphic processes and magmatism, (2) the timing of Au mineralization and vein formation. In the following, we will discuss some constraints on the genesis of the Muruntau deposit derived in the light of available, in particular, more recent data as reviewed in the preceding paragraphs.

8. Discussion

8.1. Regional and stratiform-like enrichment of gold

The role of gold, which may have been enriched in the sedimentary rocks already during deposition, is not yet well studied. Despite repeated claims in the literature, there seem to be no

reliable data constraining the mode of gold occurrence (secondary, primary clastic, fine-dispersed or adsorbed on carbonaceous matter) in the meta-sedimentary and meta-volcanic rock packages outside the Muruntau deposit (Golovanov et al., 1998b). The discussion is therefore restricted to enhanced gold content of several tens to hundreds of ppb established by whole rock analyses. Similarly, we have not found published data constraining the possible role of carbonaceous matter or of organic carbon in these rocks, although such carbon has been repeatedly argued to act as the carrier of adsorbed or finely dispersed gold. According to Rusinova et al. (1996), only high-ordered graphite was identified in the unaltered metamorphic packages. It remains therefore an open question whether the enhanced gold content in the host rocks outside the deposit resulted from accumulation during sedimentation or from subsequent metasomatic alteration. One possible pass-way for late gold-bearing fluids in the Variegated Besapan (or Kosmanachi Suite) was formed by the nearly bedding-parallel Sangruntau-Tamdytau shear zone. Gold may have been enriched, for example, during the formation of the early, pre- or synmetamorphic "flat" quartz veins or during formation of high-temperature gold-rich metasomatites.

Two arguments point clearly against an isochemical syn-sedimentary – epigenetic mechanism of gold enrichment at Muruntau. Firstly, zones of gold depletion, from where the gold has been extracted to be subsequently transported and re-precipitated in the vein structures and ore-bearing metasomatites (by analogy, e.g., to the well documented redistribution of carbon) could not be identified. Secondly, calculations by Kotov and Poritskaya (1990) demonstrated that the potential gold resources in the metamorphic rocks outside the deposit are far too small to explain the established giant economic reserves of the Muruntau deposit.

8.2. The role of carbon

Although the prominent role of black shales in deposit formation at Muruntau is controversial, the possible role of carbon is worth noting. Carbon may be found throughout the deposit in various forms: as well-ordered graphite enclosed in metamorphic quartz or as calcite in carbonate-rich layers, lenses or cements in the metamorphic wall rocks, as hydrothermal disordered graphite and as carbonate at the vein selvages, in veins and breccias bodies and as carbon dioxide, methane, and higher hydrocarbons trapped in fluid inclusions (e.g., Rusinova et al., 1996; Graupner et al., 2001a). As demonstrated before, the role of carbonate minerals within the vein structures increases from the early to the late vein types. Higher amounts of disordered graphite were also found in late veins, breccia bodies and reactivated faults, in particular, close to and within the southern Fault zone. In the fluids, there is a tendency for increasing CO_2 and decreasing CH_4 contents during fluid evolution. It seems that carbon may have played a key role not so much in a debatable fixation of gold in the unaltered host rocks, but rather in gold mobilization, transport and, finally, in its precipitation in the quartz veins and metasomatites. The carbon from the host rocks was apparently only redistributed as indicated by the stable isotope data. It seems, however that additional carbon was supplied by the hydrothermal fluids into the vein system (Graupner et al., 2001a). Besides some nitrogen and chlorine, carbon species are the only (and dominating) compounds in the fluids which may have significantly influenced the solubility and complexation behavior of the gold (cf. Marakushev and Khokhlov, 1992). Note that up to now, H_2S was found only in very low concentrations and restricted to late vein quartz (Wilde et al., 2001). The amount of sulfides in the deposit is generally low. Nevertheless, a possible role of sulfidation during gold precipitation cannot be ruled out considering the common occurrence of iron sulfides in the wall rocks (e.g., Wall et al., 2004). Clearly, relations between higher hydrocarbons, methane, graphite and carbon dioxide reflect not only fluid evolution leading to phase separation (Graupner et al., 2001a), but also changing redox conditions within the fluids during gold precipitation.

8.3. Mineralization and tectonics: regional distribution of gold deposits

Several studies on the structural control of magmatism and hydrothermal activity indicated that the main tectonic elements defining the geological setting of the gold ore mineralization at Muruntau are regional fault zones. Muruntau is located just at the intersection of the subhorizontal, left-lateral, east-west tending Sangruntau-Tamdytau shear zone with the steeply-dipping, left-lateral, northeast-tending Muruntau-Daughyztau shear zone (e.g., Drew et al., 1996). Other Au and Au-Ag deposits in this area, which are exposed within the Paleozoic outcrops, are grouped along these two faults: (1) The Amantaitau, Daughyztau, Vysokovoltnoe and Kolchik deposits are located to the southwest. (2) The Myutenbai deposit is found to the southeast and the Besopan and Kosmanachi deposits to the west from Muruntau. Moreover, there seems to be a general decrease in deposit size, formation temperature and an increase in the role of silver in the ores with increasing distance from the Muruntau deposit (e.g., Bierlein and Wilde, 2010). This situation highlights the importance of deep crustal (meso-to hypozonal) processes in the formation of gold systems in the Kyzylkum area.

8.4. Timing of metamorphism, magmatism, metasomatism, and vein formation

Although absolute age data do not provide very precise information on the timing of the main tectonic, magmatic and hydrothermal events involved in deposit formation, we have some clear time evidence to define some principal genetic aspects for Muruntau. First of all, intense tectonic, magmatic and hydrothermal activity in the Muruntau area falls into an interval between late Carboniferous and late Triassic (from about 320 to about 220 Ma) with a peak in the Permian (300–260 Ma). It appears, therefore, very likely that these are the time brackets for formation of the main gold mineralization (Bierlein et al., 2006). Interestingly, exactly the same conclusion was reached much earlier by Gar'kovets et al. (1970) analyzing regional geological data of gold mineralization in the Tien Shan area. Secondly, regional metamorphism finished in the early Devonian at about 400 Ma, well before the peak of magmatic and hydrothermal activity in the region. The main magmatic activity falls in a time interval between 305 and 285 Ma (late Carboniferous–early Permian); as discussed in section 7.1.3, an age close to 300 Ma is more likely. It remains, however, an open question whether some later magmatic events have to be considered as well. Results reported by Zarembo (1968) and Nemchin (2002, personal communication cited in Kempe et al., 2015) indicate some additional magmatic activity in the early Triassic (at about 255 Ma). Likewise, the age of lamprophyre and kersantite magmatism in the region remains equivocal although there are indications that it may have occurred closely in time to the main granite magmatism at 290–300 Ma.

According to Sm-Nd, Rb-Sr and K-Ar data, the formation of Au-rich potassic metasomatites and of high-temperature Au-bearing group 2 quartz veins roughly overlap in time (275–280 Ma). These age data are, however, in some conflict with the higher Re-Os arsenopyrite ages clustering around 290 Ma as defined by Morelli et al. (2004, 2007). Note that although the latter measurements are more precise, the former results were obtained utilizing three

independent isotope systems. It is not yet feasible to resolve a possible age difference between the main granite magmatism on the one hand and the high-temperature alteration and vein formation on the other (e.g., Morelli et al., 2007; Kempe et al., 2015). Likewise, there may have been a time overlap between granite magmatism and high-temperature hydrothermal activity. On the other hand, the isotope data clearly demonstrate that there were at least three periods of hydrothermal activity distinctly separated from each other in time: (1) Sm-Nd isotope systematics of scheelite I yield strong evidence that the early scheelite I in the flat veins must have been formed long before the later scheelite II in the cross-cutting stockwork structures, although it is not yet possible to define the absolute formation age for scheelite I. This inference supports similar conclusions made from geological and mineralogical observations as reviewed in section 5.2. The apparent isochron age of 350 Ma for scheelite I is well below the Rb-Sr and K-Ar closure ages of the metamorphic sequences quoted in the previous paragraph. Nevertheless, a formation of the ductile deformed "flat" veins during or before the intense folding of the Besapan rocks could not be excluded or verified. (2) A second stage of hydrothermal activity is commonly linked to the formation of the main Au-bearing quartz veins (group 2 "Central" and surrounding stockwork veins) and to potassic alteration at about 280–290 Ma. Both processes occurred at relatively high temperatures around 400–420 °C as indicated by thermodynamic data for the alteration assemblages, the mineral assemblages present in the veins and fluid inclusion data. (3) At least one, but possibly two or more late and low-temperature hydrothermal events are indicated by disturbed or late Rb-Sr, K-Ar and Ar-Ar ages of vein systems, mica and adularia. One event seems to be adequately constrained at about 220 Ma (late Triassic) by Rb-Sr, K-Ar and Ar-Ar isotope data for adularia-bearing veins. Possibly, another event occurred at about 240–250 Ma (early Triassic), but more efforts are needed for clarification. As we have shown, the first and the second hydrothermal events are considered to be related to economic gold precipitation. Nevertheless, the main ore mineralization is related to the formation of group 2, cross-cutting and high-temperature quartz veins and of the enveloping biotite and K-feldspar-rich metasomatites.

Closer examination of the Au-rich "Central" quartz veins revealed that there were at least two consecutive stages of gold precipitation in these veins, which are not yet resolved from each other in time by isotope research. During the early phase, moderate Ag-bearing, small idiomorphic Au I crystals precipitated simultaneously with normally zoned, hydrothermal quartz. Similar gold formed in the altered K-rich wall rocks. Subsequently, these veins (and in particular, the quartz) were strongly affected by brittle deformation. During this event, phase separation occurred within the fluids and a Ag-poor, commonly larger and anhedral Au II formed within grain interstitials and, again, in the adjacent wall rocks (Graupner et al., 2005a).

8.5. Breccia-related mineralization?

We should consider here the occurrence of breccia textures within the ore bodies in some more detail. Marakushev and Khokhlov (1992), Drew et al. (1996) and Bierlein and Wilde (2010) noticed the frequent occurrence of breccia textures in the metasomatic wall rocks. Marakushev and Khokhlov also described a common observation of local breccia controlling gold distribution within the biotite metasomatites. The features described by these authors apparently differ from the fault-controlled breccia normally met within late alteration assemblages close to the southern Fault zones mentioned in paragraph 5. Earlier, two types of breccia (one fault-controlled and another related to veining in the stockwork) were described by Bendik (1969). Graupner et al. (2000) described breccia textures common in vein quartz of the "Central" veins revealed by CL. These textures control the distribution of Au II. Breccia textures were also noticed by Kempe et al. (2001a,b) for scheelite II, monazite and allanite, respectively. Similar observations were reported by Bierlein and Wilde (2010) for arsenopyrite. Graupner et al. (2005a) found that breccia textures are common not only within vein quartz of "Central" veins but widely involve adjacent wall rocks. These observations raise the question on the nature of these breccia textures. Although Drew et al. (1996) related breccia formation to the activity of fault zones cross-cutting the deposit, we suggest here that the observed features are difficult to explain by a simple shear model. Considering the column (or cone-like) geometry of the ore bodies, we argue that the textures described within and adjacent to the "Central" veins may represent hydrothermal breccia (Bierlein and Wilde, 2010) or even an explosion breccia (caused by hydraulic fracturing) instead of tectonic breccia. To our knowledge, there were no special investigations on this subject so far.

8.6. Crustal and mantle sources

For the evaluation of the nature of the circulating fluids, several isotope and geochemical signatures have been examined. The resulting picture is, however, not as clear as may be expected. Initial isotope ratios of Sr and Nd defined for the vein mineralization and the ore-bearing metasomatites represent crustal signatures and indicate equilibrium with the host rocks (as are the stable isotope ratios of S and C). As discussed by Kostitsyn (1996) and Kempe et al. (2001a), these findings for Sr and Nd are not a proof for a metamorphic source of the fluids, but rather point to intense fluid-wall rock interaction. The trace-element signatures of the hydrothermal quartz also speak against a metamorphic fluid (Monecke et al., 2002). On the other hand, intense Sr and Nd isotope exchange between the fluids and magmatic or sedimentary carbonate rocks may be excluded. The isotope signatures for O and some noble gases (Ne, Kr, Xe; Graupner et al., 2006) point to an involvement of near-surface or even atmospheric gases. Br/Cl ratios and He isotope characteristics as well as some C isotope data indicate the involvement of sub-crustal, juvenile sources (Graupner et al., 2006). As demonstrated, it is difficult to relate gold mineralization to granite magmatism using the above criteria; the only hint at a possible role of granite magmatism is the close association with gold mineralization in space and time. Clearly, the formation of the contact aureole around the granite intrusion has changed the rock properties dramatically and, consequently, promoted extensive veining during deposit formation. On the other hand, genetic links to lamprophyre and kersantite magmatism remain also rather speculative.

8.7. Muruntau – a unique world-class Au deposit

One point of special interest is the unique size of the Muruntau deposit. Some authors have discussed this issue to some extent (Marakushev and Khokhlov, 1992; Drew et al., 1996; Konstantinov et al., 2000; Wilde et al., 2001; Wall et al., 2004; Bierlein et al., 2006; Bierlein and Wilde, 2010). According to Marakushev and Khokhlov (1992), two processes led to the occurrence of an extensive gold mineralization: (1) enrichment of gold and carbon in the host rocks and (2) interaction of these host rocks with lamprophyric magmas. Except for the particular mechanism suggested for gold redistribution, this concept is similar to the syn-/epigenetic model for "Kyzylkum-Type" gold deposits as outlined in section 7.2. Wall et al. (2004) acknowledged the special features of the host rocks (interbedding of conformable and brittle rocks, hornfels

formation etc.) allowing extended fracturing and permeability. These authors also suggested an important role of Devonian to Carboniferous carbonates as a seal on top of the hydrothermal system. According to Wall et al. (2004) a key role comes from a granite pluton at depth forming the hornfels aureole, supplying heat and auriferous fluids rich in S, As and W. These conclusions overlap to some extent with suggestions made earlier by Drew et al. (1996). The latter authors considered a long-lasting tectonic evolution as the essential condition for the formation of extensive gold mineralization: (1) regional metamorphism and the development of schistosity, (2) thrusting with related shear zones, (3) flat vein formation, (4) activation of the Muruntau-Daughyztau fault with stockwork formation, and (5) later waning stages. The role of the granite intrusion as a heat source was also acknowledged. Similarly, Wilde et al. (2001) stressed the long-lasting, polychronous formation of Muruntau which they see as the key-condition for the formation of a super-large gold deposit. According to Bierlein and Wilde (2010), the long-lasting evolution resulted in a combination of characteristics typical of two or more types of gold deposits.

We acknowledge the polygenetic nature of the ore-forming processes at Muruntau. Certainly, the formation of group 1 veins as well as of various group 3 veins and related metasomatites had an important impact on the concentration and redistribution of the gold within the deposit. However, the unique size of Muruntau is mainly defined by the giant hydrothermal system which has formed group 2 veins and the ore-bearing potassic metasomatites. We therefore suggest that the main ingredients for the formation of the super-large hydrothermal system, which distinguish Muruntau from other deposits in the region and elsewhere, are: (1) the intersection of two regional fault zones (Tamdytau-Sangruntau and Muruntau-Daughyztau) permitting quick ascent of fluids and, possibly, magmas from lower crustal levels; (2) the related high temperature (400–450 °C) of the ore-forming fluids as reflected by fluid inclusion characteristics and the alteration and vein mineral assemblages. The high temperature resulted in intense fluid-wall rock interaction; (3) the formation of a hornfels aureole in rocks including some with a relatively high porosity (psammites) allowed extensive veining on one hand and large-scale metasomatic infiltration and alteration on the other during high-temperature hydrothermal activity. One additional factor of importance may have been the inferred formation of pipe- or cone-like explosion breccia. Clearly, this latter assumption has to be explored in more detail. Our conclusions are similar to those drawn by Konstantinov et al. (2000) suggesting that the intersection of regional fault zones, the widespread occurrence of high-temperature potassic metasomatism and the poly-stage formation are the main conditions leading to the formation of a super-large gold deposit at Muruntau.

9. Outlook

According to our recent knowledge, it is highly unlikely that the Muruntau deposit is a classical metamorphic gold deposit, although there are some “metamorphic” isotope signatures – other geochemical and isotope markers are clearly non-metamorphic. There are no data clearly supporting a synsedimentary origin of the gold besides the enhanced gold contents in the Besapan Sequence. Similarly, the knowledge on the pre- or syndeformation “flat” quartz veins is still restricted. The main granite magmatism at Muruntau is at least close in time to the main hydrothermal activity, but there are no signs for an exchange of matter between the granitoids and the hydrothermal system(s). Exchange of matter with the hydrothermal system(s) is also not indicated for the lower Tasgazkan Sequence and the upper sedimentary dolomite. On the other hand, rather extensive and intensive high-temperature interaction is seen between the fluids and the wall rocks leading to the formation of Au-bearing metasomatites. An involvement of lower crustal- or mantle-related material or systems is indicated. There is, however, still no clarity concerning the heat source (granitoids or other magmatic systems, mantle plumes etc.) and the source of the elements enriched during hydrothermal activity as, for example, U, Th, W, As and, in particular, Au. Possibly, crustal thinning as assumed by Bierlein et al. (2006) was a global key factor in this respect.

Summarizing, considerable progress has been reached in the understanding of the genesis of the giant Muruntau gold deposit during the last decades. Nevertheless, fundamental problems still need to be addressed. So, the occurrence of low-level gold enrichment around the deposit is still to be studied in a systematic manner. Certainly, more efforts are needed in the field of absolute age determination to better constrain the timing of metamorphism, magmatism and hydrothermal activity. Systematic investigation of the U-Pb zircon age distribution in the unaltered host rocks outside the deposit may help to unravel their real sedimentation ages. Additional Rb-Sr and K-Ar or Ar-Ar investigations and fission track and/or U-Th-Sm-He studies on the same rock packages may be helpful to verify the thermal history of regional metamorphism and – inside the ore field – of hydrothermal activity. To constrain the timing of granite magmatism and of various hydrothermal events, studies on other mineral isotope systems (e.g., U-Th-Pb of rutile, monazite and/or allanite) may be helpful. Of particular importance are systematic studies on the dikes and the granite intrusions with the aim to verify their absolute and relative age relationships, petrology, alteration characteristics and the time relations to various vein systems and alteration styles. Hopefully, it would be possible to resolve absolute time relations between magmatism, metasomatism and veining more exactly. In this context, the genetic classification of vein types considering possible variations in mineral associations within each type should be verified. Other points still open for discussion are the possible role of granite and lamprophyre magmatism in the formation of gold mineralization and the association of gold with such “unusual” elements as tungsten and uranium.

Acknowledgments

The authors are indebted to A.A. Kremenetsky for his continuous support and early access to site and data since the early 1990s. Without the help provided by him and his colleagues of IMGRE Moscow and in Uzbekistan, our research at Muruntau would not have been possible. He supported our group during field work, in literature search and by providing numerous samples. Multiple field campaigns were supported by the Navoi Mining and Metallurgical Complex, Zarafshan Central Mine Board, Uzbekistan and, in particular, by A.I. Obraztsov.

S. Niedermann from the GFZ Potsdam is greatly acknowledged for noble gas analysis. We greatly benefited from the cooperation with various other expert scientists including V.J. Wall and G. Hall (who involved some of the authors during 2002–2004 in a project sponsored by CRC-PMD and Placer Dome), R. Morelli, R.A. Creaser, E.T.C. Spooner, C.J. Bray, J. Götze, B.V. Belyatsky, N. Rodionov, S.A. Sergeev, D.I. Matukov, V. Shatov, R. Koneev, M. Rafailovich, I.Golovanov and others. Our research was generously supported by several grants from DAAD, DFG (Wo 489/15-1, 15-2; KL 692/11-1, 11-2), NSERC, NHM CERCAMS, IGCP (IGCP-473) and other organizations. We wish to thank all these people and institutions. This paper is a contribution to the IGCP project 592 sponsored by IUGS and UNESCO.

We thank Prof. Franco Pirajno for his helpful critical comments on the manuscript.

References

Abrajevitch, A., Van der Voo, R., Levashova, N.M., Bazhenov, M.L., 2007. Paleomagnetic constraints on the paleogeography and oroclinal bending of the Devonian volcanic arc in Kazakhstan. Tectonophysics 441, 67–84.

Abramovich, Y.L., 1969. Distribution of iron, manganese, copper and minor elements in Devonian carbonate rocks at Muruntau (Central Kyzylkum). Doklady Akademii Nauk SSSR 186 (4), 928–931 (in Russian); English version: 1969, Doklady Akademii Nauk SSSR 186, 227–229.

Abrejevitch, A., Van der Voo, R., Bazhenov, M.L., Levashova, N.M., McCausland, P.J.A., 2008. The role of the Kazakhstan orocline in the late Paleozoic amalgamation of Eurasia. Tectonophysics 455, 61–76.

Akhber, D.Ya., Mushkin, I.V., 1976. The Kyzyl-Kum-Nurata deep fault, Tien Shan. Geotektonika (1), 95–102 (in Russian); English version: 1976, Geotectonics 10(1), 58–62.

Akhmedzhanov, M.A., Tsoj, R.V., Korsakov, V.S., Abduazimova, Z.M., Borisov, O.M., 1979. System of stratigraphical units in pre-Mesozoic rocks of Central Kyzylkum and adjacent areas. Uzbekskij Geologicheskij Zhurnal (3), 21–25 (in Russian).

Alekseyev, V.B., 1979. Succession of deformations in the Besopan suite (Paleozoic?), Kyzylkum. Geotectonica 13 (5), 58–66 (in Russian); English version: 1979, Geotectonics 13: 375–381.

Allen, M.B., Şengör, A.M.C., Natal'in, B.A., 1995. Junggar, Turfan and Alakol basins as Late Permian to ?Early Triassic extensional structures in a sinistral shear zone in the Altaid orogenic collage, Central Asia. Journal of the Geological Society 152, 327–338.

Allen, M.B., Anderson, L., Searle, R.C., Buslov, M., 2006. Oblique rift geometry of the West Siberian Basin: tectonic setting for the Siberian flood basalts. Journal of the Geological Society 163, 901–904.

Alyoshin, A.P., 1994. Evolution of mineralizing solutions and physicochemical characteristics of gold precipitation at the Muruntau deposit (Central Kyzylkum, Uzbekistan). In: 9th IAGOD Symposium, Beijing, China, v. 2, pp. 444–445 (extended abstract).

Askarov, F.A., Bigaeva, A.R., 1965. On the absolute age of magmatic events in the Kyzylkum desert. Uzbekskij Geologicheskij Zhurnal 4, 54–62 (in Russian).

Badalova, R.P., Palej, L.Z., 1965. Principal features of gold mineralization in Western Uzbekistan. Geologiya rudnykh mestorozhdenij 7 (5), 38–46 (in Russian); Englisch abstract: 1968, Economic Geology 63, 852.

Basov, V., 2015. The World Top 10 Gold Mines. http://www.mining.com (accessed: 17.06.2015).

Bendik, A.T., 1969. Geological position and formation conditions of the Muruntau ore field in the general geological patterns of the area. In: Khamrabayev, I.Kh (Ed.), Rudnye formatsii i osnovnye cherty metallogenii zolota v Uzbekistane. FAN, Tashkent, pp. 150–164 (in Russian).

Bendik, A.T., Kasavchenko, G.V., Sher, S.D., 1969a. On the problem of ore formation at Muruntau. In: Khamrabayev, I.Kh (Ed.), Rudnye formatsii i osnovnye cherty metallogenii zolota v Uzbekistane. FAN, Tashkent, pp. 189–192 (in Russian).

Bendik, A.T., Zarembo, Yu.G., Kasavchenko, G.V., 1969b. Special features of the localization and distribution of gold mineralization at Muruntau – morphological types of ore bodies. In: Khamrabayev, I.Kh (Ed.), Rudnye formatsii i osnovnye cherty metallogenii zolota v Uzbekistane. FAN, Tashkent, pp. 164–173 (in Russian).

Berger, B.R., Drew, L.J., Snee, L.W., 1994. An epoch of gold riches: the late Paleozoic in Uzbekistan, Central Asia. SEG Newsletters (16), 1–11.

Bel'kova, L.N., Ognev, V.N., 1971. Age and origin of gold mineralization at Muruntau. Doklady Akademii Nauk SSSR 197 (6), 1383–1386 (in Russian); English version: 1971, Doklady Akademii Nauk SSSR 197, 100–102.

Bierlein, F.P., Wilde, A.R., 2010. New constraints on the polychromous nature of the giant Muruntau gold deposit from wall-rock alteration and ore paragenetic studies. Australian Journal of Earth Sciences 57, 839–854.

Bierlein, F.P., Groves, D.I., Goldfarb, R.J., Dubé, B., 2006. Lithospheric controls on the formation of provinces hosting giant orogenic gold deposits. Mineralium Deposita 40, 874–886.

Biske, Yu.S., Seltmann, R., 2010. Paleozoic Tian-Shan as a transitional region between the Rheic and Urals-Turkestan oceans. Gondwana Research 17, 602–613.

Bojtsov, V.E., Ivanov, P.A., Pilipenko, G.N., 1996. A geological-genetic model for the formation of uranium-gold deposits. In: Litvinenko, V.S., Smyslov, A.A., Sokolovskij, A.K. (Eds.), Unique Ore Deposits of Russia. Principal Characteristics of Formation and Setting. Izd. Gornogo Universiteta, St. Peterburg, pp. 50–62 (in Russian).

Brown, S.M., Fletcher, I.R., Stein, H.J., Snee, L.W., Groves, D.I., 2002. Geochronological constraints on pre-, syn-, and postmineralization events at the world-class Cleao gold deposit, Eastern Goldfields Province, Western Australia. Economic Geology 97, 541–559.

Bukharin, A.K., Maslennikova, I.A., Zhuravleva, I.T., Mambetov, A.M., 1984. On the age of the Taskazkan and Besapan sequences (lower Paleozoic) in the Kyzylkum and their analogies in the Nuratau. Byulleten' Moskovskogo Obshchestva Ispytatelej Prirody. Otdel geologicheskij 59 (3), 57–68 (in Russian).

De Boorder, H., 2012. Spatial and temporal distribution of the orogenic gold deposits in the Late Palaeozoic Variscides and Southern Tianshan: how orogenic are they? Ore Geology Reviews 46, 1–31.

Dolgopolova, A., Seltmann, R., Armstrong, R., Belousova, E., Pankhurst, R., Konopelko, D., Koneev, R., 2013. Sr-Nd-Hf-Pb isotope mapping of Tien Shan in Uzbekistan. In: Proceedings of the 23rd Annual V.M. Goldschmidt Conference, Florence, Italy, 25–30 August 2013, Mineralogical Magazine 77(5), 1001 (abstract).

Drew, L.J., 1993. Geology of the Tamdy Mountains, Uzbekistan. US Geological Survey Miscellaneous Investment Map I–2386,1: 50,000-scale.

Drew, L.J., Berger, B.R., Kurbanov, N.K., 1996. Geology and structural evolution of the Muruntau gold deposit, Kyzylkum desert, Uzbekistan. Ore Geology Reviews 11, 175–196.

Ecomomos, R.C., Paterson, S.R., Said, L.O., Ducea, M.N., Anderson, J.L., Padilla, A.J., 2012. Gobi–Tianshan connections: field observations and isotopes from an early Permian arc complex in southern Mongolia. Geological Society of America Bulletin 124, 1688–1701.

Ermolaev, N.P., Chinenov, V.A., Khoroshilov, V.L., Goryachkin, N.I., 1994. Characteristics of the ore-forming fluids in gold and silver deposits in black shales. Geokhimiya (8/9), 1275–1286 (in Russian).

Ezhkov, Y.B., Rakhimov, R.R., 2012. Ore-magmatic systems in gold-ore districts of Uzbekistan: criteria for prognosis and search of large deposits as a base for extending their perspectives. Geologiya i mineral'nye resursy 4, 23–35 (in Russian).

Faure, G., 1986. Principles of Isotope Geology. Wiley & Sons, New York, 589 pp.

Gar'kovets, V.G., 1969. Pre-Paleozoic ore mineralization in Uzbekistan. Sovetskaya Geologiya (12), 51–59 (in Russian).

Gar'kovets, V.G., 1971. Syngenetical-epigenetical gold deposits of the Kyzylkum-Type. Sovremennoe sostoyanie ucheniya o mestorozhdeniyakh poleznykh iskopaemykh. Izd. AN UzSSR, Tashkent, pp. 53–55 (in Russian).

Gar'kovets, V.G., 1973. On the definition of the Kyzylkum-Type syngenetic-epigenetic deposits. Doklady Akademii nauk SSSR 208 (1), 163–165 (in Russian).

Gar'kovets, V.G., 1975. Lithological and geological-structural control of gold ore localization in deposits of the Kyzylkum-Type. Doklady Akademii nauk SSSR 222 (1), 193–196 (in Russian).

Gar'kovets, V.G., 1978. On formation conditions of syngenetic-epigenetic deposits of carboniferous ore formation (on the example of Uzbekistan)Carboniferous deposits and ore content of the Precambrian and lower Paleozoic. Academy of Sciences of the USSR, Frunze, Conference abstracts 28–29 (in Russian).

Gar'kovets, V.G., Babaev, K.L., Davletov, I.K., Malakhov, A.A., Palej, L.Z., Rakhmatullaev, K.R., 1970. General characteristics of gold metallogeny of the Tien Shan. In: Smirnov, V.I. (Ed.), Zakonomernosti razmeshcheniya poleznykh iskopaemykh, vol. 9. Problemy metallogenii Tyan′ Shanya, Nauka, Moskva, pp. 182–193 (in Russian).

Glorie, S., De Grave, J., Buslov, M.M., Elburg, M.A., Stockli, D.F., Gerdes, A., Van den Haute, P., 2010. Multi-method chronometric constraints on the evolution of the Northern Kyrgyz Tien Shan granitoids (Central Asian Orogenic Belt): from emplacement to exhumation. Journal of Asian Earth Sciences 38, 131–146.

Goldfarb, R.J., Taylor, R.D., Collins, G.S., Goryachev, N.A., Orlandini, O.F., 2014. Phanerozoic continental growth and gold metallogeny of Asia. Gondwana Research 25, 48–102.

Golovanov, I.M., Savchuk, Y.S., Voronkov, A.K., Khorvat, V.A., Shvetsov, A.D., Yudalevich, Z.A., 1998a. Geology of the Muruntau ore field. In: Shayakubov, T.S. (Ed.), Zolotorudnoe Mestorozhdenie Muruntau. FAN, Tashkent, pp. 78–164 (in Russian).

Golovanov, I.M., Protsenko, V.F., Arifulov, C.K., Dunin-Barkovskaya, E.A., 1998b. Mineral associations and peculiarities of economic gold ores. In: Shayakubov, T.S. (Ed.), Zolotorudnoe Mestorozhdenie Muruntau. FAN, Tashkent, pp. 222–319 (in Russian).

Golovanov, I.M., Voronkov, A.K., Obraztsov, A.I., Savchuk, Y.S., Shvetsov, A.D., 1998c. Condition of ore localization. In: Shayakubov, T.S. (Ed.), Zolotorudnoe Mestorozhdenie Muruntau. FAN, Tashkent, pp. 343–371 (in Russian).

Golovko, A.V., Kaminsky, F.V., 2008. Lamproitic Karashoho diamond deposit in Uzbekistan located within the Hercynian Tyan-Shan system. In: 9th International Kimberlite Conference, Extended Abstract No. 91KC – A – 00007.

Golovko, A.V., Kaminsky, F.V., 2010. The Shoshonite-Absarokite-Picrite Karashoho Pipe, Uzbekistan: an unusual Diamond Deposit in an Atypical tectonic environment. Society of Economic Geologists, Inc., Economic Geology 105, 825–840.

Graupner, T., Götze, J., Kempe, U., Wolf, D., 2000. CL for characterizing quartz and trapped fluid inclusions in mesothermal quartz veins: Muruntau Au ore deposit, Uzbekistan. Mineralogical Magazine 64 (6), 1007–1016.

Graupner, T., Kempe, U., Spooner, E.T.C., Bray, C.J., Kremenetsky, A.A., 2001a. Microthermometric, laser Raman spectroscopic, and volatile-ion chromatographic analysis of hydrothermal fluids in the Paleozoic Muruntau Au-bearing quartz vein ore field, Uzbekistan. Econcomic Geology 96 (1), 1–23.

Graupner, T., Kempe, U., Götze, J., Wolf, D., Irmer, G., Kremenetsky, A.A., 2001b. Au deposition and remobilization in the Muruntau "Central" quartz veins: evidence from SEM, cathodoluminescence and fluid inclusion data. In: Piestrzynski, A., et al. (Eds.), Mineral deposits at the Beginning of the 21st Century (6th SGA-SEG Meeting). Swets and Zeitlinger Publishers, Lisse, pp. 747–750.

Graupner, T., Kempe, U., Klemd, R., Schüssler, U., Spooner, E.T.C., Götze, J., Wolf, D., 2005a. Two stage model for the Muruntau (Uzbekistan) high grade ore structures based on characteristics of gold, host quartz and related fluids. Neues Jahrbuch Mineralogie Abhandlungen 181 (1), 67–80.

Graupner, T., Kempe, U., Wall, V.J., Seltmann, R., Köhler, S., Shatov, V., 2005b. Mass transfer during alteration and Au precipitation at Muruntau: alteration behaviour of different rock types. In: Mao, J., Bierlein, F.P. (Eds.), Mineral deposit Research: Meeting the Global Challenge (8th SGA Meeting). Springer, Berlin, Heidelberg, pp. 1317–1320.

Graupner, T., Niedermann, S., Kempe, U., Klemd, R., Bechtel, A., 2006. Origin of ore fluids in the Muruntau gold system: constraints from noble gas, carbon isotope and halogen data. Geochimica et Cosmochimica Acta 70, 5356–5370.

Graupner, T., Niedermann, S., Rhede, D., Kempe, U., Seltmann, R., Williams, C.T., Klemd, R., 2010. Multiple sources for mineralizing fluids in the Charmitan gold(-tungsten) mineralization (Uzbekistan). Mineralium Deposita 45, 667–682.

Gusev, A.I., Gusev, N.I., 2012. Fluid regime and petrology of shoshonitic granitoids from the super-giant gold-ore deposit Muruntau. Fundamental'nye Issledovaniya (6), 13–18 (in Russian).

Hall, G., Wall, V., 2007. Geology works: the use of regional geological maps in exploration. In: Milkereit, B. (Ed.), Proceedings of Exploration 07: Fifth Decennial International Conference on Mineral Exploration, pp. 51–60.

Herrington, R.J., Zaykov, V.V., Maslennikov, V.V., Brown, D., Puchkov, V.N., 2005. Mineral deposits of the Urals and links to geodynamic evolution. Economic Geology 100th Anniversary Volume, 1069–1095.

Herrington, R., Brown, D., Hawkins, T., Smith, M., Yakubchuk, A., Maslennikov, V., Fershtater, G., Krasnobaev, A., 2008. Nature of the boundary between the East European Craton, the Uralides and the Altaids: implications for metallogenic correlations. In: CERCAMS-12 Workshop "Metallogeny of Central Asia from Kazakhstan to Xinjiang – Research in Progress". The Natural History Museum, London, pp. 25–26. November 2008, p. 11 (abstract).

Heubeck, C., 2001. Assembly of central Asia during the middle and late Paleozoic. In: Hendrix, M.S., Davis, G.A. (Eds.), Paleozoic and Mesozoic Evolution of Central Asia: From Continental Assembly to Intercontinental Deformation, vol. 194. Geological Society of America Memoir, pp. 1–22.

Ivanov, G.A., Sabdyushev, S.S., 1974. Structure of thrust sheets in the Tamdytau, central Kyzylkum, as shown by seismic exploration. Doklady Akademii nauk SSSR, Earth Sciences Section 216, 94–95 (in Russian).

Kempe, U., Oberthür, T., 1997. Physical and geochemical characteristics of scheelite from gold deposits: a reconnaissance study. In: Papunen, H. (Ed.), Mineral deposits: Research and Exploration – where Do They Meet? Balkema, Rotterdam, pp. 209–212.

Kempe, U., Trinkler, M., Wolf, D., 1991. Yttrium und die Seltenerdfotolumineszenz natürlicher Scheelite. Chemie der Erde 51 (4), 275–289.

Kempe, U., Belyatsky, B.V., Kremenetsky, A.A., Wolf, D., Krymsky, R.S., 1997. Mantle influence on the genesis of the super-large Au deposit Muruntau (Uzbekistan): constraints from geochemistry and isotope composition of scheelite. In: Hatton, C.J. (Ed.), Plumes, Plates and Mineralization. University of Pretoria, pp. 51–52 (abstract).

Kempe, U., Monecke, T., Oberthür, Th., Kremenetsky, A.A., 1999. Trace elements in scheelite and quartz from the Muruntau/Myutenbai gold deposit, Uzbekistan: constraints on the nature of the ore-forming fluids. In: Stanley, C.J., et al. (Eds.), Mineral Deposits: Processes to Processing, vol. 1. Balkema, Rotterdam, pp. 373–376.

Kempe, U., Graupner, T., Wolf, D., Kremenetsky, A.A., 2000. Fluid migration and wall rocks of the Muruntau Au deposit (Uzbekistan): which processes resulted in ore precipitation? In: Bouchot, V., Moritz, R. (Eds.), A GEODE-GEOFrance 3D Workshop on Orogenic Gold Deposits in Europe with Emphasis on the Variscides. BRGM, Orléans, pp. 112–113 (abstract).

Kempe, U., Belyatsky, B.V., Krymsky, R.S., Kremenetsky, A.A., Ivanov, P.A., 2001a. Sm-Nd and Sr isotope systematics of scheelite from the giant Au(-W) deposit Muruntau (Uzbekistan): implications for the age and sources of gold mineralization. Mineralium Deposita 36, 379–392.

Kempe, U., Graupner, T., Wolf, D., Kremenetsky, A.A., 2001b. Unusual REE fractionation and occurrence of monazite-(La,Ce) in single monazite grains from a "Central" gold-quartz vein at Muruntau (Uzbekistan). In: Piestrzynski, A., et al. (Eds.), Mineral Deposits at the beginning of the 21st century. Balkema, Rotterdam, pp. 767–770.

Kempe, U., Seltmann, R., Graupner, T., Wall, V.J., Matukov, D., Sergeev, S., 2004. SHRIMP U-Pb zircon dating of Hercynian granite magmatism in the Muruntau gold district (Uzbekistan). In: Khanchuk, A.I., Gonevchuk, G.A., Mitrokhin, A.N., Simanenko, I.F., Cook, I.J., Seltmann, R. (Eds.), Metallogeny of the Pacifics Northwest: Tectonics, Magamtism and Metallogeny of Active Continental Margins. Dalnauka, Vladivostok, pp. 210–213.

Kempe, U., Seltmann, R., Graupner, T., Rodionov, N., Sergeev, S.A., Matukov, D.I., Kremenetsky, A.A., 2015. Concordant U-Pb SHRIMP ages of U-rich zircon in granitoids from the Muruntau gold district (Uzbekistan): timing of intrusion, alteration ages, or meaningless numbers. Ore Geology Reviews 65, 308–326.

Khokhlov, V.A., 1990. Petrology of metamorphic and metasomatic processes in the Muruntau ore field. In: Osobye kharakteristiki geologii i mineralizatsii v Yuzhnom Tienshane. SAIGIMS, Tashkent, pp. 37–47 (in Russian).

Khokhlov, V.A., Savchuk, Y.S., Khorvat, V.A., 1998. Metamorphic alteration of ore-hosting rocks. In: Shayakubov, T.S. (Ed.), Zolotorudnoe Mestorozhdenie Muruntau. FAN, Tashkent, pp. 165–194 (in Russian).

Koneev, R.I., 2003. Gold ore deposits of Uzbekistan: systematic and formation conditions. In: Akhmedov, N.A. (Ed.), Problems of Ore Deposits and Maximizing the Prospecting Efficiency. Uzbekistan, Tashkent, pp. 200–202 (in Russian).

Koneev, R.I., Ignatikov, E., Turesebekov, A., Aripov, U., Khalmatov, R., Kodirov, O., Usmanov, M., 2005. Gold ore deposits of Uzbekistan: geochemistry and nanomineralogy of tellurium and selenium. Geochemistry, Mineralogy and Petrology 43, 102–107.

Koneev, R.I., Khalmatov, R.A., Mun, Yu.S., 2010. Nanomineralogy and nanogeochemistry of ores from gold deposits of Uzbekistan. Zapiski Rossijskogo Mineralogicheskogo Obshchestva (2), 1–14 (in Russian); English version: 2010, Geology of Ore Deposits 52(8), 755–766.

Konopelko, D., Biske, G., Seltmann, R., Eklund, O., Belyatsky, B., 2007. Hercynian postcollisional A-type granites of the Kokshaal Range, Southern Tien Shan, Kyrgyzstan. Lithos 97, 140–160.

Konstantinov, M.M., Nekrasov, E.M., Sidorov, A.A., Strujkov, S.F., 2000. Gold Giants of Russia and World. Nauchnij Mir, Moscow, 272 pp.

Korhonen, J.V., Fairhead, J.D., Hamoudi, M., Hemant, K., Lesur, V., Mandea, M., Maus, S., Purucker, M., Ravat, D., Sazonova, T., Thebault, E., 2007. Magnetic Anomaly Map of the World; Map Published by Commission for the Geological Map of the World, Supported by UNESCO, first ed. GTK, Helsinki, ISBN 978-952-217-000-2 http://ftp.gtk.fi/WDMAM2007/. (15 August 2010).

Koroteev, V.A., de Boorder, H., Necheukhin, V.M., Sazonov, V.N., 1997. Geodynamic setting of the mineral deposits of the Urals. Tectonophysics 276, 291–300.

Kostitsyn, Y.A., 1991a. Rb-Sr isotope system of granite from the Altyntau (Central Kyzylkum): open for the rocks and closed for feldspar. Geokhimiya (10), 1437–1443 (in Russian); English version: 1992, Geochemistry International 29(5), 76–82.

Kostitsyn, Y.A., 1991b. Rb-Sr System of Rocks and Minerals from the Muruntau Deposit. Ph.D. Thesis. Institute of Geochemistry and Analytical Chemistry, Soviet Academy of Sciences, Moscow, 23 pp (in Russian).

Kostitsyn, Y.A., 1993. Rb-Sr isotope study of the Muruntau deposit: dating of ore veins by the isochron method. Geokhimiya (9), 1308–1318 (in Russian); English version: 1994, Geochemistry International 31(4), 53–64.

Kostitsyn, Y.A., 1994. Rb-Sr isotope study of the Muruntau deposit: ore-bearing metasomatites. Geokhimiya (4), 486–497 (in Russian); English version: 1994, Geochemistry International 31(11), 21–34.

Kostitsyn, Y.A., 1996. A Rb-Sr isotope study of the Muruntau deposit: magmatism, metamorphism and mineralization. Geokhimiya 34 (12), 1123–1138 (in Russian); English version: 1996, Geochemistry International 34(12), 1009–1023.

Kostitsyn, Y.A., Rusinova, O.V., 1987. Rb-Sr dating of a quartz-adularia hydrothermal vein by the use of a monomineral isochron. In: Metody izotopnoj geologii. GEOKHI, Moscow, pp. 123–125 (abstract; in Russian).

Kotov, N.V., Poritskaya, L.G., 1990. A generalized genetic model of gold accumulation in gold-sulfide ore metasomatic formations in black shales (Central Kyzylkum). Geologiya i Geofizika (11), 49–57 (in Russian); English version: 1990, Soviet Geology and Geophysics 31(11), 46–53.

Kotov, N.V., Poritskaya, L.G., 1991. Peculiarities of geology, mineral associations in metasomatites and problems of genesis of the Muruntau gold deposit (Central Kyzylkum). Zapiski Vessoyuznogo Mineralogicheskogo Obshchestva 120 (4), 59–69 (in Russian); English version: 1992, International Geology Review 34(1), 77–87.

Kotov, N.V., Zverev, Yu.N., Poritskaya, L.G., 1993. Gold Ore Formation in Black Shales (Central Kyzylkum). Nevskii Kur'er, St. Petersburg, 112 pp. (in Russian).

Kotov, N.V., Poritskaya, L.G., Gembitsky, V.V., 1995. Native Gold at Deposits of Western Uzbekistan. Nevskii kur'er, St. Petersburg, 116 pp. (in Russian).

Kol'tsov, A.B., Kostitsyn, Y.A., 1995. Isotope-termodynamic modeling of skarnoid formation at Muruntau. Geokhimiya (4), 512–523 (in Russian); English version: 1995, Geochemistry International 32(12), 67–80.

Kol'tsov, A.B., Rusinova, O.V., 1997. Quartz-biotite-K – feldspar metasomatites of Muruntau: genesis and a formation model. Petrologiya 5 (1), 81–90 (in Russian); English version: 1997, Petrology 5(1), 74–82.

Kraft, M., Kampe, A., 1995. Rohstoffwirtschaftliche Länderberichte der BGR: XXXVIII Usbekistan. Schweizerbart, Stuttgart, 137 pp.

Kremenetsky, A.A., 1994. Ore-forming processes in black shales: Muruntau gold ore deposit. In: Rongfu, Pei (Ed.), IX IAGOD Symposium, Abstracts, vol. 2, pp. 443–444.

Kremenetsky, A.A., Lapidus, A.V., Skryabin, V.Y., 1990. Depth evaluation of gold mineralization in black shales of the Central Kyzylkum desert according to deep drill hole SG 10. In: Ovchinnikov, L.N. (Ed.), Geological and Geochemical Methods of Depth Evaluation of Economic Deposits. Nauka, Moscow, pp. 59–139 (in Russian).

Kremenetsky, A.A., Mintser, E.F., Islamov, F.I., 1996. Evolution of ore-magmatic systems – criteria for prognosis, search and evaluation of gold-rare metal deposits. Razvedka i Okhrana Nedr 6 (8), 29–34 (in Russian).

Kryazhev, S.G., 2002. Isotopic-geochemical Regime of the Muruntau Gold Deposit Formation. TsNIGRI, Moscow, 91 pp. (in Russian).

Kryazhev, S.G., Kudryavtsev, S.G., 1995. Fluid regime during formation of the quartz vein stockwork at Murntau according to oxygen isotope composition of quartz. In: XIV Simpozium po geokhimii izotopov, Moscow, Russian Academy of Sciences. Abstracts, 124 (in Russian).

Kudrin, V.S., Solov'yev, S.G., Stavinskiy, V.A., Karabdin, L.L., 1990. The gold-copper-molydenum-tungsten ore belt of the Tien Shan. Geologiya rudnykh mestorozhdeniy 32 (4), 13–26 (in Russian); English version: 1990, International Geology Review 32(9), 930–941.

Laurent-Charvet, S., Charvet, J., Monié, P., Shu, L., 2003. Late Palaeozoic strike-slip shear zones in eastern central Asia (NW China): new structural and geochronological data. Tectonics 22 (2), 1009–1101.

Levashova, N.M., Degtyarev, K.E., Bazhenov, M.L., 2012. Oroclinal bending of the Middle and Late Paleozoic volcanic belts in Kazakhstan: paleomagnetic evidence and geological implications. Geotectonics 46, 285–302.

Loshchinin, V.P., Chistyakov, P.A., Mansurov, M.M., Surgutanova, D.M., Min'kin, M.I., 1986. Metamorphic alteration of Ordovician-Silurian sediments in the Muruntau ore field. Zapiski Uzbekskogo Otdeleniya Vsesoyuznogo Mineralogicheskogo Obshchestva (39), 153–161 (in Russian).

Makarova, Z.A. (Ed.), 1974. Map of the Anomalous Magnetic Field of the Territory of the USSR and Adjacent Marine Areas, 1:2 500 000. USSR Ministry of Geology, VSEGEI, Leningrad.
Marakushev, A.A., Khokhlov, V.A., 1992. A petrological model for the genesis of the Muruntau gold deposit (Western Uzbekistan). Geologiya rudnykh mestorozhdenij (1), 38–57 (in Russian); English version: 1992, International Geology Review 34(1), 59–76.
Mirkamalov, R.Kh., Chirikin, V.V., Kharin, V.G., Khan, R.S., 2012a. On the age of granitoid and metamorphic complexes in the Tian-Shan fault belt (Uzbekistan). Geologiya i mineral'nye resursy (1), 5–14 (in Russian).
Mirkamalov, R.Kh., Chirikin, V.V., Khan, R.S., Kharin, V.G., Sergeev, S.A., 2012b. Results of U-Pb (SHRIMP) datings of granitoid and metamorphic complexes of the Tien Shan folded belt (Uzbekistan). Vestnik St. Petersburg University 7 (1), 3–25 (in Russian).
Monecke, T., Kempe, U., Götze, J., 2002. Genetic significance of trace element content in metamorphic and hydrothermal quartz: a reconnaissance study. Earth and Planetary Science Letters 202, 709–724.
Morelli, R.M., Creaser, R.A., Seltmann, R., 2004. Rhenium – osmium geochronology of arsenopyrite from the giant Muruntau Au deposit, Uzbekistan. In: Khanchuk, A.I., Gonevchuk, G.A., Mitrokhin, A.N., Simanenko, I.F., Cook, I.J., Seltmann, R. (Eds.), Metallogeny of the Pacifics Northwest: Tectonics, Magmatism and Metallogeny of Active Continental Margins. Dalnauka, Vladivostok, pp. 510–513.
Morelli, R.M., Creaser, R.A., Seltmann, R., Stuart, F.M., Selby, D., Graupner, T., 2007. Age and source constraints for the giant Muruntau gold deposit, Uzbekistan, from coupled Re-Os-He isotopes in arsenopyrite. Geology 35 (9), 795–798.
Mukhin, P.A., Savchuk, Y.S., Kolesnikov, A.V., 1988. Position of the "Muruntau lens" within the collage of metamorphic units in the Southern Tamdytau (Central Kyzylkum desert). Geotektonika (2), 64–72 (in Russian); English version: 1988, Geotectonics 22(2), 142–148.
Mushkin, I.V., Akhber, D.Ya., Oranskiy, N.I., Chernyavskiy, Yu.A., 1973. Block structure and endogenic metallogeny in western Uzbekistan. Sovetskaya Geologiya (12), 70–80 (in Russian); English version: 1975, International Geology Review 17(2), 125–133.
Musin, R.A., 1981. Typomorphism of Quartz, Pyrite and Gold from Gold Ore Deposits in Uzbekistan. FAN, Tashkent, 144 pp. (in Russian).
Natal'in, B.A., Şengör, A.M.C., 2005. Late Palaeozoic to Triassic evolution of the Turan and Scythian platforms: the pre-history of the Palaeo-Tethyan closure. Tectonophysics 404, 175–202.
NGMK, 2015. Surface Mining – Last Update 03_March_2015 (accessed: 16.04.2015). http://www.ngmk.uz/en/about/mining/182-openmining.
Obraztsov, A.I., 1998. Principles of the Formation and Localization of the Gold Deposits in the Muruntau Ore Field. Summary of the habilitation thesis, Zarafshan, 24 pp. (in Russian).
Obraztsov, A.I., 2009. Development of concepts on ore deposit morphologies. Otechestvennaya Geologiya (3), 96–100 (in Russian).
Obraztsov, A.I., Belenko, A.P., 1997. Special features of the geological structure of Muruntau and methods for an estimation of its resources. Theoriya I Praktika Rasrabotki Mestorozhdeniya Muruntau Otkrytym Sposobom. FAN, Tashkent, pp. 18–25 (in Russian).
Palej, L.Z., 1968. Age and geological setting of gold-ore mineralization in Central Asia. Sovietskaya Geologiya (3), 125–128 (in Russian).
Palej, L.Z., Sher, S.D., 1970. On the absolute age of gold mineralization in Uzbekistan. In: Smirnov, V.I. (Ed.), Zakonomernosti razmeshcheniya poleznykh iskopaemykh, vol. 9. Nauka, Moscow, pp. 195–290 (in Russian).
Petrovskaya, N.V., 1968. On classification of gold ores in Uzbekistan. Geology of Ore Deposits/Geologiya Rudnykh Mestorozhdenij 10 (3), 3–16 (in Russian).
Porshnyakov, G.S., 1983. Stages in the formation of the tectonic structure in different segments of the Hercynides in southern Tian Shan and the Pamirs. In: The Tectonics of the Tien Shan and Pamirs. Nauka, Moscow, pp. 66–77 (in Russian).
Protsenko, V.F., 1987. Formation of gold mineralization in black shales of western Uzbekistan. Zapiski Uzbekskogo otdeleniya Vsesoyuznogo Mineralogicheskogo Obshchestva (40), 23–30 (in Russian).
Protsenko, V.F., Rubanov, A.A., 1991. Convective-metasomatic formation of rare-metal mineralization in black shales and granitoids of western Uzbekistan. In: Barabanov, V.F. (Ed.), Mineralogiya i geokhimiya vol'framovykh mestorozhdenii, vol. 4. Izd. LGU, Leningrad, pp. 242–252 (in Russian).
Protsenko, V.F., Arifulov, C.K., Khorvat, V.A., 1998. Metasomatites. In: Shayakubov, T.S. (Ed.), Zolotorudnoe Mestorozhdenie Muruntau. FAN, Tashkent, pp. 195–222 (in Russian).
Rafailovich, M.S., Shevkunov, A.G., Koloskova, S.M., Ezhkov, Yu.B., 2013. Tungsten mineralization in large gold deposits located in black shales of Central Asia. Geologiya i mineral'nye resursy (3), 16–28 (in Russian).
Rakhmatullaev, K.R., 1980. Different ages for different gold ores types from the Muruntau ore field. Zapiski Uzbekskogo Otdeleniya Vsesoyuznogo Mineralogicheskogo Obshchestva 33, 198–202 (in Russian).
Rosenbaum, G., 2014. Geodynamics of oroclinal bending: insights from the Mediterranean. Journal of Geodynamics 82, 5–15.
Rusinova, O.V., Korolev, Y.M., Vasil'eva, M.E., 1996. XRD charateristics of carbonaceous matter from gold ore deposits in black shales. Litologija i poleznye izkopaemye (1), 89–96 (in Russian).
Sabdyushev, S.S., Usmanov, R.R., 1971. Tectonic sheets, mélanges and the ancient oceanic crust in Tamdytau (Western Uzbekistan). Geotektonika (5), 27–36 (in Russian); English version: 1971, Geotectonics (5), 283-287.
Sabdyushev, S.S., Voronov, O.A., 1990. Deep Structure of the Northern Tamdytau Based upon Results of Structural Drilling. Unpublished manuscript, 4 pp., 3 figs. (in Russian).
Safirova, E., 2014. The Mineral Industry of Uzbekistan. U.S. Geological Survey Minerals Yearbook. Uzbekistan (advance release), pp. 49.1–49.8.
Savchuk, Y.S., Procenko, V.F., Kolesnikov, A.V., 1987. Mineral associations in the tectonic structures at Muruntau. Zapiski Uzbekskogo Otdeleniya Vsesoyuznogo Mineralogicheskogo Obshchestva 40, 30–33 (in Russian).
Savchuk, Y.S., Mukhin, P.A., Meshcheryakova, L.V., 1991. Late Palaeozoic granitoid magmatism and Kyzylkum ore formations from a plate tectonics viewpoint. Geotektonika (4), 70–87 (in Russian); English version: 1991, Geotectonics 25, 326–339.
Seltmann, R., Graupner, T., Klemd, R., Kempe, U., Shatov, V., 2003. Criteria for an Exploration Model for Muruntau Style Deposits. CERCAMS Report (unpublished), NHM London, 92 pp.
Seltmann, R., Armstrong, R., Dolgopolova, A., Yakubchuk, A., Konopelko, D., Creaser, R.A., Morelli, R., Zhang, X., Chen, C., 2008. Granitic magmatism and related mineralization in the Altaids: case study from the Tienshan mineral belt. Geochemica et Cosmochimica Acta 72 (12). Supplement, 18th Annual V.M. Goldschmidt Conference, Vancouver, A846 (abstract).
Seltmann, R., Konopelko, D., Biske, G., Divaev, F., Sergei, S., 2011. Hercynian post-collisional magmatism in the context of Paleozoic magmatic evolution of the Tien Shan orogenic belt. Journal of Asian Earth Sciences 42, 821–838.
Seltmann, R., Porter, T.M., Pirajno, F., 2014. Geodynamics and metallogeny of the central Eurasian porphyry and related epithermal mineral systems: a review. Journal of Asian Earth Sciences 79, 810–841.
Seltmann, R., Shatov, V., Yakubchuk, A. (Eds.), 2015. Mineral deposits Database and Thematic Maps of Central Asia, Scale 1:1 500 000. ArcGIS 10.1 Package and Explanatory Notes, Centre for Russian and Central Eurasian Mineral Studies (CERCAMS). NHM London, 120 pp.
Shayakubov, T.S. (Ed.), 1998. Zolotorudnoe Mestorozhdenie Muruntau. FAN, Tashkent, 539 pp. (in Russian).
Shayakubov, T.S., Dalimov, T.N. (Eds.), 1998. Geology and Minerals of the Republic of Uzbekistan. Tashkent University, Tashkent, 724 pp. (in Russian).
Shayakubov, T.S., Kremenetsky, A.A., Mintser, E., Obraztsov, A.I., Graupner, T., 1999. The Muruntau ore field. In: Shayakubov, T.S., Islamov, F., Kremenetsky, A., Seltmann, R. (Eds.), Au, Ag, and Cu Deposits of Uzbekistan, GFZ Potsdam, IGCP 373 Excursion Guidebook, pp. 37–74.
Sher, S.D., 1970. Wall-rock alteration in one of the gold deposits in Middle Asia. In: Internat. Union Geol. Sci. A, No 2: Problems of Hydrothermal Ore Deposition. Schweizerbart, Stuttgart, pp. 312–315.
Sher, S.D., 1972. Structural features of the Muruntau ore field: genetic problems and conditions of localization of the stockwork mineralization. Trudy TsNIGRI 101, 143–154 (in Russian).
Toovey, L.M., 2011. Gold mining in the Republic of Uzbekistan (accessed: 16.04.2015). http://goldinvestingnews.com/13349/gold-mining-in-the-republic-of-uzbekistan.html.
Tourtelot, H.A., 1979. Black shale – its deposition and diagenesis. Clays and Clay Minerals 27 (5), 313–321.
Uspenskij, Y.I., Aleshin, A.P., 1993. Patterns of scheelite mineralization in the Muruntau gold deposit, Uzbekistan. International Geology Review 35, 1037–1051.
Vasilevsky, B.B., Koneev, R.I., Rustamov, A.I., Turesbekov, A. Kh., Ignatikov, E.N., Mirtalipov, D.Y., Rakhimov, R.R., 2004. New data on the composition of gold ores of the Muruntau deposit. TsNIGRIi Moscow: Rudy i Metally 2 (3), 67–79 (in Russian).
Vikhter, B.Y., Khazan, K.E., Zarembo, Y.G., 1986. Relations between gold and tungsten mineralization in Southern Tien Shan. In: Barabanov, V.F. (Ed.), Mineralogiya i geokhimiya vol'framovykh mestorozhdenii, vol. 4. Izd. LGU, Leningrad, pp. 307–316 (in Russian).
Van der Voo, R., Levashova, N.M., Skrinnik, L.I., Kara, T.V., Bazhenov, M.L., 2006. Late-orogenic, large-scale rotations in the Tien Shan and adjacent mobile belts in Kyrgyzstan and Kazakhstan. Tectonophysics 426, 335–360.
Voronkov, A.K., 1976. Peculiarities of lithology of metamorphic rocks of the Besapan Suite in the Proterozoic of the Cetral Kyzylkum. Uzbekskij Geologicheskij Zhurnal (1), 70–73 (in Russian).
Voronkov, A.K., Yakovlev, V.G., 1980. On the sources of metals in silver mineral associations in the Central Kyzylkum. Zapiski Uzbekistanskogo otdeleniya Vsezoyuznogo Mineralogicheskogo Obshchestva 33, 114–117 (in Russian).
Vorotnikov, V., 2014. Uzbekistan plans to increase gold production. Engineering and Mining Journal (6), 82–87.
Wall, V.J., 2004. Muruntau, Uzbekistan: Preliminary Report on CERCAMS Research Project (Unpublished), Spring Hill, Australia, 69 pp.
Wall, V.J., Graupner, T., Yantsen, V., Seltmann, R., Hall, G.C., 2004. Muruntau, Uzbekistan: a giant thermal aureole gold (TAG) system. In: Muhlig, J., Goldfarb, R., Vielreicher, N., Bierlein, F., Stumpfl, E., Groves, D.I., Kenworth, S. (Eds.), SEG 2004, Centre for Global Metallogeny, University of Western Australia, vol. 33, pp. 199–203 extended abstracts.
Wilde, A.R., Layer, P., Mernach, T., Foster, J., 2001. The giant Muruntau deposit: geologic, geochronologic, and fluid inclusion constraints on ore genesis. Economic Geology 96, 633–644.
Windley, B.F., Alexeiev, D.V., Xiao, W., Kröner, A., Badarch, G., 2007. Tectonic models for accretion of the Central Asian Orogenic Belt. Journal of the Geological Society of London 164, 31–47.
Yakubchuk, A., Cole, A., Seltmann, R., Shatov, V., 2002. Tectonic setting, characteristics, and regional exploration criteria for gold mineralization in the Altaid

orogenic collage: the Tien Shan province as a key example. Society of Economic Geologists Special Publication 9, 177–201.
Yakubchuk, A.S., Shatov, V.V., Kirwin, D., Edwards, A., Tomurtogoo, O., Badarch, G., Buryak, V.A., 2005. Gold and base metal metallogeny of the Central Asian Orogenic Supercollage. Economic Geology 100th Anniversary Volume, 1035–1068.
Yardley, B.W., Cleverley, J.S., 2015. The role of metamorphic fluids in the formation of ore deposits. In: Jenkin, G.R.T., Lusty, P.A.J., Mcdonald, I., Smith, M.P., Boyce, A.J., Wilkinson, J.J. (Eds.), Ore Deposits in an Evolving Earth, Geological Society, London, Special Publications, 393(1), pp. 117–134.
Yudalevich, Z.A., Levchenko, I.V., 1981. Metallogenetic role of dikes in western Uzbekistan. Zapiski Uzbekskogo Otdeleniya Vsesoyuznogo Mineralogicheskogo Obshchestva 34, 201–207 (in Russian).
Yudalevich, Z.A., Gayzeev, A.A., Divaev, F.K., Ronkin, Y.L., 1991. Characteristics of internal structure, age and ore mineralization of the Koshrabad intrusion (South Tien Shan). In: Stroenie i dinamika litosfery Tyan'-Shanya. SAIGIMO, Tashkent, pp. 33–61 (in Russian).
Zairi, N.M., Kurbanov, N.K., 1991. Isotopic-geochemical model of ore genesis in the Muruntau ore field. Sovietskaya Geologiya (8), 64–69 (in Russian); English version: 1992, International Geology Review 34(1), 88–94.
Zairi, N.M., Kostitsyn, Y.A., Protsenko, V.F., Kol'tsov, A.B., Kotov, N.V., 1998. Age of gold mineralization and physical-chemical of formation. In: Shayakubov, T.S. (Ed.), Zolotorudnoe Mestorozhdenie Muruntau. FAN, Tashkent, pp. 404–448 (in Russian).
Zarembo, Y.G., 1968. Main Characteristics of Stages of Ore Formation in the Muruntau Deposit (Western Uzbekistan). Voprosy geologii mestorozhdenij zolota i zolotonosnykh rajonov, vol. 79. Trudy TsNIGRI, pp. 279–290 (in Russian).
Zonenshain, L.P., Kuzmin, M.I., Natapov, L.M., 1990. Geology of the USSR: a Plate Tectonic Synthesis. American Geophysical Union, Washington, DC. Geodynamic Series, 21, 242 pp.